Zeitschrift: IABSE congress report = Rapport du congrès AIPC = IVBH Kongressbericht

Band: 8 (1968)

Rubrik: V. New practices in concrete buildings

V

Développements nouveaux relatifs aux bâtiments de grande hauteur en béton

Neue Entwicklungen bei Beton-Hochhäusern

New Practices in Concrete Buildings

Va

Problèmes spéciaux aux bâtiments de grande hauteur (murs de contreventement, stabilité élastique des poteaux, effets de gradients thermiques, problèmes constructifs)

Spezielle Probleme bei Hochhäusern (Schubwände, Stabilität der Stützen, thermische Einflüsse, konstruktive Probleme)

Special Problems of Tall Buildings (Shear Walls, Stability of Columns, Effect of Thermal Gradients, Construction Problems)

Leere Seite
Blank page
Page vide

DISCUSSION PRÉPARÉE / VORBEREITETE DISKUSSION / PREPARED DISCUSSION

Special Problems of Tall Buildings (Shear Walls, Stability of Columns, Effect of Thermal Gradients, Construction Problems)

Problèmes spéciaux aux bâtiments de grande hauteur (murs de contreventement, stabilité élastique des poteaux, effets de gradients thermiques, problèmes constructifs)

Spezielle Probleme bei Hochhäusern (Schubwände, Stabilität der Stützen, thermische Einflüsse, konstruktive Probleme)

ALFRED A. YEE
Alfred A. Yee & Associates, Inc.
1441 Kapiolani Boulevard
Honolulu, Hawaii 96814

The authors' subject is one of great interest in view of the increasing world population. In this area of design there is a need for more information to define physiological and psychological response limits. Although some information is available on tolerable structural movements based on frequency of vibration and displacement, these should be extended in scope to cover a wider range of frequencies and displacements. There should be further development of response criteria based in terms of acceleration with regard to discomfort for the human body is most sensitive to this aspect of motion. It is recognized that criteria for comfort can be difficult to establish since personal reactions to vibration vary among individuals.

There is a need for more sophisticated wind measuring devices to obtain wind gust readings within fractions of a second. This information can be valuable in determining dynamic responses of structures. Further statistic and probabilistic studies should be undertaken in order to develop a more rational design criteria for earthquake and wind loads.

The importance of energy absorption and ductility in multistory frames is well recognized by all engineers. This, however, may not be easily achieved in reinforced concrete or prestressed concrete building frames unless more emphasis is given to the detailing of primary joints between columns, beams, girders and shear elements. This is now especially important in view of the potential increase in the use of precast units for the construction of high rise buildings. It may be more advantageous to precast such primary joints between columns, beams and girders and locate the splicing points between these precast units in an area midway between the primary joints in order to optimize the quality of construction and ultimate behavior of the critical column-beam-girder intersections. For instance, Figure 1 shows a method of high rise building construction utilizing precast column-beam elements in combination with pretensioned precast concrete floor slabs. The interaction of the columns and beams at the factory-produced joints will furnish the necessary energy absorption and ductility required in the resistance of lateral dynamic forces. The bending moments due to lateral forces are usually minimal at the splice points shown and these locations will be required primarily to transmit shear under the action of lateral forces. These connections, therefore, can be simply fabricated by means of

grouted sleeves joining the column reinforcing bars and cast in situ splices for the beams. This prefabrication concept provides considerable economic benefit through the advantage gained by factory work replacing a large part of in situ work in the multistory structure.

Minimum depth in structural framing systems is important for multistory buildings not only from the point of view of cost savings but also with regard to the increasingly strict height limitations now being introduced in recent zoning and building set-back regulations. Figure 2 shows the cross section of a 33-story apartment building recently constructed under strictly regulated height limitations. The basic structural concept utilizes a 3-1/2 inch thick precast prestressed concrete slab soffit in composite action with a 2-1/2 inch thick cast in situ reinforced concrete topping making a total overall depth of 6 inches in a clear span of 26 feet. The maximum overall slab span from center line of beam to center line of wall support is 30 feet 7 inches. This thin slab was built to achieve these spans through the combined use of prestressing steel and lightweight aggregate concrete. It was found that when local pumice lightweight aggregate was prestressed its stiffness increased to the extent that it developed only two thirds the deflection for dead and live load of that experienced by similar construction using regular weight blue basalt aggregate concrete. This appeared to be an unusual phenomenon inasmuch as standard reinforced concrete using this same lightweight aggregate would develop about double the deflection experienced by similar construction with regular weight aggregate. The minimum thickness of these slabs enabled the builder to construct an extra story height within the restricted building height envelop as regulated by local building ordinances.

Weight is a critical factor in the construction of multistory buildings. If lightweight aggregate concrete is used in place of standard weight concrete, the reduction in total dead weight of the building means a reduction in earthquake response forces, reduction in the reinforcing required for each basic element such as floor slabs, beams, walls, columns and finally a reduction in the size of the footings and the requirements for foundation piling. However, the apparent initial disadvantage in the use of lightweight concrete because of its normally increased unit cost per cubic yard of material has discouraged many designers from investigating it further. In the building project shown in Figure 2, a structural cost comparison was made on alternate designs using various lightweight aggregate concrete combinations versus all standard weight concrete construction and it was proven that although there was a premium of $5.00 per cubic yard on the lightweight aggregate concrete, the use of this material throughout the entire building would result in a savings of $113,100. Figure 3 is a summary of this comparative cost analysis.

Other factors that can influence multistory construction cost are methods of framing with relation to the utilities that must be accommodated. One of the framing methods that has often been successfully employed in the past few years is the interrupted beam system whereby alternate spans of the beams are cantilevered off the columns and stopped short of the midspan, thus allowing a break for the passage of air conditioning ducts. This is an effective way to reduce the floor to floor height in multistory buildings and such reduction of height means a reduction in each run of stairs, elevator shafts, plumbing stacks, vertical duct work, area of exterior perimeter walls, overturning moment, etc.

The most desirable multistory building design solution requires a complete integration of numerous factors balancing structural methods and speed of construction with accommodation of electrical, mechanical and other utilities to produce the most functional, economical and aesthetic end product. The writer agrees with the authors that, "Structural design is still almost as much of an art as a science ...".

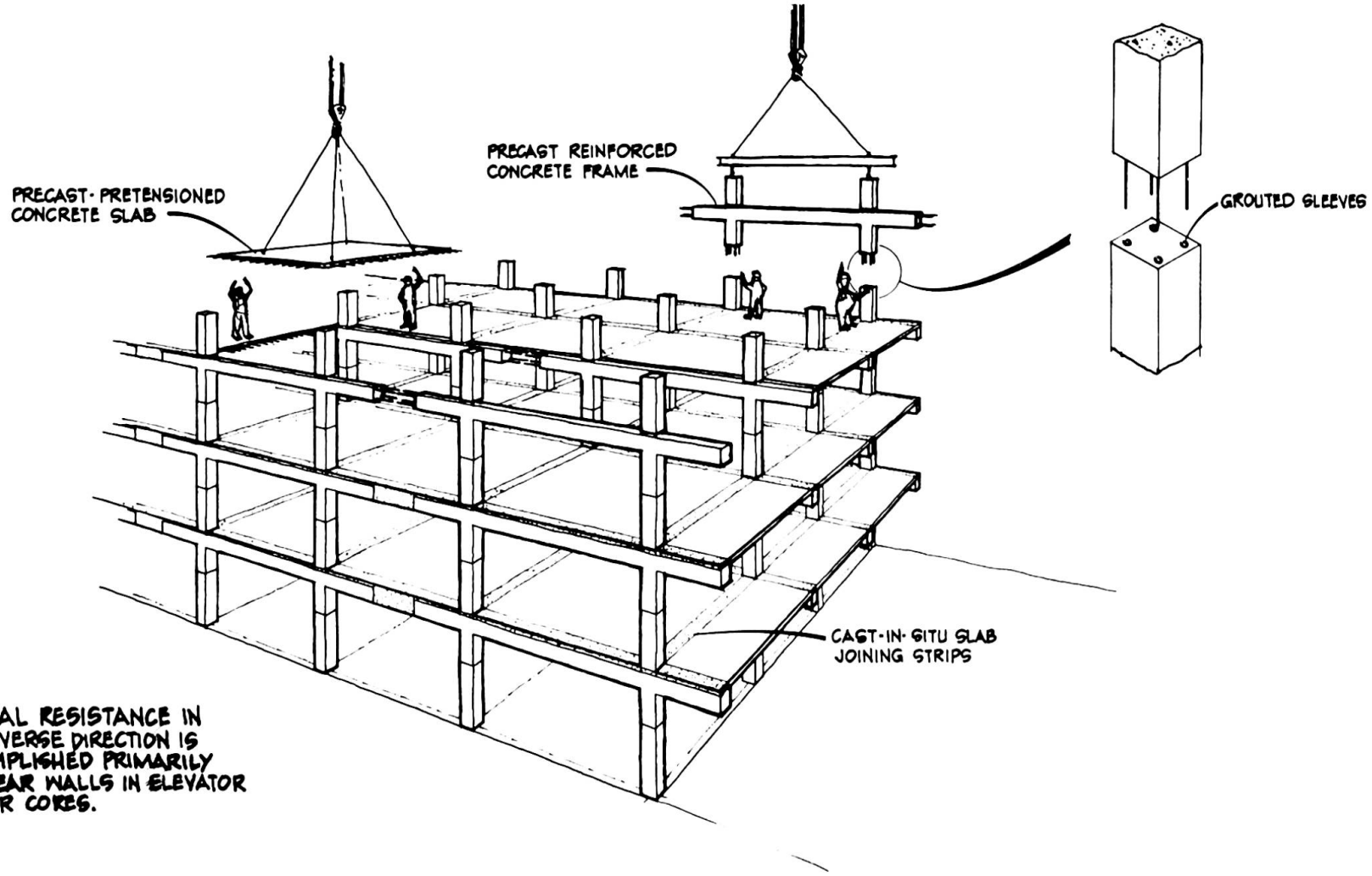
PRECAST-PRETENSIONED CONCRETE SLAB
PRECAST REINFORCED CONCRETE FRAME
GROUTED SLEEVES
CAST-IN-SITU SLAB JOINING STRIPS
NOTE: LATERAL RESISTANCE IN TRANSVERSE DIRECTION IS ACCOMPLISHED PRIMARILY BY SHEAR WALLS IN ELEVATOR & STAIR CORES.

FIGURE 1

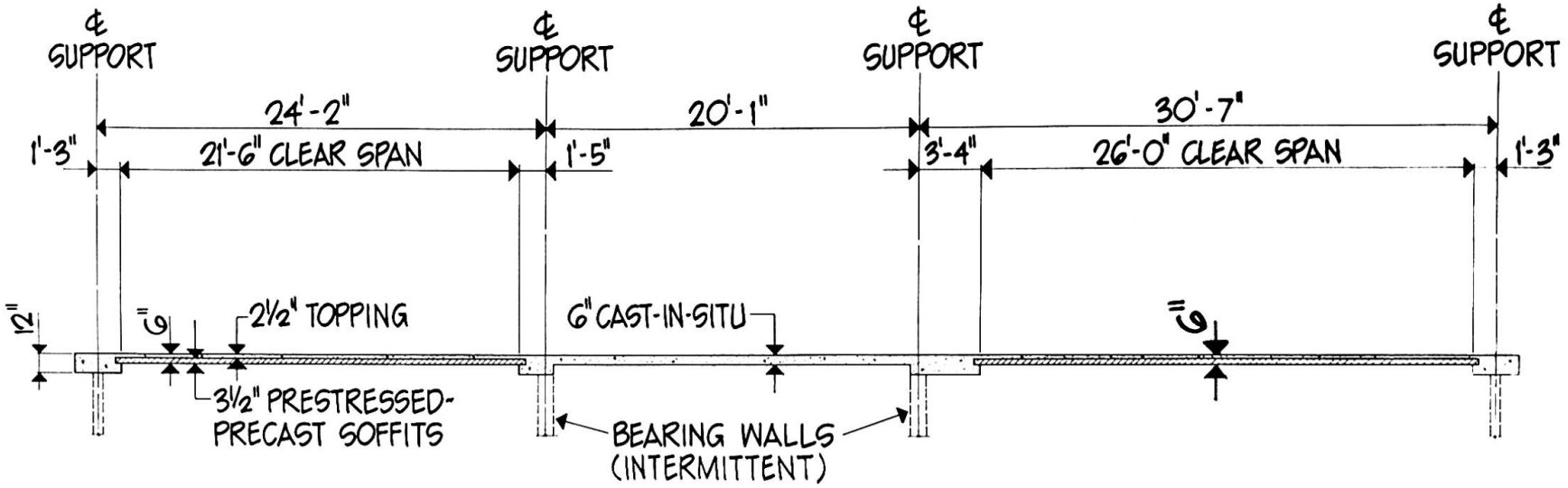

TYPICAL APARTMENT FLOOR CROSS SECTION

FIGURE 2

COMPARATIVE COST ESTIMATE WITH VARIOUS COMBINATIONS OF AGGREGATE TYPES BASED ON TYPICAL BAY EXTRAPOLATION

Schemes	Reinforcing Costs	Concrete Costs	Pile Costs	Pile Cap Deductions	Totals
SCHEME I Blue Basalt Concrete throughout	$481,700	$264,400	$590,000	$ -	$1,336,100
SCHEME II Lightweight Concrete Topping and Beams - Blue Basalt Concrete Planks, Walls and Columns	434,100	296,400	574,000	800	1,303,700
SCHEME III Lightweight Concrete Topping, Beams and Planks - Blue Basalt Concrete Walls and Columns	387,200	299,400	552,000	1,900	1,236,700
SCHEME IV Lightweight Concrete throughout	380,300	315,700	530,000	3,000	1,223,000

TOTAL DIFFERENCE - SCHEME IV TO SCHEME I $113,100

Based on the Following Unit Costs:

Lightweight concrete @ $25.00/cu. yd.*
Regular weight concrete @ $20.00/cu. yd.*

A-15 reinforcing steel @ $.16/lb.**
A-432 reinforcing steel @ $.17/lb.**

200T piles @ $10.00/ft. (prestressed concrete)

* Material only
** In-place cost

FIGURE 3

SUMMARY

The importance of energy absorption and ductility in multistory building frames is well recognized by all engineers and the most important area of consideration is the detailing of primary joints between columns, beams, girders and shear wall elements. For factory fabrication there appears to be some advantage in precasting joints between primary members and locating splicing points at positions of minimum moments under lateral forces. In view of increasing building height restrictions, some advantages can be gained in minimizing the depth of structural framing systems. The use of lightweight concrete for weight reduction in multistory buildings is especially desirable in seismic areas.

RÉSUMÉ

L'importance de l'absorption de l'énergie et de la ténacité dans les portiques à étages multiples est bien connue par tous les ingénieurs. L'intérêt primordial est porté vers les joints principaux entre colonnes, poutres, traverses et éléments de mur de cisaillement. Pour la fabrication industrielle, il apparaît avantageux de préfabriquer les joints entre éléments primaires, et de placer des raccords aux endroits de moment minimum sous charge latérale. Vu les restrictions de plus en plus sévères de la hauteur des bâtiments, il peut être avantageux de minimizer la hauteur du système de portiques. L'emploi de béton léger réduisant le poids dans les structures élevées est particulièrement recommandé dans les zones sismiques.

ZUSAMMENFASSUNG

Frühzeitig ist die Wichtigkeit der Energieabsonderung sowie die Biegbarkeit in Stockwerkrahmen von allen Ingenieuren erkannt worden; der wichtigste Teil der Betrachtung ist der der Hauptknoten zwischen Stützen, Unterzug (Träger), Hauptträger und Scheiben. Für die Herstellung scheint es vorteilhaft, die Verbindungen zwischen Haupteleme̊nten vorzufertigen und Montagestösse dort anzubringen, wo das Moment infolge seitlicher Kräfte minimal bleibt. Aus der Sicht der wachsenden Beschränkung von Gebäudehöhe können einige Vorteile durch die Minimalisierung der Rahmentiefe gewonnen werden. Die Anwendung leichten Betons zur Gewichtsabminderung in vielstöckigen Gebäuden ist besonders in erdbebengefährdeten Gebieten erwünscht.

New Practices in Concrete Buildings

Développements nouveaux relatifs aux bâtiments de grande hauteur en béton

Neue Entwicklungen bei Beton-Hochhäusern

PAUL ROGERS
F. ASCE
Structural Engineer
Los Angeles, California

INTRODUCTION

The authors are to be commended for their concise presentation of the practices in concrete high-rise buildings. Their description is applicable where only wind forces act laterally against the buildings. In areas of high seismicity, both the design and construction is markedly different.

Professors N. M. Newmark and W. J. Hall are presenting, at this Congress, an extensive paper on the Dynamic Behavior of Reinforced Concrete Buildings. It is the philosophy expressed in their paper which led the Structural Engineers Association of California, (SEAOC) to initiate new procedures in the design of high-rise buildings.

Damaging earthquakes seem to indicate that, in order to safeguard life and property, the building frames have to resist lateral forces brought about by the earthquakes, and, furthermore, such building frames to be able to absorb energies without failures. The implementation of these criteria, however, is not a simple matter. Attempts to design within the elastic range would create buildings beyond economic feasibilities.

Forty years of evolution in producing a realistic design procedure has resulted in the latest SEAOC requirements which, for high-rise structures particularly, demand a ductile, energy absorbing rigid frame, with the following behavior:

a. Minor earthquake: No damage to the building.

b. Moderate earthquake: No structural damage, although minor damage to enclosing materials may be expected.

c. Major earthquake: Considerable non-structural damage, but the reinforced concrete frame absorbs the excess energy through ductile yielding and formation of elasto-plastic hinges.

EARTHQUAKE INTENSITIES. While no location may be guaranteed against earthquakes, past histories have been used for the production of a map of seismic probability.

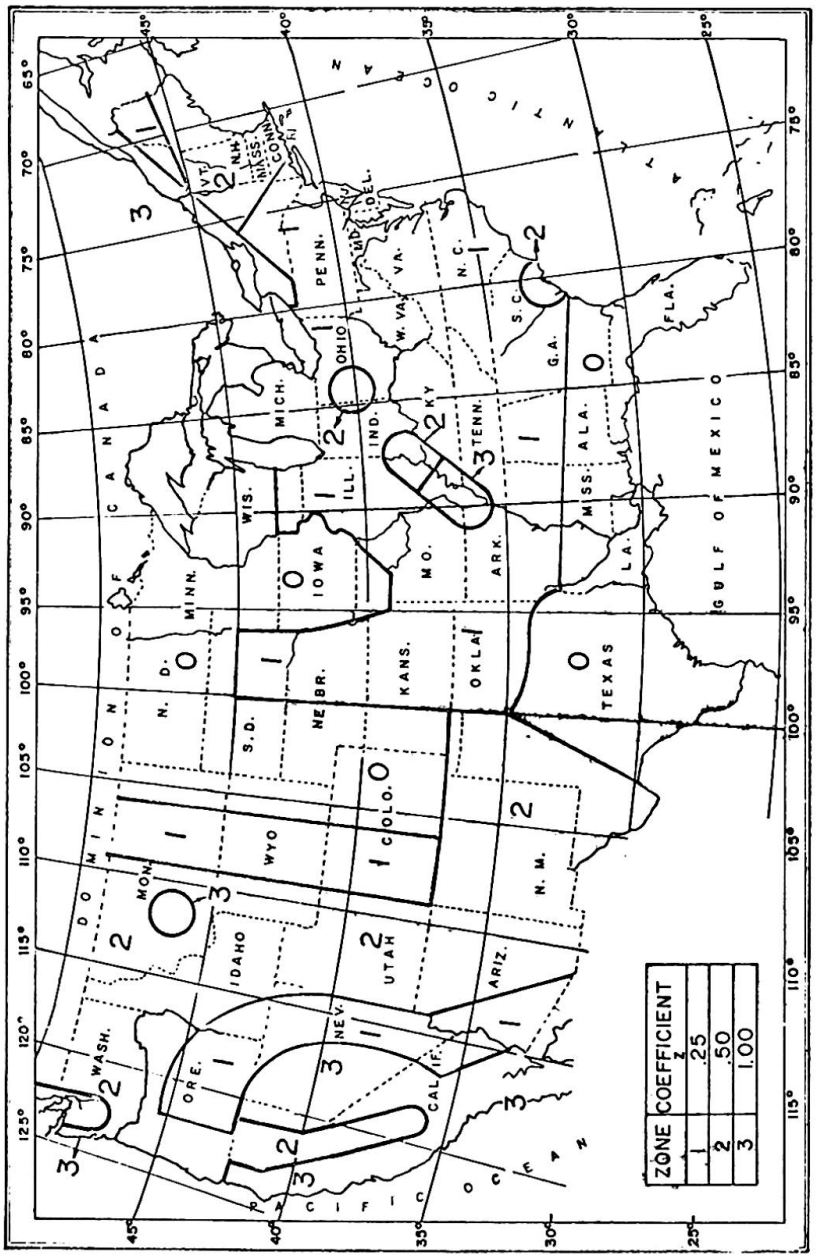

FIG. 1.
EARTHQUAKE ZONES AND COEFFICIENTS "Z"

This map is now in process of revision (e.g.: Substantial earthquakes were registered in Denver, Colorado, a zero intensity location on the map.) In the calculation of seismic lateral forces a coefficient "Z" to be employed. The value "Z" varies according to the probability zone, such as:

Zone 0: "Z"= 0; Zone 1: "Z"= 0.25; Zone 2: "Z"= 0.50;
Zone 3: "Z"= 1.00.

FORCE FACTOR "K". Dependent on the framing system employed, a coefficient "K" is to be used:

HORIZONTAL FORCE FACTOR "K" FOR BUILDINGS OR OTHER STRUCTURES(1)

TYPE OR ARRANGEMENTS OF RESISTING ELEMENTS	VALUE OF K(2)
All building framing systems except as hereinafter classified.	1.00
Buildings with a box system as defined in Section 2313(b).	1.33
Buildings with a dual bracing system consisting of a ductile moment resisting space frame and shear walls designed in accordance with the following criteria: 1. The frames and shear walls shall resist the total lateral force in accordance with their relative rigidities considering the interaction of the shear walls and frames. 2. The shear walls acting independently of the ductile moment resisting space frame shall resist the total required lateral force. 3. The ductile moment resisting space frame shall have the capacity to resist not less than 25 per cent of the required lateral force.	0.80
Buildings with a ductile moment resisting space frame designed in accordance with the following criteria: The ductile moment resisting space frame shall have the capacity to resist the total required lateral force.	0.67
Elevated tanks plus full contents, on four or more cross-braced legs and not supported by a building.(3), (4), (5).	3.00
Structures other than buildings and other than those set forth in Table 23-D.	2.00

(1) Where prescribed wind loads produce higher stresses, these loads shall be used in lieu of the loads resulting from earthquake forces.

(2) The coefficients determined here are for use in the State of California and in other areas of similar earthquake activity. For areas of different activity, the coefficient may be modified by the building official upon advice of seismologists and structural engineers specializing in aseismic design.

(3) The minimum value of KC shall be 0.12 and the maximum value of KC need not exceed 0.25.

(4) For overturning, the factor J as set forth in Section 2313(h) shall be 1.00.

(5) The torsional requirements of Section 2313(g) shall apply.

High-rise buildings in excess of 160 ft. (± 49 m.) can only be of ductile system, with a "K" factor of 0.80 or 0.67. There is a penalty for use of shear walls, as stated above; however, shear walls may be necessary to restrict drift either against seismic or wind forces; or they are difficult to eliminate due to architectural layouts. (Enclosure walls around stairs and elevators. Solid cast-in-place stairs act as trusses similar to shear walls.)

The minimum seismic base shear, in the direction of each of the main axes is to be:

$$V = ZKCW, \text{ where}$$

W= total dead load, (KIPS) $\quad W = \sum_{i=1}^{n} w_i$

$C = \dfrac{0.05}{\sqrt[3]{T}}$; (C= 0.10 for one and two-story buildings.)

$T = \dfrac{0.05 h_n}{\sqrt{D}}$; (T= 0.10 x number of stories above the base for rigid frame high-rises.)

= fundamental period of vibration in seconds in the direction under consideration. Properly substantiated data is also acceptable. (Such as computer calculations.)

h_n= total height of building above base. (ft.)

D= dimension of building in the direction of applied forces. (ft.)

In order to account for the higher modes of vibration and for whipping forces, the base shear "V" is to be distributed as follows:

$$F \text{ top level} = 0.004V \left(\frac{h_n}{D_s}\right)^2 \leq 015V, \qquad (F_t = 0 \text{ if} \left(\frac{h_n}{D_s}\right) \leq 3)$$

$$F_x \text{ at level } x = \frac{(V - F_t)\, w_x h_x}{\sum_{i=1}^{n} w_i h_i}, \quad \text{where}$$

D_s= plan dimension of the vertical lateral force resisting system(ft)

wi, wx= that portion of "W" which is located at or is assigned to level "i" or "x" respectively.

TORSIONAL MOMENTS. As a rule, high-rise structures should be designed for a minimum torsional eccentricity of 5% of maximum building dimension.

OVERTURNING. Every high-rise building to resist the overturning effect caused either by wind or earthquake. For the latter there is a modified moment:

$$M_{o.t.} = J\left(F_t\, h_n + \sum_{i=1}^{n} F_i h_i\right) \quad \text{where}$$

$$J = \frac{0.6}{\sqrt[3]{T}} \leq 1.$$

SPECIAL PROVISIONS. Ductile frame buildings of 160 ft. or higher are subject to several restrictive provisions. The most important ones are enumerated as follows:

1. The main ductile moment resisting frame has to be cast-in-place monolithic reinforced concrete. Other members may be precast, prestressed, composite, etc.

2. The Ultimate Strength Design Method (USD) is specified for ductile frames.

3. The following load factors are to be used:

$U = 1.40 (D + L + E)$ where $U = .90 D \pm 1.25E$ = (suggested) $.90 D \pm 1.35E$

D= Dead Load
L= Live Load
E= Earthquake Force

4. Under no conditions should plastic hinges be formed in columns but only in beams preferably near the columns.

5. In order to insure ductility both columns and beams at end near the joints shall be of confined concrete. Concrete may be confined by closely spaced ties, or stirrup-ties.

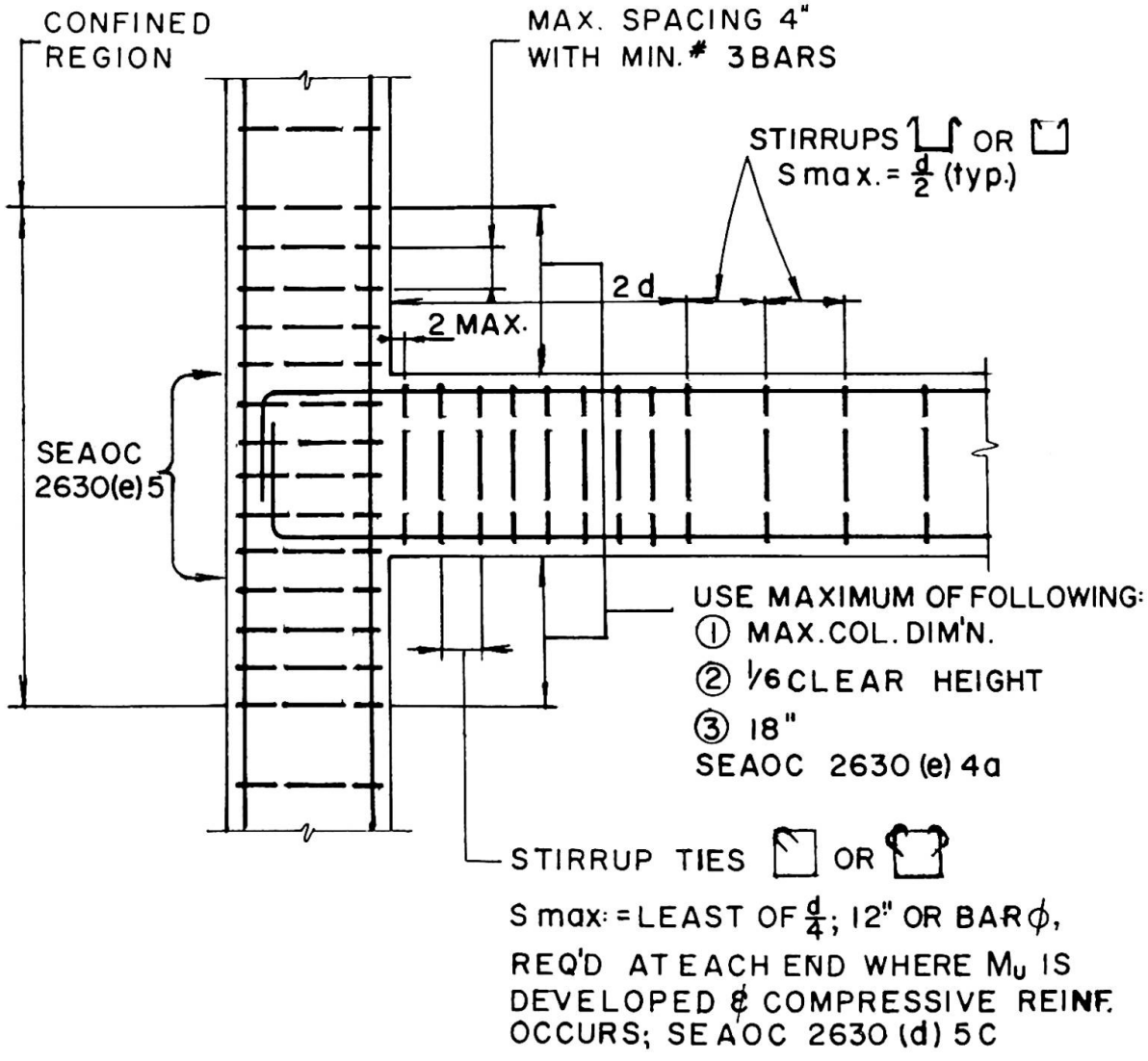

FIG. 2

COLUMN - BEAM JOINT REINFORCEMENT

WEB REINFORCEMENT MIN. # 3 BARS IN ACCORDANCE WITH ACI, CHAPTER 17 --- SEAOC 2630(d)5

M_U^A & M_U^B = ULTIMATE MOMENT CAPACITY OF MEMBER OF OPPOSITE SENSE.

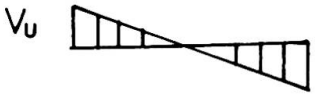

$$V_U \geq \frac{M_U^A + M_U^B}{L} + 1.4\,V(D+L)$$ --SEAOC 2630(d)5a(30-5)

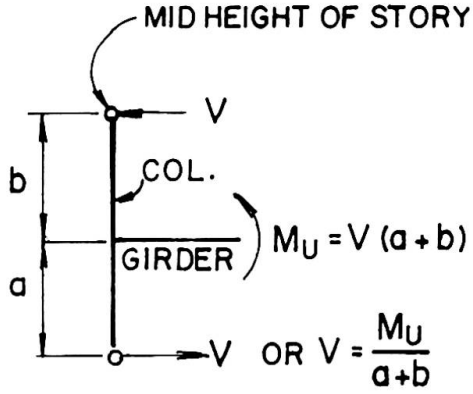

$V_U = T - V$ ---------- SEAOC 2630 (C) 5

DESIGN IN ACCORDANCE WITH ACI 318 CHAPTER 17, SPECIAL TRANSVERSE REINFORCEMENT REQ'T MAY GOVERN... SEAOC 2630 (C) 4

FOR COLUMNS WITH GIRDER FRAMING ON ALL FOUR SIDES ONE HALF OF THE SPECIAL TRANSVERSE REINFORCEMENT IS REQUIRED.

FIG. 3

GIRDER - COLUMN JOINT ANALYSIS

$$V_U = \frac{M_U^T + M_U^B}{h} \quad \text{OR} = \frac{M_U^B + \frac{1}{2} M_b}{h} \quad \text{— — — — — — — — — — SEAOC 2630 C(6) 30-9 / 30-8}$$

(OMIT FACTOR $\frac{1}{2}$ FOR ONLY ONE COLUMN IN TOP CONNECTION.

$V_U = V_C = A_v f_y \frac{d}{s}$ — — — — — — — — — — SEAOC 2630 (e)6 30-7

WHERE $V_C = v_c bd$ — — — — — — — — — — ACI 318 CHAPTER 17

EXCEPT FOR $\frac{P}{Ag} < 0.12 f'c$, $V_C = 0$.

A_V = TOTAL AREA OF TRANSVERSE REINF. IN TENSION WITHIN DISTANCE BETWEEN TIES

FOR SPIRALS USE $^2/_3$ A_V — — — — — SEAOC 2630 (e) 6

FOR SPIRALS:

MIN. VOLUME SPIRAL $P_s = 0.45\left(\frac{Ag}{Ac} - 1\right)\frac{f'c}{fy}$ - ACI 913 (b) (9-1)
BUT NOT LESS THAN REQUIRED BY — — SEAOC 2630 e (6)

FOR HOOPS:

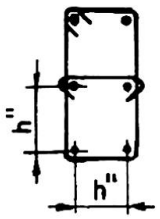

MIN.: 2 P_s
SUPPLEMENTARY CROSS TIES; NOT TO EXCEED 25% OF TOTAL TIE VOLUME ¢ SHALL HAVE STANDARD HOOKS AND ENGAGE EXTERIOR HOOP ¢ VERTICAL BAR.

$h'' < \frac{2A''_{sh}\, f_y'' h}{p'' a f_y''}$ — — — — — — — SEAOC 2630 (e) 6 30-6

IF $h'' <$ MAX. COLUMN DIMENSION, PROVIDE NECESSARY OVERLAPPING HOOPS — SEAOC 2630 (e) 4 C

FIG. 4

ANALYSIS FOR COLUMN TRANSVERSE REINFORCEMENT

6. Only intermediate grade reinforcing steel (A-15, 40,000 psi yield point) shall be used in flexural members. (This restriction will be lifted as soon as the ductility requirements of high strength steel will be guaranteed.) Higher strength steel (A-432, 60,000 psi yield point) may be used in columns.

7. Compact sections are prescribed both for columns and beams.

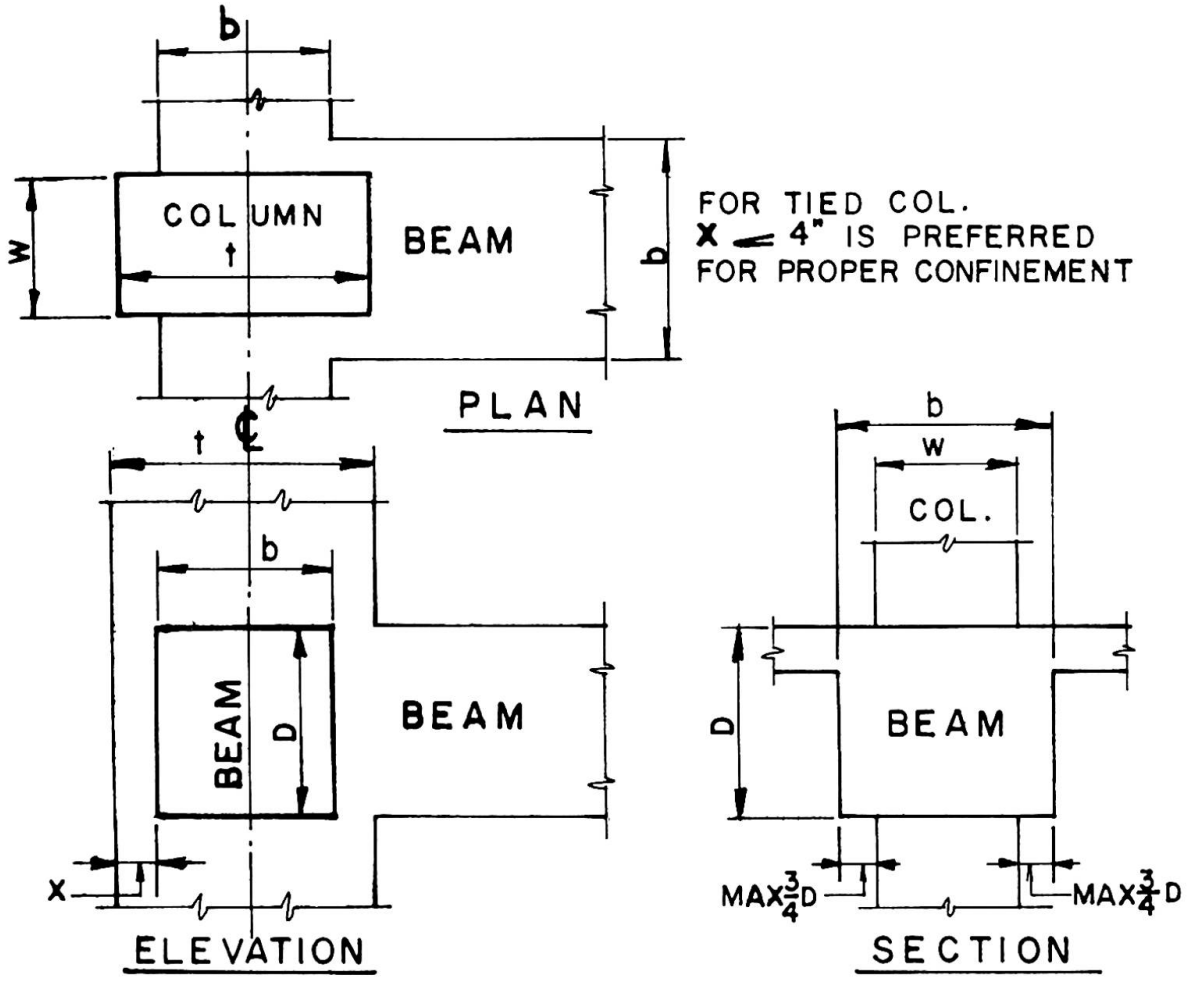

BEAMS: $\frac{b}{D} \geq 0.4$

OR 10" $\leq b \leq$ W + MAX.($\frac{3}{4}$D) EACH SIDE OF COLUMN__SEAOC 2630(d)1

$b \geq \frac{3}{4}t$ OR $\frac{3}{4}$ W (RECOMMENDED) _ _ _ _ _ _ _ _ _ _ _ _ SEAOC 2630(e)40

COLUMN: $\frac{W}{t} \geq 0.4$

W OR t OR ϕ OF ROUND COL. $\geq$ 12" _ _ _ _ _ _ _ _ _ _ SEAOC 2630(e)1

DESIGN: FOR $\frac{P}{Ag} \geq 0.12 f'_c$ WHERE Ag = (W) (t)

M_U OF COL. WITH $P > M_U$ OF BEAMS. FOR $\frac{P}{Ag} < 0.12 f'_c$ COLUMN SHALL CONFORM AS FLEXURAL MEMBER _ _ _ _ _ SEAOC 2630(C)7

FIG. 5

SEAOC CODE LIMITATIONS ON FRAME DIMENSIONS.

8. The requirements under (7.) eliminate, until further studies are conducted, the use of flat slabs and flat plates as systems of unproven ductility.

9. In order to avoid brittle failures, not only minimum but also maximum reinforcements are prescribed.

10. Extreme attention is to be given to splices and anchorages.

11. Shear walls must be provided with strong boundary members designed to carry all vertical loads attributed to the shear walls including overturning axial forces. Thus, in case of failure of a shear wall during an earthquake, the boundary members would take over and insure safety against collapse.

CONCLUSIONS

The recently adopted Code provisions of the SEAOC permit now the construction of reinforced concrete high-rise buildings. (Previously only buildings less than 160 ft. in height could be built of reinforced concrete.) The writer has designed a 21-story medical building and a 26-story office building using the ductile frame reinforced concrete principles as described in this discussion.

SUMMARY

Reinforced concrete high-rise buildings in seismic areas have to be designed and constructed differently from the customary types described in the author's presentation. This discussion attempts to describe the present state of art for earthquake resisting high-rise buildings in the Western States of the United States.

RÉSUMÉ

Les bâtiments élevés en béton armé situés dans des zones sismiques doivent être projetés et construits différemment des types habituels décrits par l'auteur. La discussion essaye de faire le point sur les méthodes actuelles employées dans l'Ouest des Etats-Unis pour des bâtiments élevés résistants aux secousses sismiques.

ZUSAMMENFASSUNG

Hohe Stahlbetongebäude in Erdbebengebieten müssen anders als die üblichen, in des Verfassers Darstellung beschriebenen Typen entworfen und durchgeführt werden. Dieser Beitrag versucht, in den derzeitigen Stand der Bauweise erdbebensicherer, hoher Gebäude in den Weststaaten der USA Einblick zu geben.

Leere Seite
Blank page
Page vide

Design of Tall Buildings of Lightweight Superstructure

Projection de bâtiments élevés de construction légère

Entwurf hoher Gebäude im Leichtbau

JOHN DE BREMAEKER
M.I. Struct.E., F.A.S.C.E.

R.N.H. TOFTS
A.M.I.C.E., A.M.I. Struct.E.

London, England

Introduction

Generally the floors in tall buildings are repetitive due to the shape of the structures. Table 1 gives an analysis of the estimated weights of the various components within typical floors of several buildings in London.1, 2, 3.

These buildings are approximately 35 storeys high with the exception of Moor House, which is 19 storeys high. It can be seen that the dead weight of the structure is 50 - 60% of the total weight and is thus by far the largest single item. Possible savings in weight on cladding, finishes and partitions are likely to be small in comparison with savings in dead weight of structure.

The average weight of structure of a typical floor including walls and columns is approximately 140 lbs/sq.ft. for a reinforced concrete frame 35 storeys high. The floor slabs vary in weight from 50 lbs/sq.ft. to 110 lbs/sq.ft. for spans up to 30 ft. with superloads of 80 lbs/sq.ft. including demountable partitions.

Those structures with light floors generally have a greater weight of walls and columns which yields a remarkably uniform average weight of structure. For lower structures of 20 storeys with spans up to 20 ft. the overall weight is approximately 120 lbs/sq.ft. and the slab weighs 85 lbs/sq.ft.

Table 1 - Weights of Tall Buildings.

	STAG PLACE		MILLBANK		DRAPERS GDNS		EUSTON CENTRE		MOOR HOUSE	
	weight lbs/ft^2	%	weight lbs/ft^2	%	weight lbs/ft^2	%	weight lbs/ft^2	%	weight lbs/ft^2	%
FLOOR SLAB	75	27.3	76	30.0	105	39.0	101	41.0	85	37.2
WALLS	60	21.8	48	18.7	37	13.8	17	6.8	22	9.6
COLUMNS	13	4.7	21	8.2	6	2.3	3	1.2	9	4.2
EXTERNAL CLADDING	20	7.3	10	3.9	14	5.4	9	3.6	10	4.2
FINISHES FLOORS CEILINGS	27	9.8	23	9.0	27	10.0	34	13.7	27	11.8
PARTITIONS	20	7.3	27	10.6	20	7.5	34	13.7	25	11.0
SUPERLOADS	60	21.8	50	19.6	60	22.0	50	20.0	50	22.0
TOTAL	275	100.0	255	100.0	269	100.0	248	100.0	228	100.0

Methods of reducing the dead weight of superstructure

Reduction in dead weight may be accomplished by the following:-

1. Use of high strength materials, i.e. high grade concrete, high tensile reinforcement or prestressed and/or precast concrete. These invariably cost more than average strength materials in common use, but reduction in weight and size may compensate.

2. The use of deeper structural sections of reduced thickness, i.e. ribbed and waffle slabs or open web joists. The deeper section increases the strength with very little increase in the weight. Increased fabrication costs are normally involved.

3. Use of lightweight materials of comparable strength to conventional materials i.e. lightweight concrete, plastics and aluminium. These usually cost more than their equivalent volume of conventional material, but the saving in weight may enable these costs to be recouped.

4. Reducing the floor spans, thus reducing the thickness of the floor. This technique is obviously limited as present day requirements are for open floor areas without supports.

5. Using the stiffness of the structural frame to withstand the horizontal loads without increasing the size of the members as determined by consideration of the vertical loads i.e. accommodating the stresses due to horizontal loads within the permitted 25% overstress (U.K. Standards).

6. The use of lightweight fire protection to structural steelwork in lieu of solid protection.

7. Special design techniques i.e. suspended structure where hangers may be used in lieu of columns and whole building loads ultimately supported on the core walls.

Factors to be balanced against savings in dead weight

Dead weight savings on structure are always desirable but must be reconciled with the other functions and also letting of the building. The importance of the latter is sometimes lost on engineers concerned primarily with structural design, but is vitally important to the client. The following factors should be balanced against the reduction in weight:-

a. Site Cost.
b. Building Cost.
c. Area of space available for letting.
d. Amenity values which may increase the prospect of letting.
e. Serviceability of the building.
f. Speed of construction.
g. Sound insulation and vibration.

TYPES OF STRUCTURE SUITABLE FOR LIGHTWEIGHT CONSTRUCTION AND EXAMPLES

a. Flat Plate Construction. In this type of construction the floors are designed as solid plates which act with columns to form a multi-storey rigid frame. The height for which this type of building is suitable is limited by the stresses within the plate floor and the deflections of the frame horizontally. Buildings up to 20 storeys can be constructed in this way, but the thickness of floors and the quantities of reinforcement required tend to make flat plate frame construction uneconomic above this limit.

The design imposes certain restrictions and advantages namely:- the external columns should be preferably inset from the face of the building; floor openings adjacent to the columns should be restricted; lightweight cladding should be used; the building should be preferably at least three bays wide to develop adequate lateral stiffness; the bay sizes should be approximately square. The compensations are that the elevators and staircases may be placed in any position; the shape of the building is not restricted; the construction is extremely simple, no shear walls are necessary, and it provides a flat soffite to the floors which may be plastered direct without false ceilings. It also reduces floor thickness to a minimum.

The trend today is to construct these buildings with light-weight concrete with a density of approximately 100 lbs/cu.ft. which reduces floor and column loadings, resulting in more economic design. In the U.K. buildings are often restricted in height and cubic content and therefore this form of construction, which takes up as little floor depth as possible, is often essential to obtain the maximum number of floors and therefore lettable area.

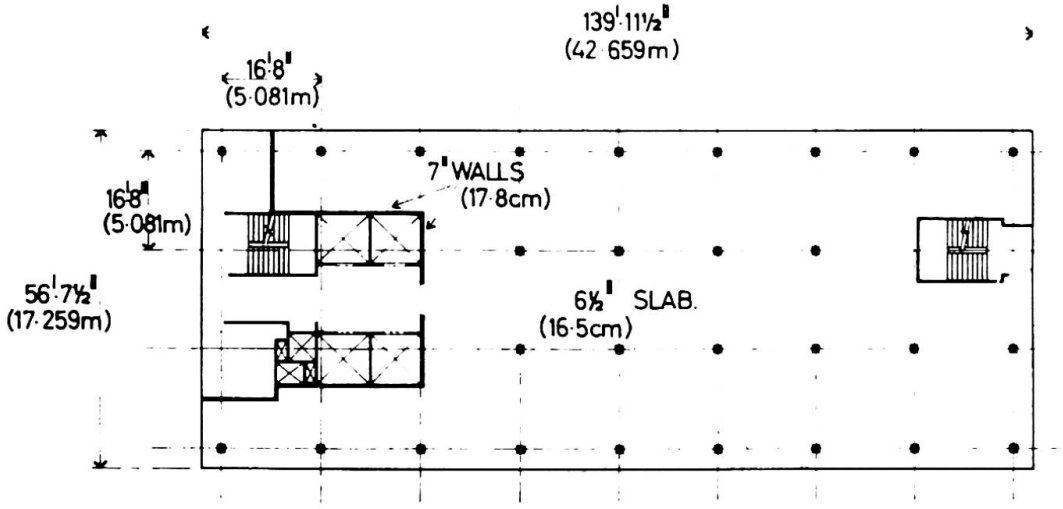

Fig. 1. MOOR HOUSE – TYPICAL FLOOR PLAN

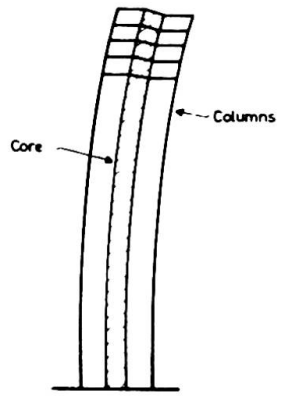

Fig. 2 FREE CANTILEVER

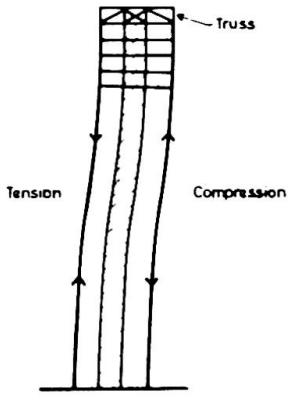

Fig. 3 TIED CANTILEVER
COLUMN – CORE INTERACTION

Figure 1 shows the floor construction of Moor House, London, 228 ft. high, and illustrates the principles outlined above. The floors are of normal gravel aggregate concrete and are only 6½ ins. thick. No column heads are provided.

b. Central Core Construction, with External Edges of Floor supported on either columns or hangers. The utilisation of the central core to withstand all lateral loads is becoming standard technique in buildings constructed in the U.K. up to 450 ft.high. Above this height the cores are rarely large enough to limit the lateral deflection of the building without increasing the thickness of the walls and columns as designed for vertical loading. The core supports a high proportion of the vertical loads of the

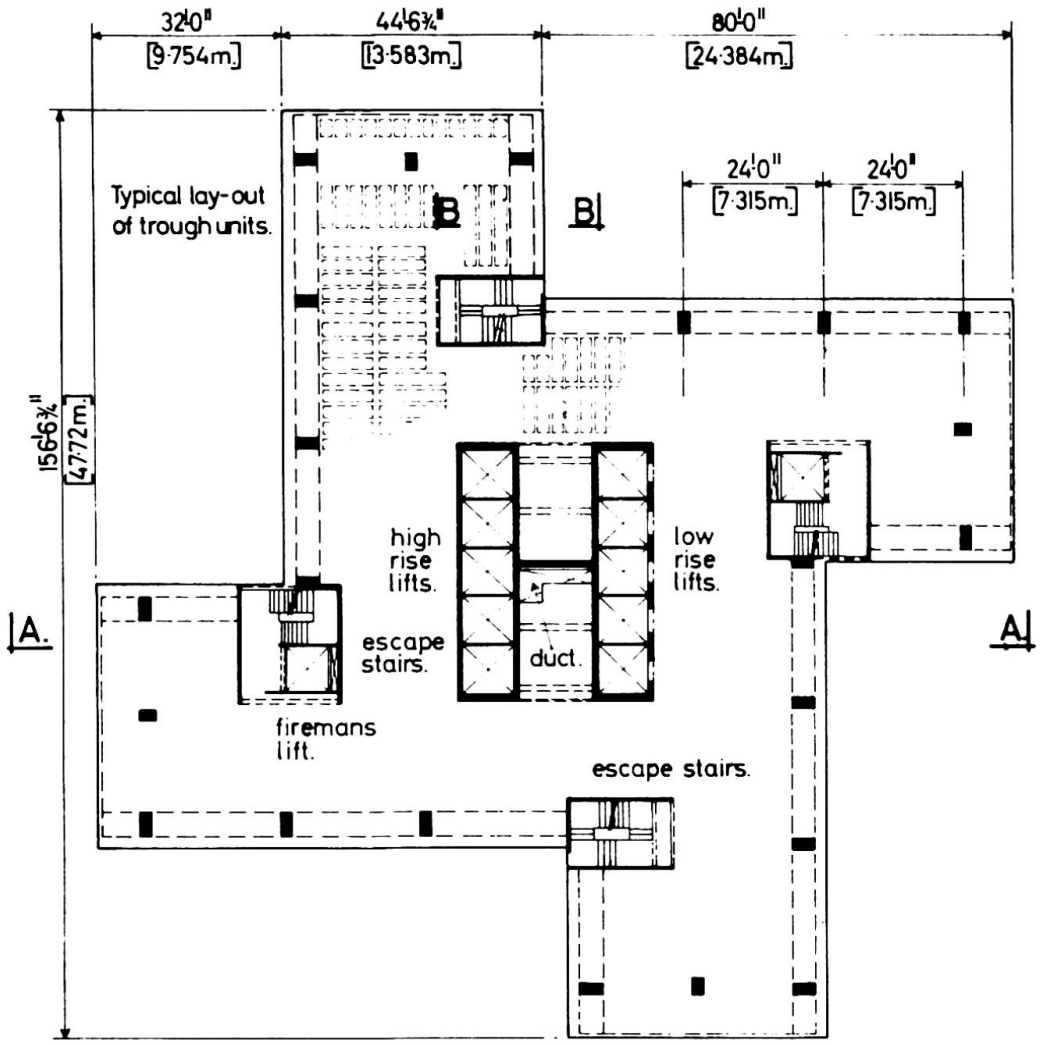

Fig. 4. – EUSTON CENTRE
TYPICAL FLOOR PLAN.

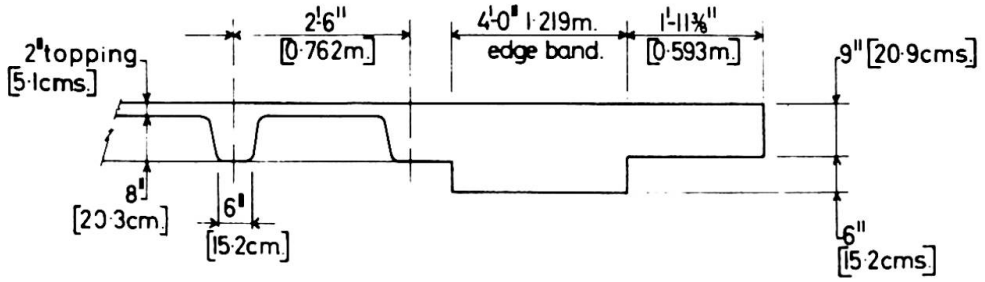

SECTION B-B.

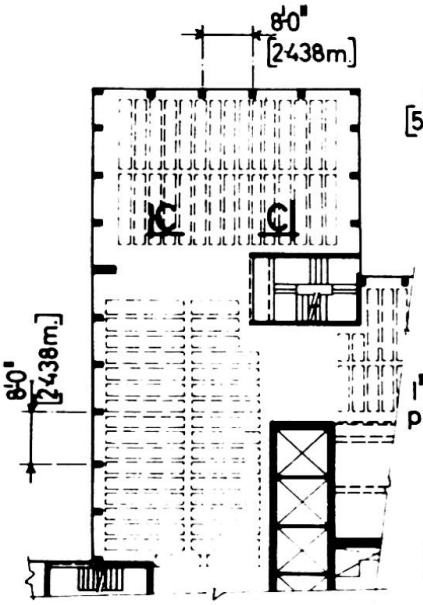

Fig.5. ALTERNATIVE FLOOR LAYOUT.

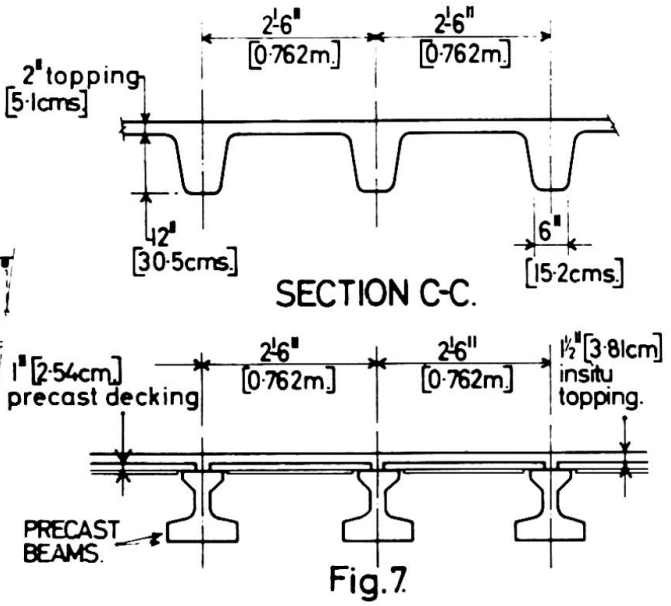

Fig.7.

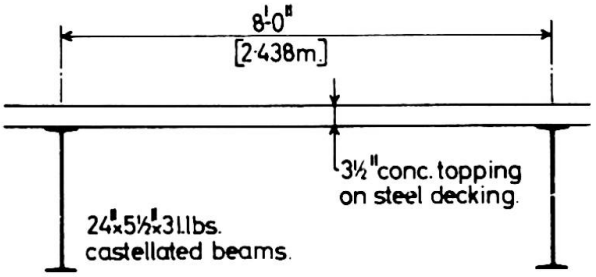

Fig.6.

Table 2 - Comparisons of alternative floor construction for Euston Centre

Case No.	Layout Fig.No.	Section Fig.No.	Ribbed Areas Wt. lbs/sq.ft.	Weight lbs/sq.ft.	% Weight	% Cost
1.	1	B - B	52	92	100	100
2.	1	-	38	64	70	107
3.	5	C - C	65	87	95	107
4.	5	C - C	48	64	69	108
5.	5	7	56	82	89	123
6.	5	6	-	42	46	125 *

* Excluding fire protection.

building thus fulfilling three functions i.e. vertical support, lateral support and service enclosures. The columns or hangers support vertical loads only, so that they may be designed to a minimum cross section and occupy as little floor area as possible.

The 35 storey Euston Tower, which is approximately 428 ft. high illustrates the principle of central core design with the external edges of the building supported on high strength (6,500 lbs/sq.in.) concrete columns. The core area and structure is limited so that 85% of the overall building area is usable.

Alternative floor constructions considered are shown on Figures 4,5,6 & 7 and Table 2.

Case 1 was in fact used and constructed using plywood formers and table forms. It provided a reasonably light structure with a minimum of reinforcement (8.5 lbs per sq.ft. including walls and columns) and a strong insitu structure to distribute lateral loads. The floor depth for the main floor areas was only 10 inches.

Case 6 using steel decking and beams was the lightest form of construction but was unacceptable due to the depth of floor construction and high cost.

Cases 2 & 4 using lightweight concrete were attractive but produced shear problems and required greater floor thickness than Case 1.

Case 3. The inclusion of structural mullions would have entailed large transfer girders at second floor level, which would have been expensive and were undesirable architecturally.

Case 5 using composite construction was more expensive than insitu construction with an increased floor thickness. Also it did not provide as rigid a structure as insitu construction and would have required a transfer girder at second floor level.

Suspended Structures

In this type of design the edges of the floors are supported by steel hangers, which are connected to cantilever trusses at the top of the building. These cantilever trusses are supported by a large central core. This arrangement produces the minimum area of external columns and provides additional dead load in the core to prevent tensile stresses being developed due to wind or lateral loading. The advantages of the method are that the contractor has the plant rooms available at an early stage in the contract, the floor space is uninterrupted by columns and there is a clear space at ground floor level which may be used for storage and access. It also allows a flexible ground floor layout. Due to the method of erecting the building from the top downwards, it is usual to build the structural floor of steel deck and castellated or lattice beams to avoid the need for formwork. Floor depths are greater than flat slab construction and building costs are usually slightly higher than an equivalent simple structure with columns.

Two examples of this form of construction are the Commercial Union Building and 20-23 Fenchurch Street, London. The difficulties of brittle fracture of the high strength steel trusses found in the latter seem to have been overcome in the P. & O. Building by using smaller made-up sections, which can be normalised instead of heavy welded Universal columns.

c. Central Core + Frame Action for Buildings over 400 ft. It is not normally economic to take all the lateral forces on the core as a vertical cantilever over 400 ft. tall, unless the core is very large; even if this is done, some account must be taken of secondary stresses induced in the remainder of the structure by consideration of the deflection of the structure. One variation is to allow the floor and columns to act integrally with the core to increase its stiffness. This solution is only practicable if the arrangement of the structural framing allows the stresses to be absorbed economically and is generally used in steel framed buildings. An alternative for reinforced concrete flat slab framed buildings is to provide trusses or beams at roof level to which the external columns are connected as shown in Figs. 2 & 3. This allows transfer of some of the tensile stresses which would otherwise develop in the core, to the external columns and therefore utilises more fully the total depth of the building. One example is Moorfields, London, 444 ft. total height and 36 storeys high, where the overall size of the floors were 66 ft. 9 in. x 202 ft. 9 in. and the core width only 21 ft.[4]

d. Hull Core Structures, where the external frame forms a hollow space tube and acts in conjunction with a central core.

No buildings, to our knowledge, have been erected in the U.K. which fall into this category, but several have been constructed in the U.S.A. One example is the World Trade Centre, New York, which is 1,350 ft. high. The principle is to use the external cladding not only to carry vertical loads but also to resist horizontal loads as a perforated box. It has the advantage that the internal floors can be constructed to give uninterrupted spans.

The external hull can be constructed in a variety of forms, either as a series of close centre mullions connected by beams at floor levels to form a series of inter-connected, very stiff portal frames, or, as a diagonal open lattice frame. The latter is particularly economical structurally since the forces within the cladding are mostly axial and result in high efficiency.

If the external cladding is constructed in steel as part of the curtain walling, it will be light in weight. If the floors are also constructed in steel joists and deck the resulting structure will be light in weight and capable of spanning 40 ft. clear without much difficulty.

This type of construction is particularly suitable in the United States where large floor areas are required and building heights are much greater than those permitted by the Planning Authorities in the U.K.

A variation on the hull core structure for buildings up to 400 ft. high is to omit the central core and use only the

external wall frame to resist wind forces. The advantage is that flat slabs may be used within the building without the encumbrance of internal concrete walls, which would slow up progress of construction on site. e.g. The 42 storey DeWitt Apartments.[5]

DESIGN OF COMPONENTS

a. Floors

The two most favoured forms of floor construction are ribbed slabs, either precast or in situ, constructed as part of a floor of uniform thickness or a steel deck floor with concrete topping supported on steel joists. The former is most used in the U.K. as it is more economical for spans up to 30 ft. Generally storey heights are approximately 10 ft. 6 in. as against 12 ft. for steel deck and beam construction. In a 35 storey block another five floors can be built within the same building envelope using a ribbed slab instead of a steel deck and beam floor.

The relative costs of the two forms of construction vary according to the country in which they are built, since the ratio of labour and material costs vary considerably. The cost per sq.ft. of floor area of the steel in a steel framed structure as built in the U.S.A. or Canada would vary from 30/- to 50/- based on U.K. costs. Cost per sq. ft. of equivalent concrete building would be 20/- to 35/-.

A ribbed floor in normal gravel aggregate concrete 10 ins. thick weighs approximately 50 lbs/sq.ft. whereas a steel deck with concrete topping weighs only 35 lbs/sq.ft. If lightweight concrete were used in a ribbed floor the weights would be almost identical. The average weight of a floor incorporating ribs is much higher than might be expected because heavier solid strips have to be provided at the edges to support the ends of ribs and transfer loads back to the columns. It would seem unlikely that the dead weight of floor construction could ever be reduced much below 40 lbs/sq.ft. since a minimum thickness of floor would be required to provide mass to damp vibration and prevent undue sound transmission through the floors.

For long spans, prestressed concrete double T beams or I beams used at 2 ft. 6 in. to 3 ft. centres with precast planks provide a rapid method of erection. So far, the use of precast elements in tall buildings has not proved as successful in speeding up erection times as could be hoped. This is largely due to the labour required in propping, making and pouring insitu portions between precast elements and making joints, and also because the core areas often determine the speed of erection. As floors act as horizontal diaphragms to transfer lateral loads back to the core, it is essential that they have rigidity and any precast scheme must be carefully detailed to provide this. Shear heads should be avoided by the use of shear reinforcement either in the form of channels, collars or flat plates providing mechanical support, or diagonally inclined "snake" reinforcement in rings round columns.

b. Columns

To avoid the introduction of heavy beams or strips spanning between columns at the edges of the building, load bearing

mullions at close centres may be used which do not project as far into the building as columns at greater centres and therefore do not break up the building area.

In order to reduce floor spans, columns may be inset a small distance to enable vertical service ducts to pass between column and cladding as shown in the Euston Centre. In this case the columns are designed in high strength concrete but even so are comparatively large in the lower storeys. At least one building (Drapers Gardens, London) has been constructed with solid steel columns (billets) to achieve the lightest weight and smallest amount of floor space occupied by columns. However, the increase in cost due to the billets is considerable and these should be carefully balanced against the increase in income due to the difference in lettable areas between concrete and steel columns.

c. Vertical Service Cores

These should be simplified as much as possible to enable them to be formed by slip-form or rapidly demountable large formwork panels; complicated core sections will slow down progress in the building as a whole. Small internal variations are most economically built in blockwork. The upper parts of the service core can be cast in lightweight concrete and in the lower parts the use of high strength concrete is essential to limit the wall thicknesses. Fire escape staircase enclosures can also contribute to the lateral strength of the building provided that this can be transmitted to the foundations. Unfortunately architectural requirements often prevent their being taken down to ground floor level.

d. Cladding

The lightest form of cladding is glass curtain walling amounting to within 3% - 4% of the total dead weight. The back-up wall to the curtain walling should be constructed in a light-weight, fire resistant material or wood-wool, rather than concrete or brickwork which has a greater density. Curtain walling has a further advantage in that it occupies a minimum thickness of wall, increasing the amount of floor area available for letting. This assumes that the exterior face of the building is fixed by the building line.

FACTORS AGGRAVATED BY LIGHTWEIGHT CONSTRUCTION

a. Thermal Movement

There is a faster build up of heat in exposed lightweight materials on the external face of the building which produces differential movement between the core and external columns. This can be overcome by making special provision in the structure to allow movement to take place, possibly by pin joints in the upper floors, or by inserting trusses to redistribute stresses between external columns. Internal partitions must be designed to allow a certain amount of distortion to take place in the frame. One method of minimising differential movement is to provide insulation to the external faces of columns to prevent such a rapid build-up. Careful detailing is required for glazing which fits between structural members of this type.

Thermal movement within the floor structure is usually

easily accommodated and in fact, the use of lightweight concrete does help to reduce this.

If columns are set on the periphery they will be fully or partially exposed and therefore subject to temperature movement, which is considerable in buildings over 400 ft. high. The columns on one face of the building will expand or contract at a much greater rate than its core or columns on the other face. This will tend to crack the partition walls and possibly the structure, if excessive. Measurements taken on tall buildings give a differential movement of between .34 in. - 1.12 in. on structures varying between 200 ft. and 450 ft.; the amount of movement varying according to the height of the building and degree of exposure of the columns. The greater the degree of exposure, the greater the differential. Some cracking where the partitions join the external columns has been noted on existing buildings, although no structural damage has been recorded, probably because the ratio of depth:span did not exceed L/200. The reasonable limit for temperature movement seems to be approximately $\frac{3}{4}$ in. up or down from the horizontal position, assuming a clear floor span of 35 ft.[5]

b. Shrinkage

Lightweight aggregate concrete has a higher shrinkage rate than conventional gravel aggregate concrete and therefore adequate tensile reinforcement must always be included to control cracking.

c. Deflection

Generally lightweight concrete structures give rise to greater deflections than conventional structures due to their lower modulus of elasticity. There has been considerable research into the properties of lightweight concrete. This suggests that initial fears that the span:depth ratio would have to be adjusted to allow for the lower modulus are unfounded, provided that the stress in the reinforcement is not increased above 27,000 lbs/sq.in. The reduction of dead weight on the structure may give rise to tensile forces within the core and unacceptable horizontal deflections. In most practicable types of structure the height:width ratio is sufficient to avoid these difficulties. Reduction in weight also serves to decrease the damping effect of the building in its response to gusting of wind, although generally the likelihood of dangerous oscillations is improbable for conventional buildings up to 600 ft. unless very slender and with $ND<25$. (Where N is the natural frequency and D a typical cross section dimension.)

d. Sound Insulation

Lightweight structures and partitions allow greater sound transmission, which although acceptable in offices, would not be so in apartments. For this reason apartments are often constructed with solid plate floors to avoid too high a noise level. In offices, false ceilings help to reduce the level of airborne sound and the insertion of glass quilt under floors will reduce the transmission of structure-borne sound. In the case of plant rooms an acceptable solution seems to be to provide a thick concrete raft which rests on a layer of insulation material which

will not transmit most of the troublesome frequencies of vibration from the plant above. If further insulation is required, wood-wool slabs may be suspended from the ceiling underneath.

References:-

1. Davies, C. Structural Engineering aspects of the Millbank Tower Block. The Structural Engineer - January 1962.

2. Mason, J. & Frost,A.D. Stag Place Development. The Structural Engineer - November 1963.

3. Frischmann, W.W., Brown, G.S., & Prahbu S.S. Features in the design and construction of Drapers Gardens Development. The Structural Engineer - February 1967.

4. Backman,P. & Dunican, P. The use of shear walls in high buildings. Tall Buildings edited by A. Coul & E. Stafford Smith. 1967.

5. Khan, F.R. & Fintel, M. Effects of column exposure in tall buildings. Journal of the A.C.I. - February 1968.

SUMMARY

The paper considers various designs suitable for lightweight superstructure, typical weights of differing construction and factors affecting the design of structural components.

RÉSUMÉ

Ce document envisage différentes conceptions convenant à des super-structures extrèmement légères, les poids types de constructions différentes et les facteurs affectant le dessin des componants structurels.

ZUSAMMENFASSUNG

Das Referat befaßt sich mit verschiedenen Entwurfen, die für leichte Aufbauten geeignet sind, sowie mit charakteristischen Gewichten verschiedener Konstruktionen und Faktoren, die den Entwurf von Bauteilen beeinflussen.

Influence Lines for Shear around Columns in Flat Plates

Les lignes d'influence d'efforts tranchants autour des colonnes aux dalles plates

Einflußlinien für Schub im Stützenbereich von Flachdecken

PAUL E. MAST
Dr.Eng.
Manager, Design Research Section
Portland Cement Association
Skokie, Illinois USA

Introduction

Shear stresses near columns in flat plate structures are caused by the column reaction. This reaction can be subdivided into a force, V_v, acting perpendicular to the plate and into a moment, M, whose vector is parallel to the plate. Only a portion of this moment, M, is transmitted to the plate by shear stresses. The remainder is transferred by bending stresses (Fig. 1).

The stress concentrations resulting from the above reactions often govern the design, i.e., they determine the required plate thickness and column periphery. It is the purpose of this paper to contribute to the evaluation of these stress concentrations.

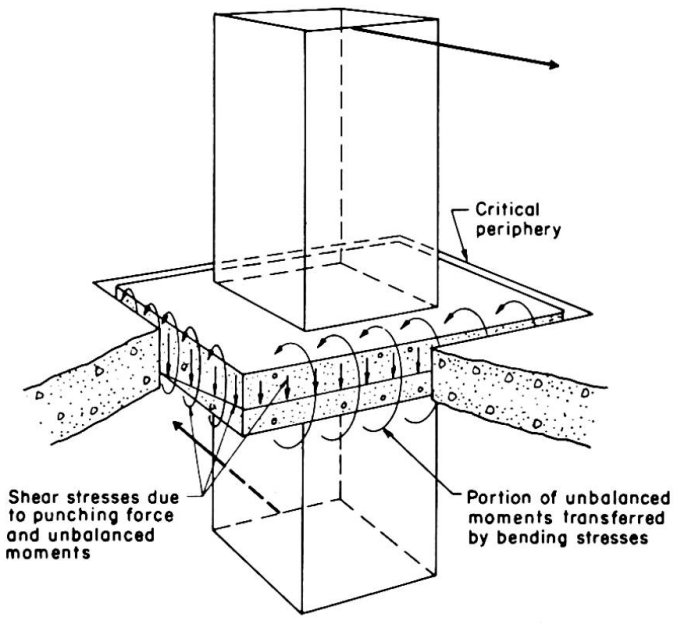

FIG. 1 TRANSFER OF UNBALANCED MOMENT

The moment transfer in the vicinity of columns has been investigated in extensive test programs [1 through 6]. While these tests resulted in design methods developed on a hypothetical basis [6 through 9], they did not reveal precisely which portion of the unbalanced moment is transferred by bending stresses and which portion by shear. The design methods commonly used in the USA [8, 9, 12] assume the moment transfer by shear to take place in accordance with the equation

$$v = \frac{V_v}{A_c} + \frac{KM}{J_c} e \qquad (1)$$

V_v = Total punching shear force

M = Total unbalanced moment

K = Percentage of unbalanced moment transferred by shear

A_c = Area of failure plane

J_c = Polar moment of inertia of failure plane

e = Distance from shear centroid to point on failure plane

Experimentally determined values for K, A_c and J_c vary and are available in tabulated form [9, Table 8-6]. The following is an approach to determine these values analytically and to evaluate the resulting shear stresses by means of influence lines.

An Analytical Method to Determine K

The deflection function of a simply-supported single-span plate strip, subject to a concentrated moment, is known [10].

$$w = \frac{M\,a}{2D\pi^2}\sum\frac{1}{n^2}\cos\frac{n\pi u}{a}\left(1+\frac{n\pi y}{a}\right)e^{-\frac{n\pi y}{a}}\sin\frac{n\pi x}{a} \tag{2}$$

Visualizing the plate supported by flexible columns at its center and applying the concentrated moment by one of these columns (Fig. 2), one can write a similar deflection function

$$w = M\frac{L}{D\pi^2}\sum_{n=1,2,3}\frac{1}{n^2}\cos\frac{n\pi}{2}\left(1+\frac{n\pi y}{2L}\right)e^{-\frac{n\pi y}{2L}}\sin\frac{n\pi(L+x)}{2L} \tag{3}$$

The boundary conditions at the remote columns are satisfied by this equation only partially. This, however, does practically not affect the stress configuration in the vicinity of the column at which the unbalanced moment is applied.

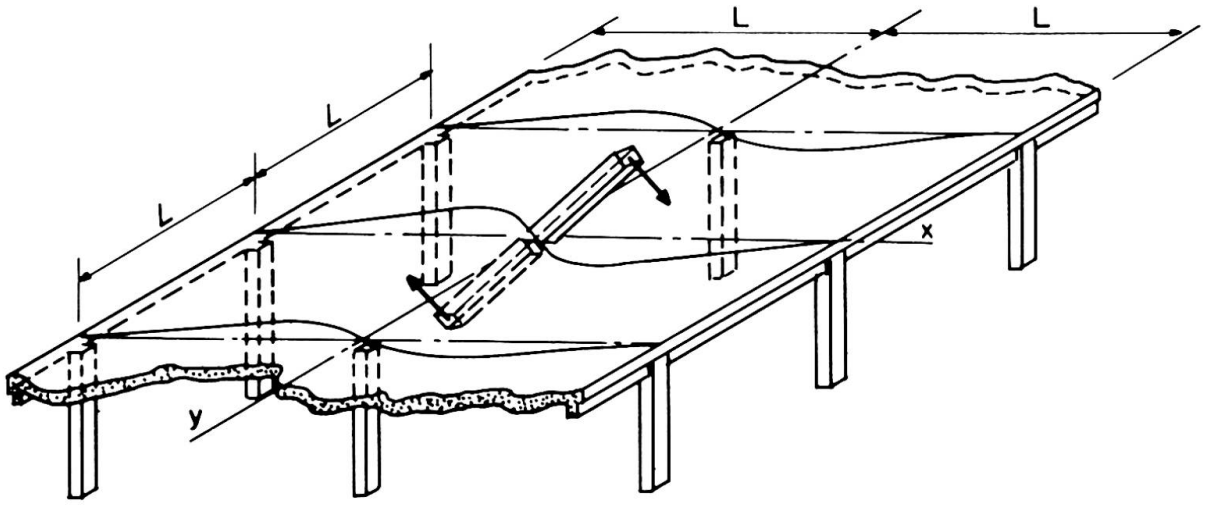

FIG. 2 CONCENTRATED MOMENT APPLIED TO FLATE PLATE

The series represented by Equation 3 converges slowly and, hence, is of limited practical use. It can be summed up, however, by means of transcendental functions [11], similar to the deflection function of a simply-supported plate strip [10]. We first determine the derivatives of the deflection function, w, with respect to the x and the y axis in closed form, and then the expressions for all bending and twisting moments and for the shear forces. It should be noted that simple expressions for the latter ones can be obtained best by determining $\partial(\Delta w)/\partial x$ and $\partial(\Delta w)/\partial y$, respectively.

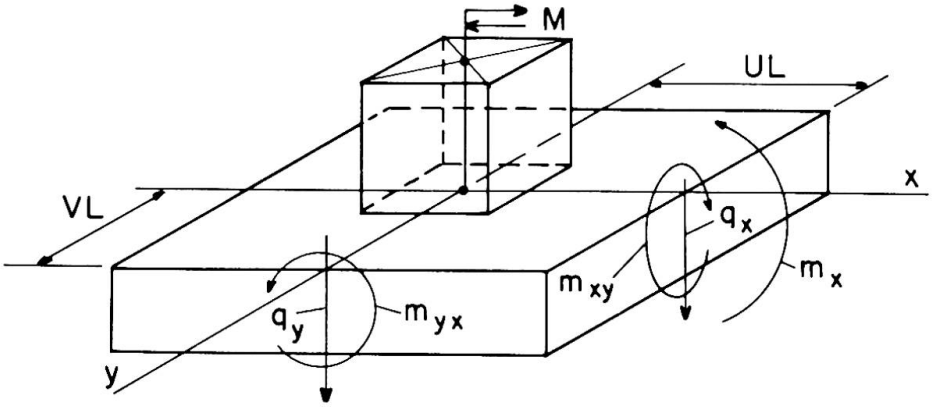

FIG. 3 SHEARS AND MOMENTS AROUND COLUMN

$$\frac{\partial w}{\partial x} = \frac{-M}{8D\pi}\left\{\log\left[2\cosh\frac{\pi y}{2L} + 2\cos\frac{\pi x}{2L}\right] + \log\left[2\cosh\frac{\pi y}{2L} - 2\cos\frac{\pi x}{2L}\right]\right.$$

$$\left. - \frac{\frac{\pi y}{2L}\sinh\frac{\pi y}{2L}}{\cosh\frac{\pi y}{2L} + \cos\frac{\pi x}{2L}} - \frac{\frac{\pi y}{2L}\sinh\frac{\pi y}{2L}}{\cosh\frac{\pi y}{2L} - \cos\frac{\pi x}{2L}}\right\} \tag{4}$$

$$\frac{\partial w}{\partial y} = \frac{M}{16D}\left(\frac{y}{L}\right)\sin\frac{\pi x}{2L}\left\{\frac{1}{\cosh\frac{\pi y}{2L} + \cos\frac{\pi x}{2L}} - \frac{1}{\cosh\frac{\pi y}{2L} - \cos\frac{\pi x}{2L}}\right\} \tag{5}$$

$$m_x = -D\left(\frac{\partial^2 w}{\partial x^2} + \nu\frac{\partial^2 w}{\partial y^2}\right)$$

$$= \frac{M}{16L}\left\{(1+\nu)\left[\frac{-\sin\frac{\pi x}{2L}}{\cosh\frac{\pi y}{2L} + \cos\frac{\pi x}{2L}} + \frac{\sin\frac{\pi x}{2L}}{\cosh\frac{\pi y}{2L} - \cos\frac{\pi x}{2L}}\right]\right.$$

$$\left. + (1-\nu)\left[\frac{-\frac{\pi y}{2L}\sinh\frac{\pi y}{2L}\sin\frac{\pi x}{2L}}{\left(\cosh\frac{\pi y}{2L} + \cos\frac{\pi x}{2L}\right)^2} + \frac{\frac{\pi y}{2L}\sinh\frac{\pi y}{2L}\sin\frac{\pi x}{2L}}{\left(\cosh\frac{\pi y}{2L} - \cos\frac{\pi x}{2L}\right)^2}\right]\right\} \tag{6}$$

$$m_{yx} = m_{xy} = -D(1-\nu)\frac{\partial^2 w}{\partial x \partial y}$$

$$= \frac{M\pi y}{32L^2}(1-\nu)\left\{-\frac{\cosh\frac{\pi y}{2L}\cos\frac{\pi x}{2L}+1}{\left(\cosh\frac{\pi y}{2L}+\cos\frac{\pi x}{2L}\right)^2}+\frac{\cosh\frac{\pi y}{2L}\cos\frac{\pi x}{2L}-1}{\left(\cosh\frac{\pi y}{2L}-\cos\frac{\pi x}{2L}\right)^2}\right\} \tag{7}$$

m_y is similar to m_x, except that the terms associated with $(1-\nu)$ are of opposite sign.

$$q_x = \frac{\partial m_x}{\partial x}+\frac{\partial m_{xy}}{\partial y} = -D\frac{\partial(\Delta w)}{\partial x}$$

$$= \frac{M\pi}{16L^2}\left\{-\frac{\cosh\frac{\pi y}{2L}\cos\frac{\pi x}{2L}+1}{\left(\cosh\frac{\pi y}{2L}+\cos\frac{\pi x}{2L}\right)^2}+\frac{\cosh\frac{\pi y}{2L}\cos\frac{\pi x}{2L}-1}{\left(\cosh\frac{\pi y}{2L}-\cos\frac{\pi x}{2L}\right)^2}\right\} \tag{8}$$

$$q_y = \frac{\partial m_y}{\partial y}+\frac{\partial m_{xy}}{\partial x} = -D\frac{\partial(\Delta w)}{\partial y}$$

$$= \frac{M\pi}{16L^2}\left\{\frac{\sinh\frac{\pi y}{2L}\sin\frac{\pi x}{2L}}{\left(\cosh\frac{\pi y}{2L}+\cos\frac{\pi x}{2L}\right)^2}-\frac{\sinh\frac{\pi y}{2L}\sin\frac{\pi x}{2L}}{\left(\cosh\frac{\pi y}{2L}-\cos\frac{\pi x}{2L}\right)^2}\right\} \tag{9}$$

To determine the value K of Eq. 1 from the above expressions, one can define it in two ways. If K is defined as that portion of the unbalanced moment M, which is not transferred between columns and slab by pure bending stresses, then K becomes

$$K = \frac{\int_0^{UL} m_{yx}dx - \int_0^{VL} q_x UL\,dy - \int_0^{UL} q_y x\,dx}{\int_0^{VL} m_x dy + \int_0^{UL} m_{yx}dx - \int_0^{VL} q_x UL\,dy - \int_0^{UL} q_y x\,dx}$$

$$= 1 - \frac{4}{M}\int_0^{VL} m_x dy \tag{10}$$

The values U and V in this expression define the assumed failure plane (Fig. 1) at which the stress configuration is to be determined (Fig. 3). The integrations can be performed numerically or, with certain approximations, in closed form as follows.

We are primarily interested in the stress configuration near the columns, where the terms which have $(\cosh\pi y/2L + \cos\pi x/2L)$ in the denominator are very small compared to the remainder of the equation. They may, therefore, be neglected. Furthermore, setting

$$\sin\frac{\pi x}{2L} = \frac{\pi x}{2L}, \text{ and } \cos\frac{\pi x}{2L} = 1 - 1/2\left(\frac{\pi x}{2L}\right)^2 \tag{11}$$

$$\text{and } \cosh\frac{\pi y}{2L} = 1 + 1/2\left(\frac{\pi y}{2L}\right)^2, \text{ and } \sinh\frac{\pi y}{2L} = \frac{\pi y}{2L} \tag{12}$$

the expression for m_x in Eq. 6 simplifies to

$$m_x = \frac{M}{4\pi L}\left\{(1+\nu)\frac{x/L}{(x/L)^2+(y/L)^2} + (1-\nu)\frac{2(y/L)^2 x/L}{[(x/L)^2+(y/L)^2]^2}\right\} \tag{13}$$

This equation can be integrated to

$$\int m_x dy = \frac{M}{2\pi}\left\{\arctan\frac{y/L}{x/L} - \left[\frac{(1-\nu)}{2}\right]\frac{(y/L)(x/L)}{(x/L)^2+(y/L)^2}\right\} \tag{14}$$

so that a closed solution for K as a function of the critical periphery (Fig. 3) becomes

$$K = 1 - \frac{2}{\pi}\left\{\arctan\frac{V}{U} - \left[\frac{(1-\nu)}{2}\right]\frac{UV}{U^2+V^2}\right\} \tag{15}$$

The above definition of K is based solely on the transfer of bending moments. There is, of course, also the possibility of expressing K in terms of the shear stresses, q_x, directly. This approach is even more justified since we are interested primarily in the maximum shear stresses along the critical periphery.

Making similar approximations as outlined before, the expression for q_x of Eq. 8 becomes

$$q_x = \frac{M}{4\pi L^2}\left\{\frac{\left[2(y/L)^2 - 2(x/L)^2\right] - \left[\frac{\pi^2}{4}(y/L)^2(x/L)^2\right]}{[(x/L)^2+(y/L)^2]^2}\right\} \tag{16}$$

Remembering from Eq. 1 how the shear stress, v, due to the unbalanced moment, M, was defined, the definition of K then becomes

$$K = \left(\frac{-q_x}{M}\right)\left(\frac{J_c}{de}\right) \tag{17}$$

where d = structural depth of the plate. While J_c and e are determined by the failure plane chosen, the shear force, q_x, as given by Eq. 16, varies, of course, along this periphery and does not suffice to define K. The required additional condition comes from the fact that the slab is built integrally with the column. This results in zero twisting moment, m_{yx}, along the column face, so that $q_x = \partial m_x/\partial x$. On the other hand, the term $\partial^3 w/\partial x^3$ is almost constant with respect to y in the vicinity of the column. It can, therefore, be assumed that the actual distribution of q_x along the column face is uniform and that it is justified to assume an average value, q_x = constant, to prevail along the assumed failure plane along the y-axis in the vicinity of the column. To find this average value, $\overline{q_x}$, one must integrate Eq. (16) as follows.

$$\overline{q_x} = \frac{1}{VL}\int_0^{VL} q_x dy$$

$$= M\frac{\pi}{32L^2}\left\{-\frac{x/L}{V}\arctan\frac{V}{x/L} + \frac{(x/L)^2 - (4/\pi)^2}{(x/L)^2+V^2}\right\} \tag{18}$$

To determine K from Eq. (17), one may use the definition of J_c from Reference 9, Eq. 8-24, so that

$$\frac{J_c}{de} = L^2\left\{\frac{4}{3}U^2 + 1/3\left(\frac{d}{L}\right)^2 + 4UV\right\} \tag{19}$$

in which the structural depth, d, of the plate may be assumed as L/40. This term is rather insignificant so that any other reasonable assumption will yield similar results. The resulting K-value for $q_x = \overline{q_x}$ can thus be expressed as a function of the critical periphery, i.e., in terms of U and V (Fig. 3)

$$K = \frac{\pi}{32}\left\{\left[\frac{4}{3}U^2 + 1/3\left(\frac{1}{40}\right)^2 + 4UV\right]\left[\frac{U}{V}\arctan\frac{V}{U} - \frac{U^2 - (4/\pi)^2}{U^2 + V^2}\right]\right\} \tag{20}$$

Another simplification suggests itself by neglecting terms in Eq. 20 which are small compared to the remainder of the equation. Hence, with

$$R = \frac{J_c}{L^2 de} \tag{21}$$

a simple expression for K results, which is within 1/2 percent identical with Eq. 20:

$$K = \frac{R}{2\pi(U^2 + V^2)} \tag{22}$$

This shows that the resulting averaged maximum shear stress, $v = \overline{q_x}/d$, due to an unbalanced moment, M, is inversely proportional to the square of the distance from the center of the column to the corner of the critical periphery:

$$v = \frac{M}{2\pi d L^2 (U^2 + V^2)} \tag{23}$$

Influence Lines for Maximum Shear Stress

As revealed by Eq. 1, the influence line for maximum shear stress is a combination of the influence lines for the column reaction, V_v, and for the unbalanced slab moment, M. Fig. 4 shows these influence lines for a typical flat plate structure extending over three spans (slab thickness: 8 in.; columns 18x18 in.; story height: 10 ft.; spans: 20 ft.; bay widths: 20 ft.). For a structure with longer spans, the ordinates of the moment influence line would, of course, be bigger, whereas the ones for V_v would remain about as shown.

In order to combine these influence lines, we multiply the ordinates of the one for M by the factor

$$Q = K\frac{A_c}{J_c}\, e \tag{24}$$

and add them to the ordinates of the one for V_v, as shown in Fig. 4c. The force, S, obtained by putting a load on the ordinates, η_s, yields the maximum shear stress as $v = S/A_c$.

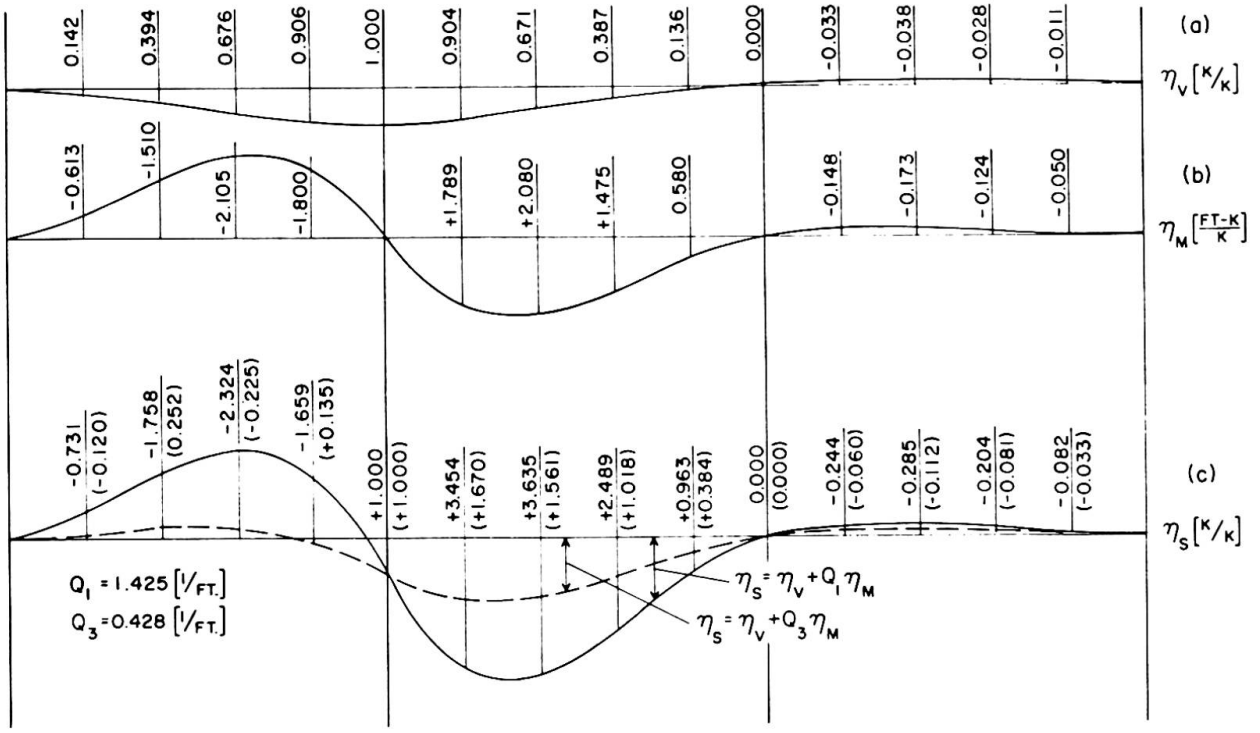

FIG. 4 INFLUENCE LINES FOR MAXIMUM SLAB SHEAR AT COLUMNS

Tables 1 through 3 tabulate K-values and the corresponding Q-factors as a function of the shape of the critical periphery, which is expressed by its coordinates, U and V. Table 1 is set up for K = 1.0. The corresponding Q-factors pertain to designs in accordance with common practice in the USA [8, 12]. Table 2 uses K-values based on the moment transfer, as defined by Eq. 15. Table 3 uses K-values based on maximum shear stress, as defined by Eqs. 20 or 22.

These Q-values in Tables 1 through 3 differ considerably, and so do the shapes of the resulting influence lines for shear. The lower portion of Fig. 4, for example, compares the influence lines based on the Q-factors from Table 1 (solid line) and from Table 3 (dashed line). The chosen coordinates of the critical periphery are U = 0.045 and V = 0.089, which comply with common practice [8, 12] for the column and slab dimensions stated above. The K-values pertaining to these Q-factors are $K_1 = 1.00$ (for $Q_1 = 1.425$) and $K_3 = 0.301$ (for $Q_3 = 0.428$). It should be noted that these influence lines resemble the ones for kern-moments in columns of continuous frames. The width of the "shear kern," measured from the centroid of the critical periphery, amounts to

V \ U		0.025	0.050	0.075	0.100
K_1	0.025				
	0.050	K_1 = constant			
	0.075	= 1.000			
	0.100				
Q_1	0.025	2.823	1.756	1.315	1.062
	0.050	2.482	1.477	1.101	0.894
	0.075	2.341	1.348	0.993	0.803
	0.100	2.264	1.274	0.928	0.747

Table 1. K and Q - Values without Plate Theory

V \ U		0.025	0.050	0.075	0.100
K_2	0.025	0.620	0.800	0.867	0.900
	0.050	0.391	0.620	0.736	0.800
	0.075	0.277	0.485	0.620	0.705
	0.100	0.213	0.391	0.525	0.620
Q_2	0.025	1.750	1.406	1.140	0.956
	0.050	0.971	0.915	0.810	0.716
	0.075	0.649	0.654	0.615	0.567
	0.100	0.482	0.499	0.487	0.463

Table 2. K and Q Values Based on Moment Transfer

V \ U		0.025	0.050	0.075	0.100
K_3	0.025	0.451	0.435	0.387	0.353
	0.050	0.308	0.431	0.445	0.427
	0.075	0.218	0.364	0.428	0.444
	0.100	0.166	0.300	0.385	0.427
Q_3	0.025	1.273	0.764	0.509	0.374
	0.050	0.764	0.637	0.490	0.382
	0.075	0.510	0.490	0.425	0.357
	0.100	0.375	0.383	0.358	0.319

Table 3. K and Q Values Based on Maximum Shear

$$k = 1/Q = J_c/KA_c e \tag{25}$$

Evaluation of Influence Lines

The variation of the influence lines (Fig. 4c) shows that the shape of the critical periphery and the theoretical assumptions of moment transfer affect the shear stresses around a column in two ways: First, there is a direct effect due to the magnitude of the factors associated with V_v and M, i.e., the magnitude of the variables K, J_c, A_c, and e. The other effect results from the positioning of the live load as determined by the positive and negative regions of the influence lines.

In designing multi-span frames, we are used to positioning the live load either on the two spans at both sides of a column (Case A) or on just one span, i.e., to the left or to the right of a column (Case B). The first arrangement, Case A, results in a maximum punching force, V_v, whereas the latter one, Case B, results in a maximum unbalanced moment, M. We will investigate these two loading conditions with respect to the maximum shear stress which they produce. Furthermore, we will see what effect partial loading of the span has, i.e., loading up to the zero-point of the influence lines (Case C).

The influence lines of Fig. 4c represent two extremes. The solid line ($K_1 = 1.00$; $Q_1 = 1.425$) puts the maximum emphasis on the unbalanced moment, whereas the dashed line assumes a big portion of the unbalanced moment being transferred by bending ($K_3 = 0.301$; $Q_3 = 0.428$). Shear stresses obtained from these influence lines cannot be compared directly because the ones for $K_1 = 1.00$ may be reduced by the provision of flexural reinforcement [8]. It is for this reason that the resulting shear stresses are compared separately in Tables 4 and 5. In other words, these tables are meant to show the significance of the live load positioning only.

In comparing Cases A through C, the dead-to-live load ratio is important. We assume a feasible range of live loads varying from 50 lb./sq.ft. to 100 lb./sq.ft. Considering the slab thickness given, other factors affecting the dead-to-live load ratio are the type of concrete (lightweight or normal weight) and, due to load factors, the design method used (Ultimate Strength Method or Working Stress Method [12]).

$K_1 = 1.000$ $Q_1 = 1.425$	Ultimate Strength				Working Stress			
	Normal weight		Lightweight		Normal weight		Lightweight	
Live Load:	50	100	50	100	50	100	50	100
Case A	112	159	95	142	69	96	58	84
Case B	171	278	154	261	102	162	91	150
Case C	173	280	155	263	103	163	92	152

Table 4. Shear Stresses (psi) as Function of Live Load Positioning

$K_3 = 0.301$ $Q_3 = 0.428$	Ultimate Strength				Working Stress			
	Normal weight		Lightweight		Normal weight		Lightweight	
Live Load:	50	100	50	100	50	100	50	100
Case A	124	172	104	152	77	104	64	91
Case B	124	173	104	154	78	105	64	92
Case C	130	185	110	165	80	111	67	98

Table 5. Shear Stresses (psi) as Function of Live Load Positioning

The values of Tables 4 and 5 were computed in compliance with standard practice [8, 12] by means of a computer program [13]. They show that it is always the live load position for maximum positive span moments (Case B) which causes maximum shear stresses at the columns. They, furthermore, show that the increase in shear stress due to extending the live load to the zero-point of the influence lines (Case C) is insignificant. It should be mentioned that some building codes [12] call for only 75 percent of the live load to be applied in pattern loading, whereas 100 percent of the live load must be placed on all spans. Under this condition it is possible that the positioning of Case A governs, especially when the spans are short and, therefore, the η_M are small compared to the η_V (Fig. 4). The loading of spans which are not adjacent to the column is insignificant due to the restraining effect of the remote columns.

It should be noted that the experimentally determined K-values [9, Table 8-6] correspond well with the K-values of Table 3, if the critical periphery is at least d/2 away from the face of the column. This is reasonable since the theoretical assumption of a concentrated moment is justified only in view of the theorem of St. Venant, i.e., at some distance away from the point of application. Numerical refinements are, of course, always possible by using series expansions of the applied moment and of the boundary reactions.

The K-values and Q-factors depend on the shape of the critical periphery and, thereby, on the column size. In addition to this primary effect, the column size affects, of course, the shape of the influence lines for V and M. Visualizing the latter one as the deflection curve due to a unit moment applied at the joint, one could expect the ordinates, η_M, to decrease with increasing

column stiffness. In reality, however, these ordinates increase, because of the smaller joint rotation. They would diminish to zero, of course, if the columns had no stiffness at all. Doubling the column stiffness in the example, for which influence lines are shown in Fig. 4, would result in an increase of the ordinates, η_M, by about 30 percent.

Summarizing the above, it can be stated that all of these factors, the assumed shape of the critical periphery, the stiffness ratio between slabs and columns, the slab spans, and the theoretical assumptions of moment transfer have an effect on the shape of the influence lines. As far as the critical live load positioning is concerned, however, Case B (Tables 4 and 5) will usually be the governing one.

References

1. "Laboratory Study of a 45-Foot Square Flat Plate Structure," S. A. Guralnick and R. W. LaFraugh, Journal of the American Concrete Institute, Vol. 60, pp. 1107-1185, Sept. 1963.

2. "Experimental Investigation of Flat Plate Floors," I. Rosenthal, Journal of the American Concrete Institute, Vol. 56, pp. 153-166, Aug. 1959.

3. "Beitrag zur spannungs optischen Untersuchung des räumlichen Spannungszustandes im Stützenbereich von Flachdecken," K. Ritter, Dissertaion, Karlsruche 1961.

4. "Modellstatische Untersuchung punktförmig gestützter schiefwinkliger Platten unter besonderer Berücksichtigung der elastischen Auflagernachgiebigkeit," A. Mehmel and H. Weise, Deutscher Ausschuss für Stahlbeton, Vol. 161, Berlin 1964.

5. "Experimental Determination of the Transmission of Column Moments to Flat Plate Floors," G. R. Frederick and F. P. Pollauf, University of Toledo.

6. "Shearing Strength of Reinforced Concrete Slabs and Footings Under Concentrated Loads," J. Moe, Development Department Bulletin D47, Portland Cement Association, April 1961.

7. "Transfer of Bending Moment Between Flat Plate Floor and Column," J. DiStasio and M. P. van Buren, Journal of the American Concrete Institute, Proceedings Vol. 57, No. 3, pp. 299-314, Sept. 1960.

8. "Commentary on Building Code Requirements for Reinforced Concrete (ACI 318-63)," Report of ACI Committee 318, Publication SP-10, American Concrete Institute, pp. 64-65, 1965.

9. "Shear and Diagonal Tension," Report of ACI-ASCE Committee 326, Journal of the American Concrete Institute, Proceedings Vol. 59, Section 807, pp. 382-386, 1962.

10. "Flächentragwerke," K. Girkmann, 5th Edition, Springer Verlag, pp. 188-189, Wien 1959.

11. "Praktische Funktionenlehre," F. Tolke, Vol. 1, 2nd Edition, Springer Verlag, pp. 369-372, Berlin 1950.

12. "Building Code Requirements for Reinforced Concrete (ACI 318-63)," ACI Committee 318 Report, American Concrete Institute, pp. 88-89, June 1963.

13. "Computer Program for the Analysis and Design of Flat Plates and Continuous Concrete Frames," Paul E. Mast, Portland Cement Association, XS6815, 1968.

SUMMARY

An analytical method is developed to determine the stress configuration in flat plates subject to column moments. The results are presented in closed form for values, K, as a function of the shape of the critical periphery. These values agree well with test results. Influence lines for maximum shear stress are drawn for the bounds of the feasible range of K-values. Their evaluation shows that live load on alternate spans usually governs. The effect of partial loading of spans, however, is insignificant.

RÉSUMÉ

On présente une méthode analytique pour déterminer les efforts aux dalles plates produits par les moments aux colonnes. Les résultats sont présentés en formules fermées définissant les valeurs K, qui sont des fonctions du profil de la périphérie critique. Les valeurs s'accordent avec les résultats expérimentaux. Les lignes d'influence d'efforts tranchants ont été tirées pour des valeurs extrêmes K à portée de service et évaluées pour des conditions différentes. L'évaluation fait preuve du fait, qu'une charge utile aux portées alternes est décisive, tandis qu'une charge partiale des portées est d'insignifiance.

ZUSAMMENFASSUNG

Der Aufsatz schlägt eine analytische Methode vor, um die Spannungen in Flachdecken zu ermitteln, welche durch Stützenkopfmomente hervorgerufen werden. Die Ergebnisse sind in geschlossenen Formeln für'K'in Abhängigkeit der Bruchform dargestellt, und sie stimmen gut mit vorhandenen Versuchsergebnissen überein. Mit den Extremen der K-Werte im brauchbaren Bereich sind Einflusslinien gezeichnet und für verschiedene Bedingungen ausgewertet. Sie zeigen, dass abwechselnd feldweise Belastung ausschlaggebend ist, dass aber teilweise Feldbelastung die Ergebnisse kaum beeinflusst.

Leere Seite
Blank page
Page vide

Load Distribution in Multi-Storey Shear Wall Structures

Répartition des charges dans des constructions à étages multiples avec murs de cisaillement

Lastverteilung in mehrstöckigen Scheibentragwerken

A. COULL A.W. IRWIN
Department of Civil Engineering
University of Strathclyde
Glasgow, Scotland

1. Introduction

Recent developments in multi-storey buildings for residential purposes have led to the extensive use of shear-walls, or cross-walls, for the basic structural system. Whilst the walls are designed primarily to resist both vertical and horizontal loads, they can in addition, by careful planning, be utilised fully for the non-structural functions of dividing and enclosing space, whilst simultaneously providing fire resistance and acoustic insulation between dwellings. By this means, efficient structural designs can be achieved. The floor slabs, which keep storey and overall heights to a minimum, act as deep beams transferring the wind loads to the vertical wall elements. The regular system of walls and slabs lends itself to industrialised building techniques, using either in-situ or precast construction.

A typical example of such slab-type structures is shown in Fig.1. Planning requirements tend to evolve parallel assemblies of walls, coupled by floor slabs or lintel beams, in conjunction with box-type assemblies surrounding lift shafts and stair wells.

The majority of studies of coupled shear-wall structures has been devoted to the problem of plane walls subjected to standard systems of loads in their own plane. In the case of a complete building, the results are strictly accurate only if the structure consists of parallel systems of identical wall assemblies, so that any lateral load is divided equally amongst them, it being assumed that all walls deflect equally due to the very high in-plane stiffness of the floor slabs.

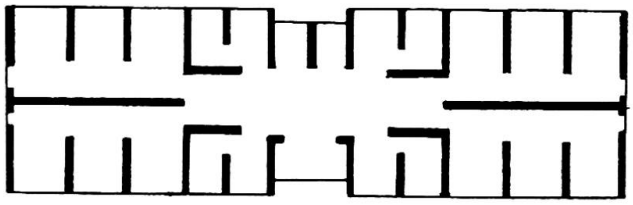

FIG. 1

If the structure consists of different forms of load bearing elements, or if, as is often the case, walls are curtailed at first floor level to provide an open concourse, considerable redistribution of load may take place. It may then become important to examine in some detail the distribution of load between the walls throughout the height of the building.

For shear-wall structures, suggestions have been made that lateral loads should be distributed amongst the walls in proportion to their stiffnesses[1]. If any coupling occurs, this process will give rise to significant errors, as may readily be seen by comparing the modes of deformation of a coupled wall and a cantilever box structure subjected to uniformly distributed loads[2]. The former bends with a reversal of curvature in the upper levels, whilst the latter bends in single curvature. In order to constrain the two to deflect equally, tensile linking forces are required in the upper levels, and compressive forces in the lower regions.

Two different methods have been developed for the analysis of coupled shear walls, the frame analogy and the continuous connection techniques. The first replaces the deep wall by a line column at the centroid, the finite depth being incorporated by the use of rigid arms to link the ends of the connecting beams to the column. The analysis is then carried out using standard frame-analysis techniques. In this case, an increase in the number of storeys leads to an increase in the degree of statical indeterminacy, and a corresponding increase in the number of equations to be solved. The second method replaces the discrete system of connecting beams by a continuous medium of the same stiffness. By assuming that the connecting beams deform with a fixed point of contraflexure, but do not deform axially, the behaviour of the system may be expressed by a single second-order differential equation, enabling a general closed solution to the problem to the obtained. This method has the advantage that the accuracy of the solution increases with an increasing number of storeys, with no extra labour involved. Because of its analytical nature, the method is less versatile in that it is more difficult to deal with variations in geometrical and stiffness parameters, although, because of the essential uniformity of the shear wall structure, this is not a serious limitation. The effects of variable thickness can easily be incorporated[3], and changes in width may be included in the general solution[4]. The accuracy of the technique has been demonstrated by numerous experimental investigations[3,4]. The discontinuities which may be present at ground floor level, where shear walls may be discontinued, may be treated by incorporating their influence in the lower boundary condition[5].

The aim of this paper is to present a method of analysis of complete multi-storey apartment-style concrete buildings, whose load-bearing structure consists essentially of parallel systems of shear wall and box elements, subjected to any system of lateral loads. The method is based on the continuous connection technique, and numerical results are presented for a typical representative structure.

2. Method of Analysis

Consider the coupled shear wall shown in Fig.2 subjected to a point load Pi applied at any height xi. The individual connecting beams of stiffness EI_p are replaced by an equivalent continuous medium or set of laminas of stiffness EI_p/h per unit height. It is assumed that the connecting beams do not deform axially so that both walls deflect equally, and that the point of contra-flexure occurs at the mid-span position in all beams. If the laminas are assumed 'cut' at their mid-points, the only force acting at the cut section is a shear force of intensity q per unit height. On considering the deformations of the cut laminas, the compatibility condition may be set up to give no resultant relative deformation at the cut, and, when used in conjunction with the moment-curvature relationships for the walls, this leads to the establishment of the following governing differential equation,

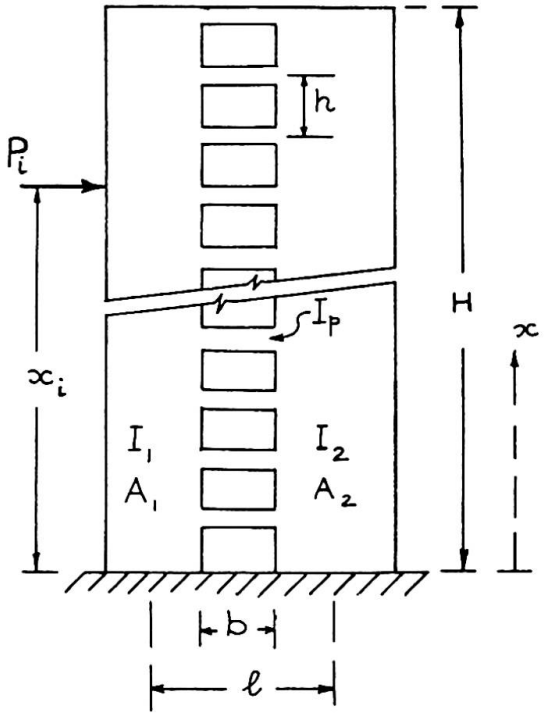

FIG. 2

$$\frac{d^2q}{dx^2} - \mu^2 q = -\alpha^2 P_i \langle x - x_i \rangle^0 \qquad (1)$$

where $\alpha^2 = \dfrac{12\ell I_p}{b^3 h I}$

and $\mu^2 = \dfrac{\alpha^2}{\ell}\left(\ell^2 + \dfrac{IA}{A_1 A_2}\right)$

For convenience in writing a single solution for the entire structure, a system of Macaulay's brackets has been employed in equation (1). These are defined in the usual manner as,

When $x < xi$, $\langle x - xi \rangle^n = 0$, $\langle x - xi \rangle^0 = 0$

When $x > xi$, $\langle x - xi \rangle^n = (x - xi)^n$, $\langle x - xi \rangle^0 = 1$

The detailed derivation of equation (1) is not given, since similar equations have been derived in detail in earlier papers for different load conditions[3,4]. The appropriate boundary conditions for the fixed and free ends, expressed in terms of the shear force intensity 'q', may be shown to be, respectively,

$$\text{At } x = 0, \quad q = 0$$

$$\text{At } x = H, \quad \frac{dq}{dx} = 0 \tag{2}$$

The solution of equation (1), subject to the boundary conditions (2), may be shown to be,

$$q = \frac{\alpha^2 p_i}{\mu^2} \cdot \frac{1}{\cosh \mu H} \left\{ \cosh \mu H \cdot \cosh \langle \mu (x - xi) \rangle^1 - \cosh \mu (H - x) - \sinh \mu (H - xi) \cdot \sinh \mu x \right\} \tag{3}$$

At any level, the axial force in the wall, tensile or compressive, is given by,

$$\begin{aligned} N &= \int_x^H q \, dx \\ &= \frac{\alpha^2 p_i}{\mu^3} \frac{1}{\cosh \mu H} \left\{ \sinh \mu (H - xi) \cdot \cosh \mu x - \sinh \mu (H - x) \right. \\ &\quad - \cosh \mu H \cdot \sinh \langle \mu (x - xi) \rangle^1 \\ &\quad \left. - \langle \mu (xi - x) \rangle^1 \right\} \end{aligned} \tag{4}$$

The corresponding bending moments in the walls are,

$$\begin{aligned} M_1 &= \left\{ p_i \langle x - xi \rangle^1 - T\ell \right\} \frac{I_1}{I} \\ M_2 &= \left\{ p_i \langle x - xi \rangle^1 - T\ell \right\} \frac{I_2}{I} \end{aligned} \tag{5}$$

since the moment carried by each wall is proportional to its stiffness, by virtue of the assumption that both walls deflect equally.

The moment-curvature relationship is,

$$EI \frac{d^2 y}{dx^2} = p_i \langle x - xi \rangle^1 - T\ell \tag{6}$$

Integration of equation (6), and inclusion of the appropriate boundary conditions at top and bottom, yields the deflection at any level,

$$y = \frac{Pi}{EI}\left\{\frac{1}{6}\left(1 - \frac{\alpha^2 \ell}{\mu^2}\right)\left(3xi \cdot x^2 - x^3 + \langle x - xi\rangle^3\right)\right.$$
$$+ \frac{\alpha^2 \ell}{\mu^4}\left[\left(x - \langle x - xi\rangle^1\right) + \frac{1}{\mu \cosh \mu H}\left(\sinh \mu(H - x)\right.\right.$$
$$- \sinh \mu H + \sinh \mu(H - xi)\ (1 - \cosh \mu x)$$
$$\left.\left. + \cosh \mu H \sinh \langle \mu(x - xi)\rangle^1\right]\right\} \qquad (7)$$

The single equation (7) yields the complete relationship between a unit load at any height xi and the deflection at any height x, enabling a complete set of influence coefficients fij (deflection at xi due to a unit load at xj) to be evaluated readily.

It may readily be shown that the same solution holds for a symmetrical shear wall containing two bands of openings, provided the parameters α and μ are defined slightly differently[3,4].

Analysis of Complete Structure

Suppose that the structure consists of a number of parallel wall assemblies. For a coupled-wall element, the load-deflection relationship is given by equation (7). For a box-type element, the corresponding load-deflection relationship may be shown to be,

$$y = \frac{Pi}{6EI}\left\{3xi^2 x - xi^3 + \langle xi - x\rangle^3\right\} \qquad (8)$$

In either case, for the k^{th} wall element, the load-deflection relationship may be expressed in matrix form as,

$$\underset{\sim}{y}_{ik} = \underset{\sim}{fij}_k \ \underset{\sim}{Pi}_k \qquad (9)$$

where $\underset{\sim}{y}_i$ and $\underset{\sim}{P}i$ are column vectors of deflections and applied loads at any chosen set of levels xi, and $\underset{\sim}{f}_{ij}$ is a square matrix of influence coefficients evaluated from equations (7) or (8). A similar relationship can be derived for each wall assembly. Fortunately, in buildings of this nature, the number of different forms of wall elements is quite small, so that only a very limited number of matrices $\underset{\sim}{f}ij$ will have to be evaluated.

For any applied load system whose resultant passes through the centre of rotation, all deflections will be the same at any given level, if it is assumed that the floor slabs are infinitely stiff in their own plane. Hence,

$$\underset{\sim}{fij}_k \ \underset{\sim}{Pi}_k = \underset{\sim}{y}_i = \text{constant for all 'k'} \qquad (10)$$

For equilibrium, the total applied load Pi at each storey level must be equal to the sum of the loads on the wall assemblies at that level. That is,

$$Pi = \sum_k \underset{\sim}{Pi}_k \qquad (11)$$

summing over all wall assemblies.

Hence, from equations (10) and (11), the complete load distribution throughout the structure may be obtained. From equation (10) the applied loads on any wall assembly 'k' may be expressed in terms of the load P_{i_1} on any particular wall 'i', say,

$$\underset{\sim}{P}i_k = \underset{\sim}{f}ij_k^{-1} \; \underset{\sim}{f}ij_1 \; \underset{\sim}{P}i_1 \tag{12}$$

Hence, from equation (11), the loads on wall 'i' become,

$$\underset{\sim}{P}i_1 = \left\{ \underset{\sim}{I} + \sum_{k=2,3,\ldots n} \underset{\sim}{f}ij_k^{-1} \; \underset{\sim}{f}ij_1 \right\}^{-1} \underset{\sim}{P}i \tag{13}$$

and the loads on all other walls follow from equation (12).

The deflections and stresses in individual wall assemblies may then be evaluated by the continuous connection solution, using equations (3), (4), (5) and (7).

Suppose, for example, that the structure consists of four, six and one element of types 'a', 'b' and 'c' respectively. Then, from equation (9),

$$\underset{\sim}{y}i = \underset{\sim}{f}ij_a \; \underset{\sim}{P}i_a = \underset{\sim}{f}ij_b \; \underset{\sim}{P}i_b = \underset{\sim}{f}ij_c \; \underset{\sim}{P}i_c \tag{14}$$

For equilibrium, $$\underset{\sim}{P}i = 4\underset{\sim}{P}i_a + 6\underset{\sim}{P}i_b + \underset{\sim}{P}i_c \tag{15}$$

or using equation (14)

$$\underset{\sim}{P}i = \left\{ 4\underset{\sim}{I} + 6\underset{\sim}{f}ij_b^{-1} \; \underset{\sim}{f}ij_a + \underset{\sim}{f}ij_c^{-1} \; \underset{\sim}{f}ij_a \right\} P_{i_a} \tag{16}$$

The loads on the wall assemblies of type 'a' become,

$$\underset{\sim}{P}i_a = \left\{ 4\underset{\sim}{I} + 6\underset{\sim}{f}ij_b^{-1} \; \underset{\sim}{f}ij_a + \underset{\sim}{f}ij_c^{-1} \; \underset{\sim}{f}ij_a \right\}^{-1} \underset{\sim}{P}i \tag{17}$$

and the loads on the other elements follow from equation (14).

If the resultant of the applied loads does not pass through the centre of rotation, but acts at a distance $3'$ from it, a torsional moment Ti of magnitude $Pi \; 3'$ is applied to the building. Owing to the high in-plane stiffness of the floor slabs, they will undergo a rigid body rotation through an angle Θi, say, such that the total displacement of the k^{th} wall assembly is equal to $yi + \Theta i 3_k$, where 3_k is the distance of the wall element from the centre of rotation.

If the twisting moments on the wall elements are neglected, the second condition of rotational equilibrium becomes, for the entire system,

$$\underset{\sim}{T}i = \sum_k \left(\underset{\sim}{P}i_k \; 3_k \right) \tag{18}$$

The second condition of equilibrium enables the additional unknown displacement $\underset{\sim}{\Theta}_i$ to be evaluated and a complete solution obtained.

By virtue of the assumption of a rigid body rotation of all floor slabs, the rotations of all wall elements may be obtained and the twisting moments evaluated in terms of the rotations Θi from standard strength of materials relationships. If the twisting movements on individual wall elements are included, therefore, the second condition of rotational equilibrium (18) must be amended to,

$$\underset{\sim}{T}i = \sum_k (\underset{\sim}{p}i_k \; 3_k) + \sum_k \underset{\sim}{T}i_k \qquad (19)$$

where Ti_k is the twisting movement on the k^{th} wall element at level xi. These twisting movements may then be expressed in terms of the rotations, and the complete solution obtained as before.

Lack of space does not permit the torsional condition to be treated in greater detail.

3. Numerical Example

In order to illustrate the results, a representative shear-wall structure of the form shown in Fig.3 (in plan) is considered. The structure consists of a central core (wall 3), heavy flank walls (walls 1), and four pairs of interior cross-walls (walls 2). It is assumed that the building is 20 storeys high, with a storey height of 8 ft.9in., the floor slabs being assumed to be 6 in. thick. For the purpose of this example, it is assumed that the building is subjected to a wind loading of intensity 10 lb/ft^2 in a direction parallel to the cross-walls.

The effective width, or stiffness, of the floor slabs may be determined by a subsidiary calculation, using such numerical techniques as the finite element or finite difference method; in the present instance, the latter was employed, using curves prepared by Qadeer and Stafford Smith[6]. In this case, the effective widths of slab connecting walls 1 and 2 are taken to be 10 ft. and 13.2 ft. respectively.

A computer program has been written to perform the entire calculations necessary for a complete analysis of the building. Because of the regularity of such structures, the program requires a relatively small amount of input data. The output consists of the influence coefficients for each type of wall unit, the loads on the various walls at each level, the bending moments, axial forces, and shear forces on all walls at each level, the stresses at the extreme fibres of each wall, and the deflection. In order to check the computation, the deflection of each wall is calculated separately.

In the present case, the influence coefficients and forces were computed at each storey level. The computed deflections for the different wall units agreed with each other to six significant figures. The results obtained are shown in Figs.4, which show (a) the percentage of the total applied load carried by each type of wall unit throughout the height of the building, and (b) the deflected form.

The results indicate that for structures of this nature, considerable variations in the load distribution can occur throughout the height of the building.

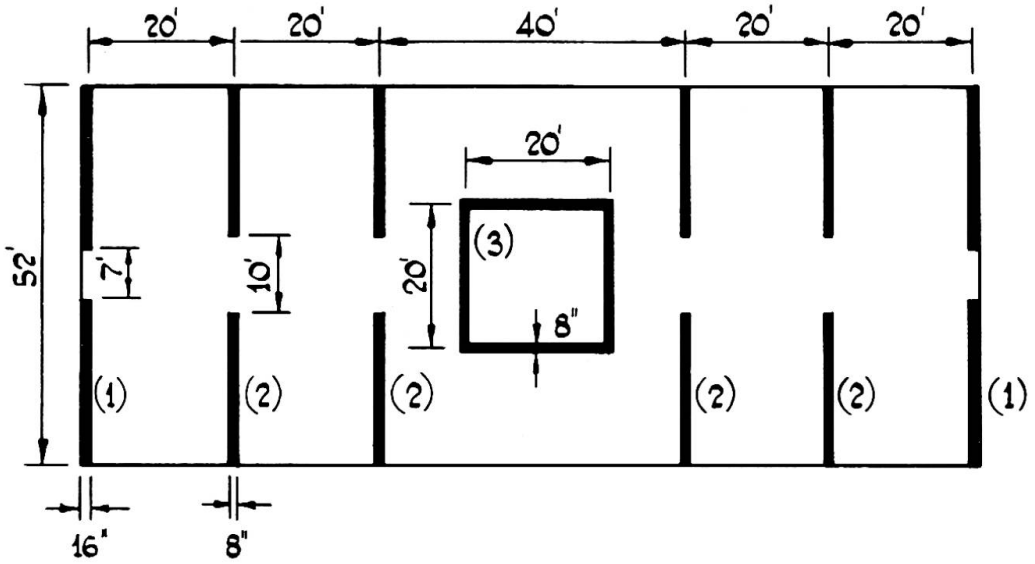
20'
20'
40'
20'
20'
52'
7'
10'
20'
20'
(3)
8"
(1)
(2)
(2)
(2)
(2)
(1)
16"
8"

Fig. 3.

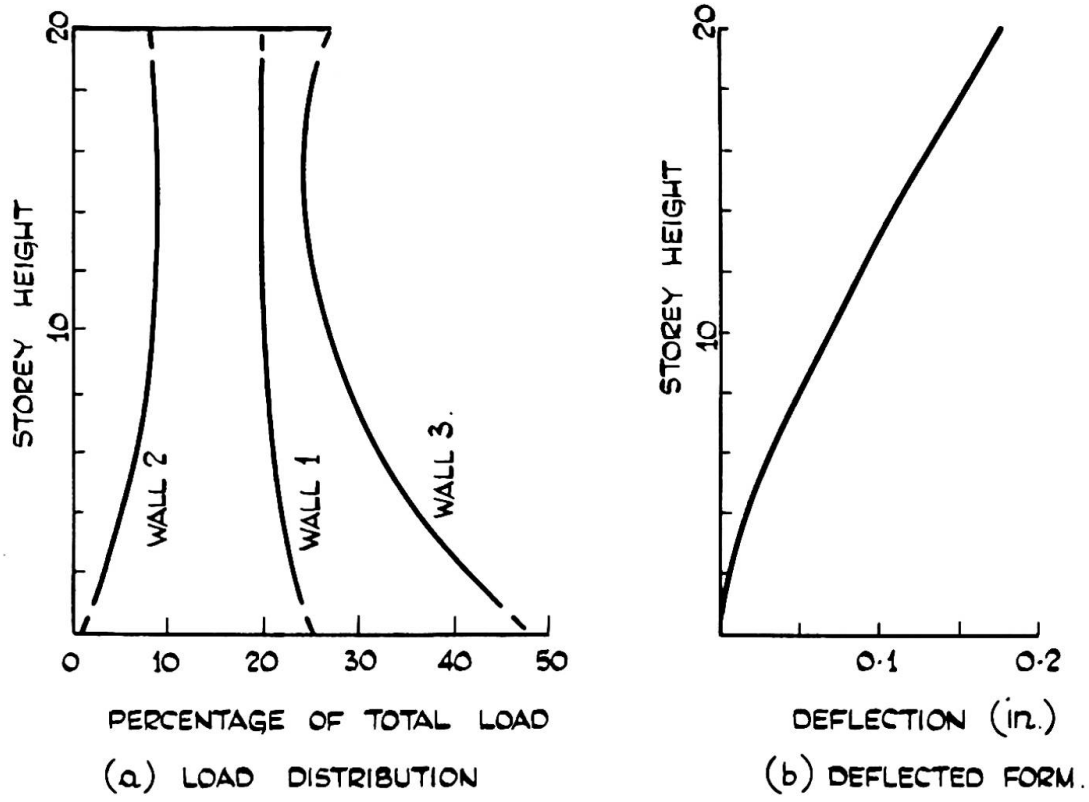
STOREY HEIGHT
20
10
WALL 2
WALL 1
WALL 3.
0
10
20
30
40
50
PERCENTAGE OF TOTAL LOAD
(a) LOAD DISTRIBUTION
STOREY HEIGHT
20
10
0·1
0·2
DEFLECTION (in.)
(b) DEFLECTED FORM.

Fig. 4.

4. Conclusions

A method has been presented for the analysis of multi-storey structures which consist essentially of parallel assemblies of coupled shear-walls. The continuous connection technique is used to determine the load-deformation characteristics of individual wall assemblies, and the complete structure is analysed using compatibility and equilibrium conditions. Any applied load system can be dealt with, and the technique can be extended to include torsion of the structure.

The analysis deals with matrices of small order, and can readily be programmed for digital computation. In order to reduce the amount of computation, the influence coefficients need not be evaluated for every storey level, since rapid variations in load distribution do not occur in regular structures of the form considered. Having regard to the form of structure and applied load, the designer can assess the number of reference levels which may be required in the analysis to give a solution which is sufficiently accurate for practical purposes. A closer spacing in the reference levels may be adopted for regions where the load distribution is changing most rapidly.

In the paper, the general solution for a coupled shear wall structure subjected to a joint load at any height is, as far as the authors are aware, presented for the first time. By simple integration, the general solution for any load form may be derived from equation (3).

References

1. Albiges, M. and Goulet, J. "Contreventement des Batiments" Annales de L'Institut Technique du Batiment et des Travaux Publics. No.149, May, 1960, pp.473 - 500

2. Khan, F.R. "Current Trends in Concrete High-Rise Buildings" Proceedings of Symposium on Tall Buildings, Ed. Coull and Stafford Smith, Pergamon Press, 1967, p.575

3. Coull, A. and Puri, R.D. "Analysis of Coupled Shear Walls of Variable Thickness" Building Science, Vol.2, 1967, pp 181-188

4. Coull, A. and Puri, R.D. "Analysis of Coupled Shear Walls of Variable Cross-section" Building Science, Vol.2, 1968, pp 313-320

5. Rosman, R. "Approximate Analysis of Shear Walls Subject to Lateral Loads" Jnl. A.C.I., Vol.61, 1964, pp 717 - 732.

6. Qadeer, A. and Stafford Smith, B. "The Bending Stiffness of Slabs Connecting Shear Walls" (submitted for publication to A.S.C.E.)

Notation The following symbols are used in this paper:

x	Height
y	Horizontal deflection
Θ	Rotation
ζ	Distance from centre of rotation
H	Total Height
h	Storey Height
b	Clear distance between walls
ℓ	Distance between centroidal axis of two walls
I_p	Moment of inertia of connecting beam
I_1, I_2	Moment of inertia of walls 1 and 2
I	$I_1 + I_2$
$A_1 A_2$	Cross-sectional areas of walls 1 and 2
A	$A_1 + A_2$
Pi	Applied load at level xi
Ti	Applied twisting moment at level xi
q	Shear force intensity in substitute connecting medium
$M_1 M_2$	Bending moments in walls 1 and 2
N	Axial force in wall
fij	Deflection at level xi due to unit load at xj
k	Suffix denoting k^{th} wall assembly

SUMMARY

A method is presented for the analysis of the distribution of load amongst the shear walls of a multi-storey apartment-style building. The method is based on the continuous connection technique. Numerical results are presented for a typical twenty-storey structure.

RÉSUMÉ

L'article présente une méthode pour l'analyse de la distribution des charges parmi les murs de cisaillement dans une maison d'appartement de beaucoup d'étages. La méthode est basée sur la technique de liaison continue. Des résultats numériques sont donnés pour un bâtiment typique de 20 étages.

ZUSAMMENFASSUNG

Dargestellt ist ein Verfahren zur Berechnung der Lastverteilung in Scheiben eines mehrstöckigen Gebäudes. Das Verfahren baut auf der durchlaufenden Gewebetechnik auf. Numerische Ergebnisse werden für ein typisches zwanzigstöckiges Haus gegeben.

Study of the Distribution of Wind Loads Between Stiffening Elements and Framing of Multi-Storey Buildings

Etude de la distribution des charges du vent entre des éléments de la rigidité et des portiques des carcasses des immeubles géants

Untersuchung über die Verteilung der Windlasten zwischen Versteifungen und Stockwerkrahmen von Hochhäusern

B.A. KOSITSYN
Cand. Techn. Sc.
(USSR)

Modern multi-storey buildings consist, as a rule, of framing, vertical diametric walls, adding transverse rigidity to the building, floors and light railing structures attached to the framework. In order to design such buildings for horizontal loads it is necessary, in general, to determine the forces arising in the structures of the framework and its deformations. The latter is required to calculate the strength of railing structures, their connections with each other and with the framework. (When designing the framework, the influence of railing structures is, commonly, not taken into account).

The present paper gives some results of the investigation of the first, most difficult part of the problem of designing framed structures with due account of the spatial behaviour of the structures.

Horizontal loads in framed buildings are taken up by vertical diametric walls and frames. Floors joined in rigid disks, serve as bracing distributing the load between the load-bearing members of the building and equalizing their transverse displacements. In very high buildings with diametric walls closely arranged, disks of floors also exert a direct affect on longi-

tudinal deformations of load-bearing members due to the resistance of floors to torsion at unequal angles of rotation of cross sections of diametric walls and frames.

When diametric walls are placed symmetrically in the plan, the three dimensional problem is reduced to a two dimensional one, viz. bending of each load-bearing member from an appropriate portion of the horizontal load, the size of which is to be determined; with asymmetric location the problem is divided in two: bending and torsion, the latter being set up by torsional moments distributed along the height of the building arising from non-coincidence of the resultants of horizontal loads with the line connecting the centres of torsion of horizontal sections of buildings.

Consider briefly the torsion.

Rigid horizontal disks formed by floors do not permit the framework to deform at torsion otherwise than by rotations of all sections round the vertical axis, and so V. Z. Vlasov's theory of thin-wall systems with closed undeformed contour of the cross section may be used for design. In fact, longitudinal forces arising in the members of the framework due to torsion may be neglected too, and making use of Bredt's postulate, shear forces in the planes of frames and diametric walls on the level of each floor can be determined on the basis of the diagram of torsional moments, which is easily drawn. These forces will give rise to local bending of posts (and rafters) of frames, and in continuous vertical diametric walls shear stresses will occur due to their effects.

When designing for bending, vertical diametric walls and frames of the framework, for simplification, may be grouped into two independent blocks with summed up parameters of stiffness, viz. flexural parameters (EJ_1 and EJ_2), characterizing the resistance of elements of blocks to sectional rotations, and shear parameters (GF_1 and GF_2) showing their resistance to shear-distortions / 2 / .

The present problem comes to determining forces $q(x)$ and $m(x)$ arising at the contact between two design blocks.

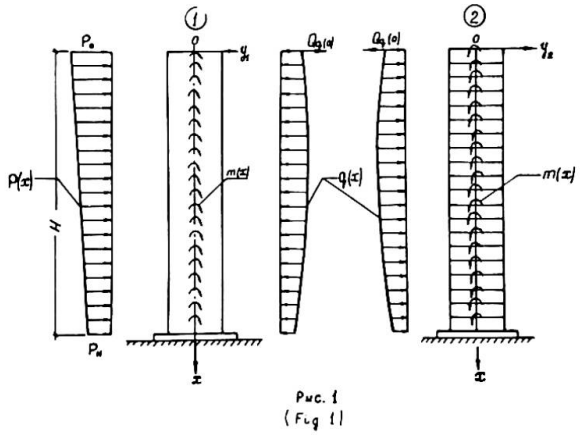

Рис. 1
(Fig. 1)

Fig. I illustrates the design scheme corresponding to the three-dimensional behaviour of structures described above with a single foundation slab under the building.

If in the design scheme the block with index 2 is the framing, then $q(x)$ is the fraction of the horizontal load resisted by the framing. Concurrently with this load there occur generally distributed bending moments $m(x)$ due to the difference in the angles of rotation of sections and resistance shown by the floors to these displacements.

Assuming the beginning of the coordinates on the upper end of the building where, as it is clear beforehand, there are no concentrated imposed bending moments, interconnected deformations of the blocks may be described by the following system of equations:

$$\begin{cases} EJ_1 y_1'' - \dfrac{EJ_1}{GF_1} M_q'' + M_q + \dfrac{EJ_1}{GF_1} M_m'' - M_m = \dfrac{EJ_1}{GF_1} |M_p|'' - |M_p|, \\ EJ_2 y_2'' + \dfrac{EJ_2}{GF_2} M_q'' - M_q - \dfrac{EJ_2}{GF_2} M_m'' + M_m = 0, \\ (y_1 - y_2) C = M_q'', \\ -\dfrac{M_m''}{\varepsilon} = \dfrac{1}{EJ_2}(M_q - M_m) - \dfrac{1}{EJ_1}(-|M_p| - M_q + M_m) \end{cases} \qquad (I)$$

In Equations (1):

M_q, M_m, M_p **are the bending moments from unknown contact forces** $q(x)$ **and** $m(x)$ **and outer load** $p(x)$ **respectively;**

$C\ [kg/cm^2]$ **is the rigidity of floors measured by the value of the linear force on contact** $\bar{q}\ [kg/cm]$ **causing reciprical transverse displacement of the blocks by a linear unit** $[cm]$ **in the direction of the force;**

$\varepsilon\ [kg\,cm/cm]$ **is the rigidity of floors thought of as longitudinal bracing measured by the value of a linear torsional moment** $\bar{m}\ [kg\,cm/cm]$ **causing torsion of the floors by an angle equal to unity.**

It should be noted that we find $M_q(x)$ **and** $M_m(x)$ **, but not directly** $q(x)$ **and** $m(x)$ **. The loads are easily determined by the formulae:**

$$q(x) = M_q''(x),$$
$$m(x) = M_m'(x) \qquad (2)$$

Solution of the system of equations (1) gives the following resolution differential equations:

$$M_m^{IV} - \left[\varepsilon\left(\frac{1}{EJ_1}+\frac{1}{EJ_2}\right)+C\left(\frac{1}{GF_1}+\frac{1}{GF_2}\right)\right]M_m^{IV} + C\left(\frac{1}{EJ_1}+\frac{1}{EJ_2}\right)M_m'' =$$

$$= -\frac{\varepsilon}{EJ_2}|M_p|^{IV} + C\varepsilon\left(\frac{1}{EJ_1 GF_2}-\frac{1}{EJ_2 GF_1}\right)|M_p|'' ; \qquad (3)$$

$$M_q = -\frac{M_m''}{\varepsilon\left(\frac{1}{EJ_1}+\frac{1}{EJ_2}\right)} + M_m - \frac{EJ_2}{\sum EJ}|M_p|$$

Boundary conditions added to Equations (3) to find the constants of integration are:

$$x=0 \qquad M_m=0, \quad M_q=0, \quad M'_q=0;$$

$$x=H \qquad M'_m=0, \quad M'_q=\frac{GF_2}{\Sigma GF}|M_P|', \quad M''_q=0.$$

The sign convention is as follows: the bending moment rotating the blocks counter clockwise and shear force of the same direction are thought of as positive. A negative sign of $M_q(x)$ **and** $M_m(x)$ **will indicate that the direction of** $q(x)$ **and** $m(x)$ **on the scheme was assumed improperly.**

When designing buildings for wind load, the latter is as a rule defined by expression $P(x)=P_0-\alpha x$ **, where** $\alpha=\frac{P_0-P_H}{H}$ **(the diagram is of a trapezium form). Floors are often taken as absolutely rigid in the plane of discs (** $c=\infty$ **) and flexible out-of-plane (** $\varepsilon=0$ **). Then** $m(x)=0$ **, the appropriate fraction of wind load resisted by the framing and forces may be determined by the formulae:**

$$M_q(x)=A\left\{\frac{B}{K}Sh\kappa x-\frac{1}{K^2}\left[(Ch\kappa x-1)+\alpha x\right]\right\}+\frac{EJ_2}{\Sigma EJ}\left(\frac{P_0x^2}{2}-\frac{\alpha x^3}{6}\right);$$

$$Q_q(x)=A\left[BCh\kappa x-\frac{1}{K}\left(P_0Sh\kappa x+\frac{\alpha}{K}\right)\right]+\frac{EJ_2}{\Sigma EJ}\left(P_0x-\frac{\alpha x^2}{2}\right);$$

$$q(x)=A\left(\kappa BSh\kappa x-P_0Ch\kappa x\right)+\frac{EJ_2}{\Sigma EJ}\left(P_0-\alpha x\right);$$

$$A=\frac{EJ_2}{\Sigma EJ}-\frac{GF_2}{\Sigma GF}; \qquad (4)$$

$$B = \frac{1}{Ch\kappa H}\left[\left(\frac{Sh\kappa H}{\kappa} - H\right)P_0 + \left(\frac{H^2}{2} + \frac{1}{\kappa^2}\right)\alpha\right];$$

$$K^2 = \frac{\frac{1}{EJ_1} + \frac{1}{EJ_2}}{\frac{1}{G \cdot F_1} + \frac{1}{G \cdot F_2}}.$$

The equation for the axis of a bent building is:

$$(\Sigma EJ)y = \left(\frac{EJ_2}{G \cdot F_2} - \frac{EJ_1}{G \cdot F_1}\right)\left[M_q(H) - M_q(x)\right] + \frac{EJ_1}{G \cdot F_1}\left[|M_p(H)| - |M_p(x)|\right] - x\left(\frac{P_0 H^3}{6} - \frac{\alpha H^4}{24}\right) + \frac{P_0 x^4}{24} - \frac{\alpha x^5}{120} + \frac{P_0 H^4}{8} - \frac{\alpha H^5}{30}. \quad (5)$$

The limit values of angles of distortion of railing structures and inner partition walls which characterize their strength and deformability, provided they are fastened rigidly to the cross frames of the framework, must not be less than the values obtained by the formulae:

$$\gamma = m_\gamma \frac{Q_q(max)}{G F_2}; \quad (6)$$

where m_γ is the safety factor stipulated by the Building Code of a particular country. The zone of the largest distortions, where $Q_q(x)$ reaches its maximum is located at one-third of the building height counting from the ground base.

To study the nature of the distribution of horizontal loads between the elements of the framework, Central Research Institute for Building Structures of Gosstroy of the USSR has carried out experiments on a large model of 30-storey buildings of an original design which were then built in a slightly changed version in Moscow / 3 /. The buildings under consideration have a broken configuration in the plan (30° angle), they consist of a rigid core, two additional vertical diametric walls on the ends of the building and framework which is enclosed between the diametric walls and the core and which bears almost all the useful load. The framework rests upon a solid foundation slab reinforced in the plane of posts of

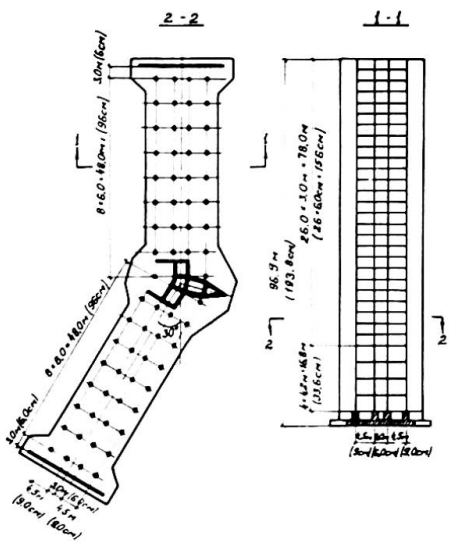

Рис 2.
(Fig 2)

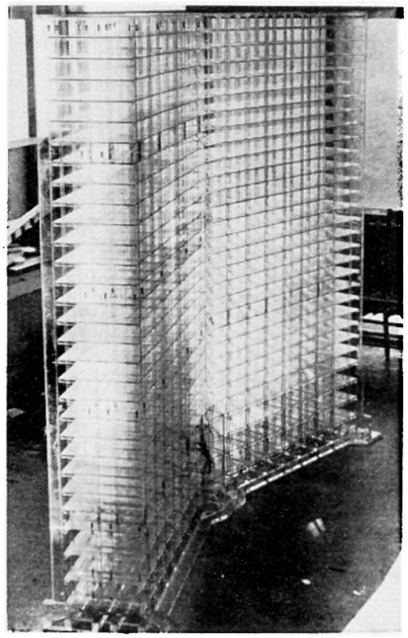

Fig. 3

frames by longitudinal and transverse ribs. Fig. 2 shows the plan and cross-section of the building, figures in brackets relate to the model.

The model was made of organic glass following the similarity conditions with the scale 1/50 (Fig. 3). The vertical load on floors was produced by small shots, and the horizontal load, the diagram of which is shown in Fig. 4, was set up through a distribution arrangement by loads hung on elastic threads pulled over pulleys.

Longitudinal deformations of the material were measured by wire strain gauges and displacements of the model were measured by indicators of 0.01 to 0.001 mm sensitivity.

The measurements have shown that transverse displacements of the model frames, core and diametric walls were practically the same. This testifies to great rigidity of discs formed by the floors despite a significant space between the diametric walls and core.

The influence of torque rigidity of the floors on longitudinal deformations of posts of frames and diametric walls has appeared to be also negligible as it should have been expected.

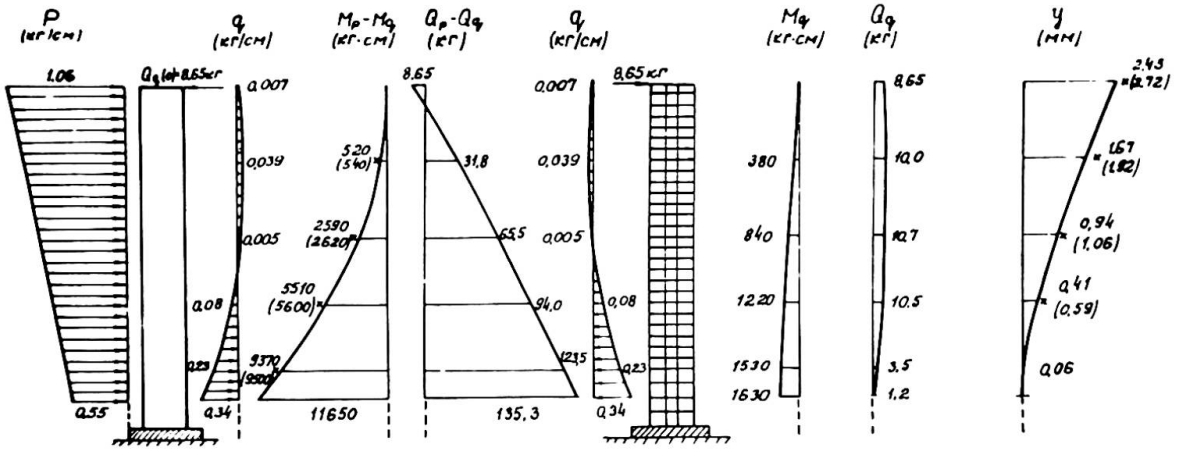

Рис. 4
(Fig 4)

The results of the design of the model under the supposition of embedment of the framework in the plane of the floor over the second floor by formulae (4), the diagrams of loads acting on framing and core, of bending moments and shear forces are given in Fig. 4. On the diagram of bending moments small crosses show the data obtained from the experiment by gauges attached to the core of the building and processed appropriately.

The data of these gauges were most stable, as well as of the indicators measuring lateral displacements; the results of measurements are also illustrated in Fig. 4 in the same way.

BIBLIOGRAPHY

1. V. Z. Vlasov, "Thin-Wall Three-Dimensional Systems", Moscow, Gosstroyisdat, 1958.

2. Transactions of Central Research Institute for Building Structures of Gosstroy of the USSR "Static Design of Large-Panelled Buildings" edited by B. A. Kositsyn, Moscow, Gosstroyisdat, 1963.

3. B. P. Voljvson, I. K. Shevchenko, D. M. Beniaminov "Model Test of a Building Being Built in Kalinin Prospect in Moscow", Moscow, Gosstroyisdat, J. Stroitelnaia Mekhanika i Raschiot Sooruzhenii, No. 5 (63), 1967.

SUMMARY

The theoretical investigations and model test results enable to conclude the following. When designing multi-storey buildings it should be born in mind that wind loads are distributed between the stiffening elements and the frames of the framework and overload the latter. The degree of the distribution of wind loads depends on the rigid characteristics of the framing and diametric walls and may be determined with a sufficient degree of precision by the approximate design method discussed in the paper.

RÉSUMÉ

Lors des calculs des immeubles géants avec des carcasses et des panneaux il faut prendre en considération les charges du vent distribuées entre des éléments de la rigidité et des portiques des carcasses ce que fait venir la sur charge les derniers. Le degré de la distribution des charges du vent dépend du rapport des caractéristiques de la rigidité des éléments de la carcasse et ce degré est déterminé avec la precision parfaite à l'aide de la méthode du calcul exposé au rapport.

ZUSAMMENFASSUNG

Man kann aus den theoretischen Untersuchungen und Versuchsergebnissen folgende Schlussfolgerungen ziehen: Bei der Berechnung der Fachwerkgebäude mit Bauplatten ist zu berücksichtigen, dass die Windbelastung eine Überbelastung des Fachwerkrahmens hervorruft und zwischen den Elementen der Steifen und des Fachwerkrahmens verteilt ist. Der Verteilungsgrad der Windbelastung hängt von dem Verhältnis der Steifigkeit der Fachwerkelemente ab und kann laut Bericht nach der Methode der Näherungsrechnung ziemlich genau bestimmt werden.

Leere Seite
Blank page
Page vide

Effects of Column Temperature, Creep and Shrinkage in Tall Structures

Effets de la température, du fluage et du retrait dans les colonnes des structures élancées

Temperatur-, Schwind- und Kriecheinflüsse in Stützen hoher Bauwerke

FAZLUR R. KHAN
Associate Partner
Chief Structural Engineer
Skidmore, Owings & Merrill
Chicago, Illinois

MARK FINTEL
Director of
Engineering Design and Standards
Portland Cement Association
Skokie, Illinois

In recent years a large number of multi-story apartment and office buildings have been built in reinforced concrete. While in the low rise buildings the effects of temperature creep and shrinkage in the columns did not substantially control the stress or design of the structure, these otherwise secondary effects may become primary and must be considered in the analysis, design and detailing of the high-rise structure. The effects of temperature, creep and shrinkage in high-rise buildings are not only structural, but also architectural in that the exterior window wall details as well as the interior partition details must be designed to incorporate relative movements caused by these factors. A brief discussion of the philosophy for planning and design procedures of high-rise buildings subjected to these effects follows:

1. Temperature Effects. Exposed columns when subjected to seasonal temperature variations change their length relative to the interior columns which remain unchanged in a controlled environment. Furthermore, if the exterior columns have difference in size and are subjected to different average temperature due to the location of glass lines, there will be relative displacement between these adjacent columns when exposed to seasonal changes.

The philosophy of design of structure with exposed columns involves one of the two basic concepts: (a) To use an effective method of analysis and design and to develop details to accommodate large expected relative movements, or (b) To plan a building for a controlled temperature movement.

When for architectural or other reasons it is not possible to limit the relative movements between the exterior column and the interior column to a reasonable value, the structural system should be analyzed by a simple and effective method such as proposed by the authors in papers published in the ACI Journal (1, 2, 3). If the analysis indicates that the stresses are acceptable and can be designed for, then only the partition details should be developed to accommodate the expected maximum distortions. However, if the initial analysis indicates extremely high stresses in the upper floors it may be advisable to hinge the floor system at the exterior columns as was done in the 38-story Brunswick Building in Chicago.

If the exterior columns are unequal in size as was used for the One Shell Plaza Building in Houston, the analysis may indicate that the glass line should be controlled in a manner that the average temperature of all the columns is approximately the same.

2. Effects of Creep and Shrinkage. With increasing height of buildings, the importance of time dependent shortening of columns and shear walls becomes more critical due to the cummulative nature of such shortening. It is known that columns with varying percentage of reinforcement and varying volume-to-surface ratio will have different creep and shrinkage strains. Increasing the percentage of reinforcement and the volume-to-surface ratio reduces strains due to creep and shrinkage. In very tall structures where a large heavy reinforced column may be adjacent to a lightly reinforcing shear wall a differential inelastic shortening causes moments in the horizontal members and also a load redistribution from the shear wall to the column which has less creep and shrinkage.

Although a large amount of research information is available on shrinkage and creep, it is not directly applicable to column of high-rise buildings but are applicable to flexural elements only. In the construction of a high-rise building columns are loaded in as many increments as there are stories above the level under consideration. Such incremental loading over a long period of time makes a considerable difference in the magnitude of creep and consequently in the differential movement and load redistribution between adjacent columns.

The significance of incremental loading was first questioned during the design of the 52-story, 715' (218m) high One Shell Plaza Building in Houston, built entirely with high strength (6,000 psi & 4,500 psi) lightweight concrete. Theoretical work to predict incremental creep was then jointly undertaken by the authors, the results of which have been submitted to ACI for publication. The Portland Cement Association at the suggestion of the senior author, undertook a series of tests with incremental loading conducted under direct supervision of Dr. Eivind Hognestad and Mr. D. Pfeifer. These results clearly pointed out the difference between the incremental loading in a column and the full load applied to a beam. The test results confirmed the authors theoretical findings indicating that the overall time vs. strain characteristics due to incremental loading surprisingly resembles the theoretical linear curve made on the basis of elastic shortening at each incremental loading. The classical creep characteristic is almost non-existent.

This linear type of creep characteristic can be translated into an "equivalent creep modulus" and can then be used to determine load redistribution between adjacent columns or columns and shear walls. Such an analysis can be made by the use of the iterative method developed by the first author (4).

References. (1, 2, 3) "Effects of Column Exposure in Tall Structures" by: Fazlur R. Khan and Mark Fintel - Part 1, ACI Journal, December, 1965; Part 2, ACI Journal, August, 1966; Part 3, ACI Journal, February, 1968. (4) "On Some Special Problems of Analysis and Design of Shear Wall Structures" by: Fazlur R. Khan - Symposium on Tall Buildings, University of Southampton, England, April, 1966.

SUMMARY

It is concluded on the basis of previous discussion that even though further research is necessary, sufficient information is now available for the design of ultra high-rise buildings in reinforced concrete to take into consideration the temperature creep and shrinkage effects both for normal weight and lightweight concrete.

RÉSUMÉ

A la suite de discussions précédentes, et malgré la nécessité de pousser les recherches, on dispose de suffisamment d'informations à l'heure actuelle pour tenir compte des effets de température, de fluage et de retrait dans les colonnes en béton armé (normal ou extraléger), dans le dimensionnement de structures très élevées en béton armé.

ZUSAMMENFASSUNG

Auf Grund vorangegangener Diskussionen und trotz der Einsicht, dass weitere Studien unerlässlich sind, kann man behaupten, dass im Moment genug Informationsmaterial zur Verfügung steht, um Temperatur-, Kriech- und Schwindeinflüsse in den Stützen extrem hoher Stahlbetonbauten, sowohl mit Normal- als auch mit Leichtbeton, bei der Bemessung zu berücksichtigen.

Leere Seite
Blank page
Page vide

Time-Dependent Performance of Reinforced Concrete Columns — Field Investigation of a 70-Story Building

Performance de colonnes en béton armé en fonction du temps — Essais sur nature d'un bâtiment de 70 étages

Zeitabhängiges Verhalten von Stahlbetonsäulen — Felduntersuchung eines 70-stöckigen Gebäudes

DONALD D. MAGURA DONALD W. PFEIFER EIVIND HOGNESTAD
Research Engineer and Manager, Concrete Products Research Section; and Director of Engineering Research (Member, U.S. Council, IABSE), resp.
Portland Cement Association, Old Orchard Road, Skokie, Illinois, U.S.A.

INTRODUCTION

Reinforced concrete buildings in the United States are being constructed to heights greater than 600 ft. (183 m). Within a story, columns shorten only a fraction of an inch. When these shortenings are added over the full height of the structure, the cumulative deformation may be several inches. Both elastic and time-dependent axial deformations of columns may therefore be important design considerations.

To determine the actual behavior of columns in tall buildings, a 70-story structure was instrumented. After columns were cast, installations were made for measuring vertical strains. These field measurements are supplemented by laboratory tests on non-reinforced specimens made with concrete taken from batches used in the building. This report describes the structure, instrumentation, laboratory tests, and initial field measurements.

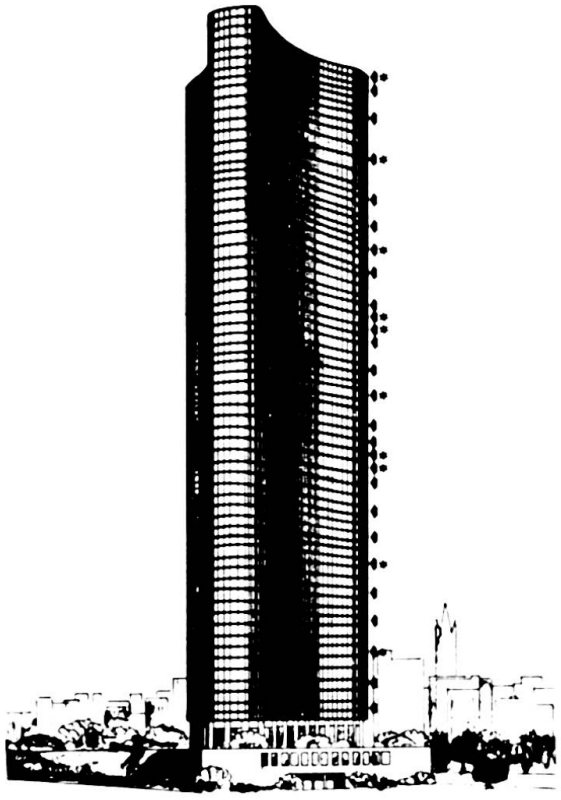

Fig. 1 - Elevation of building

DESCRIPTION OF STRUCTURE

A sketch of the structure is shown in Fig. 1. Total height above grade is 645 ft. (197 m). In plan, the building has three wings shaped as shown in Fig. 2. Each wing is 65 ft. (20 m) wide and extends 117 ft. (36 m) from the center of the building.

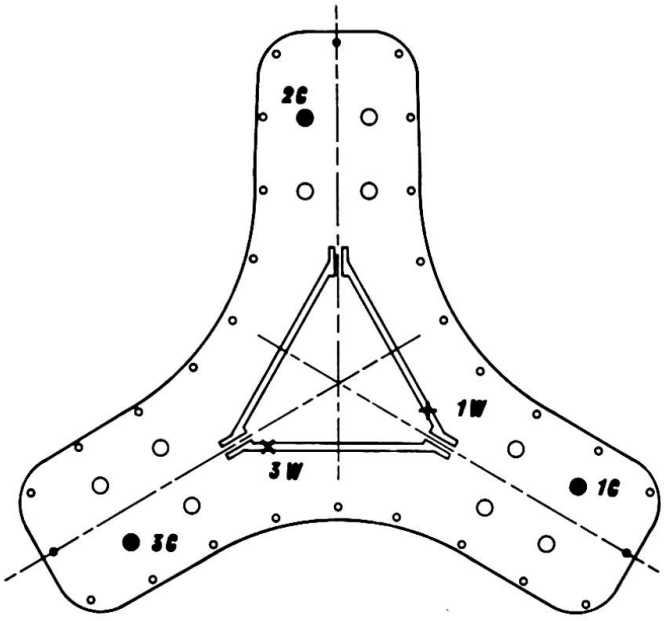

Fig. 2 - Floor Plan

The floors are flat plates 8 in. (20 cm) thick made of lightweight aggregate reinforced with high strength deformed bars. Diameter, design strength of concrete at 28 days, and design yield stress of reinforcement for the interior columns are given in Table 1. Normal weight concrete is used in the columns.

Construction of the first story of the building was started in June, 1966. The 70th story was completed in December, 1967. Weather permitting, the building was cast at the rate of one floor every three working days.

TABLE 1 -- PROPERTIES OF INTERIOR COLUMNS

Story No.	Column Diameter		Concrete Design Strength		Yield Stress of Reinforcement	
	in.	cm	psi	kg/cm²	ksi	kg/mm²
1	40	102	7500	528	75	53
11	40	102	7500	528	75	53
12	40	102	7500	528	60	42
16	40	102	7500	528	60	42
17	40	102	6000	422	60	42
29	40	102	6000	422	60	42
30	36	91	6000	422	60	42
34	36	91	6000	422	60	42
35	36	91	5000	352	60	42
43	36	91	5000	352	60	42
44	30	76	5000	352	60	42
58	30	76	5000	352	60	42
59	30	76	3500	246	60	42
68	30	76	3500	246	60	42

FIELD MEASUREMENTS

A Whittemore mechanical strain gage[1] with a gage length of 20 in. (51 cm), is used to measure vertical shortening of the columns and core walls. With an initial gage length of 20 in., the 0.0001 in. (0.0025 mm) dial gage indicates five millionths strain per dial division. Gage installations were made after the columns were cast and forms were removed. Reference discs and a portion of the Whittemore gage are shown in Fig. 3. In taking readings, the Whittemore dial gage is first set to a fixed reading over a gage length determined by a standard bar made of Invar steel. Air temperature and surface temperature of the concrete are recorded using a thermocouple connected to a potentiometer.

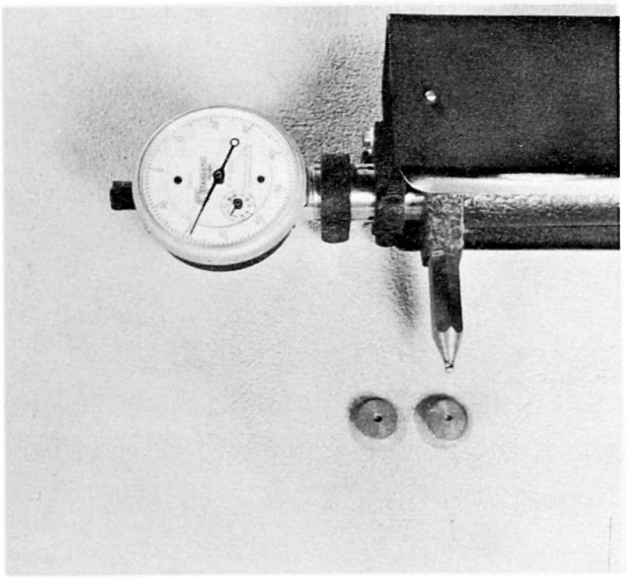

FIG. 3 - Whittemore Strain Gage

Three columns and two locations on the core wall of selected stories are instrumented. These installations are identified as 1C, 1W, 2C, 3C and 3W on Fig. 2. About every third story, Column 1C and core wall location 1W are instrumented with one gage line. Specified stories where these single gage lines are installed are indicated by arrows in Fig. 1. Asterisks in Fig. 1 indicate stories in which all three columns, each with three gage lines, and both core wall locations are instrumented. Stories above and below floors where column sizes change are monitored at installations 1C, 2C, and 3C, each with three gage lines. These gage lines are spaced at about 90 degree intervals around half the column perimeter. The more completely instrumented stories are spaced about every ten floors.

Relative humidity in Column 1C is measured with a Monfore humidity probe[2] at floors 10, 19, 43, 58 and 61. Hollow tubes are cast into these columns to permit measuring humdity at the center of the column, midway between the center and surface of the column, and about 2 in. (5cm) from the surface of the column. Temperature within the humidity wells can also be measured. Surface temperature and interior column temperature agree within ±3F (± 1.7 C).

LABORATORY TESTS

Samples of each of the four concrete mixes used in casting columns and core walls of the building were obtained and brought to the laboratory for tests. For each mix, sixteen 6 x 12-in. (15 x 30 cm) cylinders were cast at the building site. The cylinders were transported to the laboratory the day following casting. At the laboratory, the cylinders were stripped from the molds and stored at 100 percent relative humidity and 73 F (23 C) until ready for test.

Compressive strength and modulus of elasticity are measured 28, 90, and 180 days, and also one and two years after casting. At 28, 90, and 180 days, one cylinder is placed under sustained constant load to measure time-dependent shortening. The applied load produces a cylinder stress equal to 25 percent of the nominal concrete design strength. With each sustained load test, a companion cylinder having no applied load is used to measure drying shrinkage. The cylinders used in this time-dependent study are stored at 50 percent relative humidity and 73 F (23 C) once the test is started.

The coefficient of thermal expansion was measured for each of the four concrete mixes. To do this, one cylinder from each mix was taken from moist storage and sealed in copper foil. Length of these moist concrete specimens was measured at temperatures of 40, 73, and 100 F (4, 23, and 38 C).

PRESENTATION OF DATA

Because of the limited length of this paper permitted by IABSE, only data related to columns in the 1st and 30th stories will be presented and discussed. Concrete used in casting these columns are designated as A and B, respectively. Measured compressive strength and modulus of elasticity versus age for these concretes are shown in Table 2.

TABLE 2 -- MEASURED PROPERTIES OF CONCRETE

Age of Concrete	Compressive Strength, *				Modulus of Elasticity, *			
	Mix A		Mix B		Mix A		Mix B	
	psi	kg/cm²	psi	kg/cm²	10^6 psi	10^6 kg/cm²	10^6 psi	10^6 kg/cm²
28-day Design	7500	528	6000	422	5.00	0.35	4.46	0.31
28 days	7940	558	7810	549	4.80	0.34	5.01	0.35
90 days	9250	650	9530	670	5.78	0.41	4.84	0.34
180 days	9910	697	9790	688	5.84	0.41	6.16	0.43
1 year	10300	724	10210	718	6.59	0.46	6.29	0.44

* Average of two cylinders

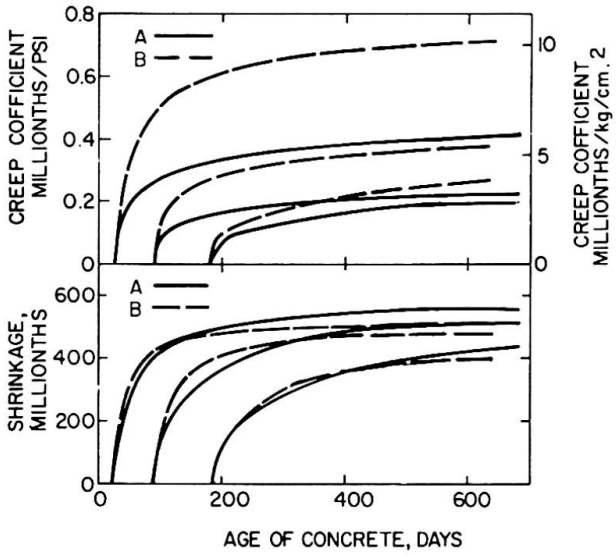

Fig. 4 - Creep and Shrinkage of Concrete

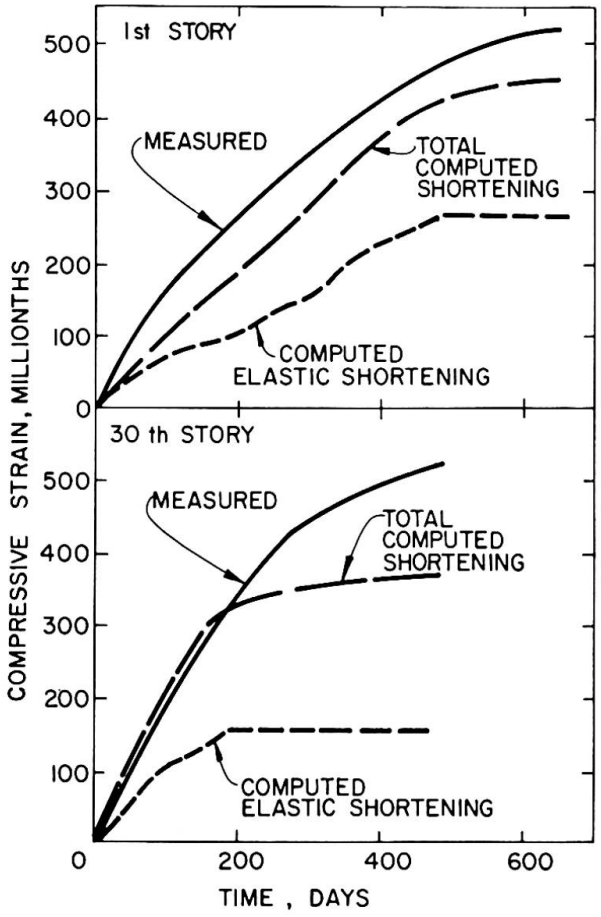

Fig. 5 - Deformation of Columns

Creep and drying shrinkage characteristics of the two field-obtained concrete mixes are shown in Fig. 4. These data are from laboratory tests of the 6x12-in. (15x30 cm) plain concrete cylinders. Cylinders were removed from moist curing and placed under test at 28, 90, and 180 days after casting.

The temperature coefficient measured in the laboratory tests was about 5 millionths per degree Fahrenheit (9 millionths per degree Centigrade). This value applies over the temperature range of 40F to 100F (4C to 38C).

Measured deformations of the reinforced columns in the 1st and 30th stories are shown in Fig. 5. The curves are the average strains for the 3 columns in each story. Strain readings are adjusted to a column temperature of 73F (23C) using the measured temperature coefficient. Temperature of the columns varied between 40F and 80F (4C and 27C) during this field investigation.

Elastic shortening was computed using the steel percentage and the measured modulus of elasticity of concrete since this value changed with time. This shortening is due to the weight of the structure alone; i. e., columns and weight of a tributary floor area used in design. Increments of load applied to a column were about 37 kips (17 t) per story. Actual time of construction was used in computing column loads. Column reinforcement was 5.5 percent in the 1st story and 3.8 percent in the 30th story.

At the end of construction, computed elastic shortening was about 260 and 160 millionths for the 1st and 30th story columns, respectively. Total measured strain was about 510 millionths in the 1st story columns at 600 days and 500 millionths in the 30th story columns at 400 days.

Relative humidity in the interior of the columns was greater than 90 percent when the column was 18 months old. Most readings at the two interior locations showed a relative humidity greater than 95 percent. Relative humidity of concrete near the surface of the column was difficult to measure accurately due to influence from the atmosphere.

TENTATIVE ANALYSIS

Time-dependent column shortening is affected by volume/surface ratio and the amount of reinforcement. By taking these two factors into account, deformation of columns in a building may be predicted from laboratory tests on small plain concrete cylinders.[3]

Hanson and Mattock[4] have shown that the amount and rate of creep and drying shrinkage of concrete decreases as the volume/surface ratio increases. Tests were made on plain concrete specimens that had volume/surface ratios from 1 to 6 in. (2.5 to 15 cm). Data from these tests were extrapolated to the volume/surface ratios of 10 and 9 in. (25.4 and 22.8 cm) for the 1st and 30th story columns. Thus, size-effects between time-dependent shortening of the laboratory test cylinders and that of the columns were determined.

Pfeifer[5] conducted tests on specimens with equal volume/surface ratio but with reinforcement varying from 0 to 8.4 percent. The tests demonstrated that time-dependent deformation decreases with increasing amounts of reinforcement. Using data from Pfeifer's tests, creep and drying shrinkage of plain concrete cylinders were related to creep and drying shrinkage of specimens with 3.8 and 5.5 percent reinforcement by interpolation. These reinforcement percentages correspond to the amounts in the 30th and 1st story columns.

Using the laboratory test data shown in Fig. 4, creep and drying shrinkage strains for concretes A and B were determined for the same time interval and stress conditions as the field measurements. These strains were modified by factors to account for volume/surface ratio and amount of reinforcement for the 1st and 30th story columns.

By this method, total computed shortenings agree satisfactorily with measured shortenings to the end of construction. Only dead load of the structure was used in computing total shortening. The differences shown in Fig. 5 between measured and computed total shortening after the end of construction may be due to live load effects.

In this tentative analysis it is assumed that effects of volume/surface ratio and amount of reinforcement may be treated separately. It is also assumed that the factors determined for these two effects can be applied to any concrete mix. The extensive test data obtained during this long-time study should permit evaluation and improvement of this analysis.

CONCLUDING REMARKS

The data described and presented in this report are examples of the initial results of a long-term study. It is intended that these measurements of the behavior of the building will be continued for ten years after construction began. Such information should lead to methods of closely predicting the performance of actual structures.

ACKNOWLEDGMENTS

These tests are being conducted with the cooperation of William Schmidt and Associates, Structural Engineers; Schipporeit/Heinrich, Architects; Harnett-Shaw and Associates/ Fluor Properties, Inc., Developers; Crane Construction Co., Inc., General Contractors; and Lake Point Tower Ltd., Owners. The field and laboratory program is being directed by personnel of the Concrete Products Research Section and the Structural Research Section of the Portland Cement Association. Particular credit is due Bernard J. Doepp and Eugene A. Valko, Technicians.

REFERENCES

1. Hanson, N.W. and Kurvits, O.A., "Instrumentation for Structural Testing," Journal of the PCA Research & Development Laboratories, 7, No. 2, 24-38 (May 1965); PCA Development Bulletin D91.
2. Monfore, G.E., "A Small Probe-Type Gage for Measuring Relative Humidity," Journal of the PCA Research & Development Laboratories, 5, No. 2, 41-47, (May 1963); PCA Research Bulletin 160.
3. Khan, F.R. and Fintel, M., "Effects of Column Creep and Shrinkage in Tall Structures -- Prediction of Inelastic Column Shortening," Proceedings ASCE Jt. Specialty Conference (EMD-STD), 17-20, Chicago, Illinois (April 1968).

4. Hansen, T. C. and Mattock, A. H., "Influence of Size and Shape of Member on the Shrinkage and Creep of Concrete," Journal of the American Concrete Institute, 63, No. 2, (February 1966) 267-290; PCA Development Bulletin D103.

5. Pfeifer, D. W., "Reinforced Lightweight Concrete Columns," to be published in Journal of the Structural Division, American Society of Civil Engineers.

SUMMARY

A 70-story reinforced concrete building has been instrumented to obtain measurements of time-dependent deformation of columns and core walls. Standard laboratory tests are being conducted on cylinders of concrete taken from batches used in casting the structure. Measurements of column shortening at two levels in the building and of characteristics of the concretes used are presented. It is intended that measurements will continue for a total of ten years after construction began. These tests should provide a correlation between laboratory test data and the performance of prototype buildings.

RÉSUMÉ

Un bâtiment en béton précontraint de 70 étages a été équipé d'instruments pour obtenir des mesures des déformations en fonction du temps sur les colonnes et les murs du noyau. Des tests de laboratoire standards sont faits sur des cylindres de béton pris des mêmes mélanges. Les mesures des raccourcissements des colonnes à deux niveaux du bâtiment et des caractéristiques des bétons utilisés sont présentés. On a l'intention de continuer les mesures pendant 10 ans depuis le début de la construction. Ces tests devraient permettre une comparaison entre les données déterminées au laboratoire et la performance de bâtiments-type.

ZUSAMMENFASSUNG

Ein siebzigstöckiges Stahlbetongebäude wurde mit Instrumenten dergestalt ausgerüstet, dass Messungen über zeitabhängige Verformungen von Säulen und Kernwänden angestellt werden konnten. Standardversuche wurden an Betonzylindern aus im Bauwerk gebrauchten Teilen durchgeführt. Es werden die Messungen der Säulenkürzung auf zwei Höhen des Gebäudes und die Betoncharakteristiken angegeben. Es ist beabsichtigt, die Messungen über zehn Jahre nach Baubeginn durchzuführen. Diese Prüfungen sollten eine Beziehung zwischen Laborversuchen und der Verformung am Versuchsgebäude ergeben.

Basic Design Considerations for the Moscow 533 Metre T.V. Tower

Considérations principales pour le projet de la tour de télévision à Moscou, 533 m haute

Grundsätzliche Berechnungsprinzipien für die Projektierung des 533 m hohen Fernsehturmes in Moskau

N.V. NIKITIN
USSR

Construction of a new 533 m TV tower was terminated at the end of 1967 (Fig.1).

Up to the level of 385 m the tower is a cone prestressed reinforced concrete tube with a sharp break in its generating line at the height of 63 m. The lower part of the cone rests on foundation containing ten separate supports which form ten open arches 17 m high each.

Beginning from the height level 385 m to 533 m (148 m) a steel telescopic pipe shaft is situated which carries radio aerials as well as TV antennas.

Within the cone and the shaft of the tower 48 floors of various premises are situated, floors N°, 5, 6, 7 are occupied by the radio transmitting station. Partially the radio transmitters are located in the upper part on the level of 348 and 353 m. Simultaneous transmission of 5 television programs is secured (one of them is in technicolour) and 6 radio programs on ultrashort wave lengths. The height of the antenna guarantees secure reception of TV and radio broadcasting programs at a distance of 120-150 km.

Three floors at the height levels 328, 331 and 334 m are taken by the restaurant. Simultaneously the restaurant can serve 288 persons. The tables are placed on the circular revolving floor.

At the height levels of 147, 269, 337 and 341 m the obser-

vation towers are located. Three of them are closed and the upper one is open (Fig.2).

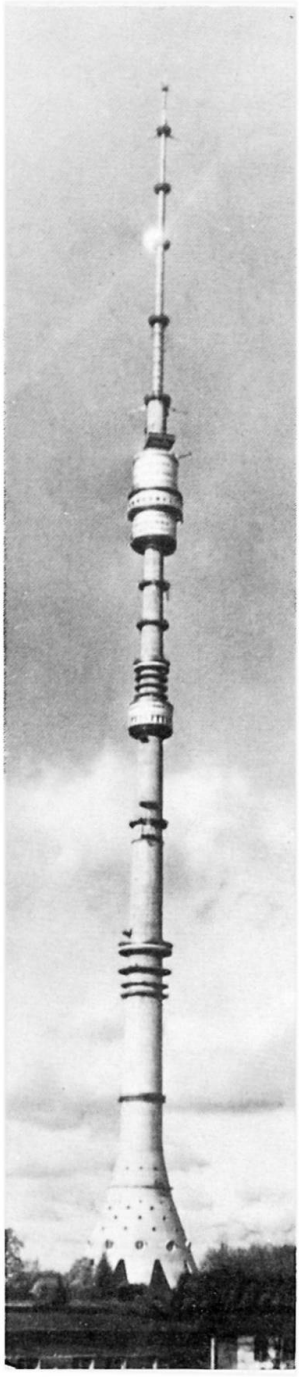

In the shaft there are 4 elevators. One of them serves the restaurant. The rise and descent takes 150 sec. at a speed of 7 m/sec.

In the shaft proper and around it on the platforms numerous technical services are located such as a receiving station for subsequent retranslation of the TV programs, meteorological apparatus, signal lights, laboratory for lightning discharges and radio relay line antennas. The shaft of the tower on top of this contains all kinds of communication, wiring for radio, TV transmissions, electric conduits, water supply pipes, sewerage and telephone.

The architectural outlook of the tower considerably is determined by the technical requirements. The lower part has large openings and being left free reveals the structural design. On this elevation the cross-section of the shell is represented. The concrete surface of the tower is left unpainted in order to better reveal the type of material used. The light aluminium constructions contrast well with rough concrete shell. The interior decoration contains modern materials: aluminium, glass, plastics.

The Basis and Foundation

On the building site the subsoil conditions are the following from top to bottom: 10-12 m of very dense loamy soil of the glacial period containing pebbles and bolders, water is at a depth of 5-6 m, further down 12-15 m more ancient deposite in form of fine dusty sands and sandy soil. Further down old dense clay and only at a depth of 40 m - rock. Under the above-mentioned circumstances it was decided to rest the tower on the upper loams with the minimum depth of foundation in order to leave as much as possible the layer of good soils between the lower part of the foundation and relatively weak lower sandy soils saturated with water.

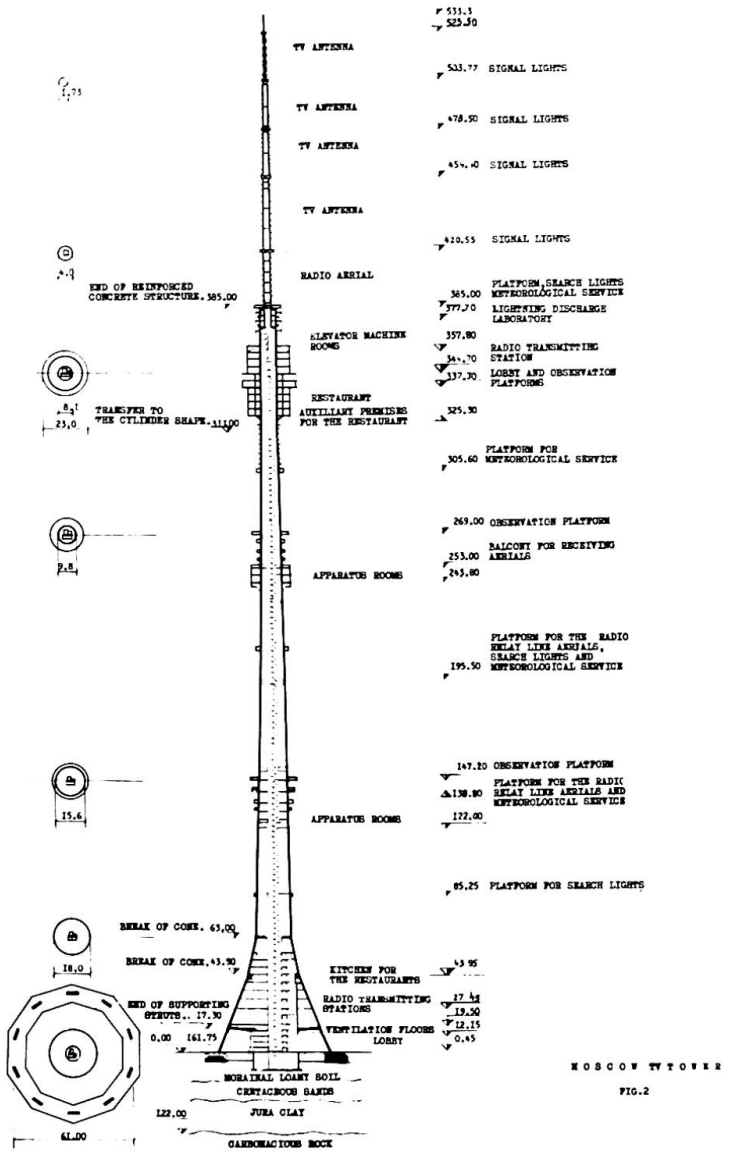

MOSCOW TV TOWER
FIG.2

The foundation of the tower has the form of 10-sided polygonal ring slab with an average diametre - 60 m, width 9.5m and the thickness 3 - 5.5 m.

When testing the soils by the method of loading the punch with the area of 600 cm^2 in the pits we have received the following values of the modules of deformation: morainal soil 800-900 kg/cm^2, underlying sand soils, loamy soils 300-400 kg per sq cm and the lower jura deposits - 300 kg per sq cm. The sedimentations of the foundations were determined at a usual supposition that the stresses under the foundation are being distributed as in a elastic homogeneous half shere 5 - 6 cm, what at subsequent observations was found to be true. Such sedimentation has no importance as far as the construction is concerned. The statical design of the foundation was carried out assuming the design scheme to be a ring continuous 10 span beam with a hinged support with a given load as the reaction of lower soils with the flat distribution of the load.

As a principal scheme for designing such a beam it is convenient to adopt a 10-sided polygon with the hinges in the middle of each side (Fig.3).

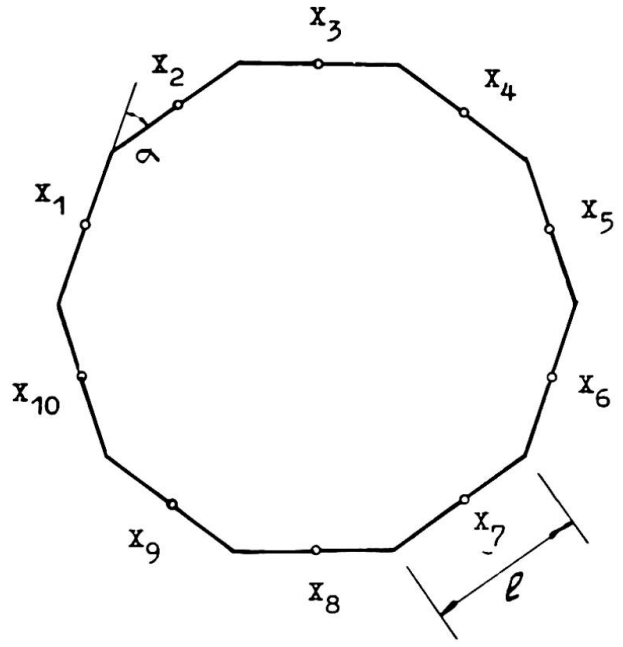

FIG.3

The hinges allow free rotation around the axis of the rod, that is they exclude the torsion moments but do not allow any shear or rotation around the axis perpendicular to the axis of the rod. In other words the hinge would allow the bending moments and the shearing stresses to appear. Under this assumption the design is reduced to solution of a system of five-member equations.

$$-x_1-2\cos\alpha x_2+(4+2\cos^2\alpha+f)x_3-2\cos\alpha x_4-x_5+$$
$$+a_{3p}+a_{35}+a_{3m}=0$$

where x are unknown torsion moments in the hinges

$$f=\frac{6\sin^2\alpha EJ}{GJ_k}$$

where E and G are modules of elasticity and shear of the concrete; J and J_k – bending and torsion moments of inertia; $a_{35}a_{3p}a_{3m}$ – the load members from the vertical loads, from the junction loads and from the uniformly distributed torsion moments.

The total weight of the tower is 31400 tons, the foundation 14500 tons soil on the foundation 5500 tons. All these loads produce stresses under the foundation equal to 2.64 kg/cm^2. The side stresses from wind loads are equal to 0.42 kg/cm^2.

When designing the foundation the necessary measures were taken to increase its durability and safety. The concrete used had according to our standards strength N^o 400, the main and cross reinforcement was increased. The protecting layer was increased to 10 cm. Along the perimetre of the foundation the reinforcement was prestressed and was formed by 10 strends according to the

number of sides of the foundation polygon. Every strend has 104 wire cables containing each 24 wires 5mm in diametre. This reinforcement was prestressed by means of jacks each one developing the stress of 57 tons in the cable. Thus, in the foundation a prestressing force was created by compression equal to 5900 tons. This prestressing permitted to reduce the tension in concrete to such a value under which one does not have to expect appearance of cracks.

Supports, the Cone and Shaft

In the cone there are 10 round openings 4 m in diametre each as well as a considerable number of other smaller ones. Over the openings special reinforced concrete awnings are provided to protect from possible fall of icicles.

At the height level 63 m a very powerful diaphragme was introduced, further on up the shaft of the tower is a cone shell with the slant of the generating line equal to 2% compared with a vertical line. The diametre of the shaft is being reduced from 18 m at a height level 63 m to 8 m at the level 311 m, further up the shaft has a cylindrical form. The thickness of the shell of the shaft within the entire cone part is constant and equal to 40 cm. In the cylindrical part it is 35 cm.

The aerial consists of 5 cylindrical sections having the following diametres: 4.0 m; 3.0 m; 2.6 m; 1.72 m; 0.72 m with the lengthes from 19 to 36 m. The sixth section 8 m long has a square cross section 16x16 cm. The sections of the aerial have the thickness from 30 to 12 mm. Inside the aerial are located the feeders from the radio transmitting sets and a lift designed for one person. The last stop of the lift is at a height of 470 m. At the sections where the cross section of the aerial is changing the ring platforms are located. To these balconies special suspended platforms are affixed. By means of these suspended platforms the possibility to reach any external point of the aerial surface is secured. The aerial is protected from corrosion by means of galvanized zinc layer or plastic materials.

The total weight of the aerial is 360 tons.

The Strends for the Prestressing of the Structure

In order to increase the rigidity and to avoid appearance of cracks the shaft of the tower was specially prestressed to create

compression in the concrete in the vertical direction. This was provided by means of a series of strends prestressed parallel to the inner surface of the shaft. Altogether there were 150 strends stressed. Thirty strends are fixed at a height of 63 m and 120 strends at a height of 43 m. At the upper part these strends are gradually fixed at 7 different horizons beginning from the height of 195 m and to the upper part only 60 strends are reaching.These strends are embedded into the ring cantilevers. The strend having a diametre of 38 mm consists of 259 wires 1.8 mm in diametre each. The wires have high quality zinc coating.

Each strend is prestressed with a force equal to 72 tons. The total stress of these strends in the lower part of the shaft reaches 10800 tons.

After the final stressing the strends were brought close to the walls of the shaft and affixed at the intervals of 7 m to the wall of the shaft. This is important since the affixed strends work as reinforcement and the strends not affixed to the walls keep their normal stress unchanged. This fact helps to gain around 10% in the safety factor.

Wind loads

When designing this tower the wind pressure was taken into consideration according to the usual norms for similar structures increased by 8%. The following wind velocities were considered:

Height above the ground level	10	20	40	100	350 and higher
Velocity in m/sec	24.7	28.7	33.1	36.6	42.7
m	0.35	0.35	0.32	0.21	0.10

Besides the statical wind load which corresponds to the above given velocities a frontal dynamic wind pressure is taken into consideration. The dynamic wind pressure is being evaluated through the coefficient ζ added to the statical pressure. By means of this coefficient the distribution of the dynamic part of the wind pressure along the height is calculated. The type of change of load pressure in terms of time is evaluated through a dynamic coefficient which is a function of the period of oscillation of the structure and its material. Having two different materials such as: reinforced concrete shaft and steel aerial the dynamic co-

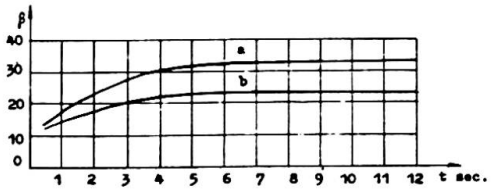

a- for metal and timber structures
b- for reinforced concrete structures

FIG.4

efficient is determined by means of interpolation- proportional to the quantity of the potential energy stored during the oscillations of the steel and reinforced concrete parts of the structure (Fig.4ab).

$$Q_m = \int \frac{M^2}{2EJ_c} \, dx$$

Aerodynamic coefficient for the cylinder part is assumed to be equal to 0.6, for all sorts of protruding parts - 1.00. At that the wind load was assumed acting on all protruding parts along the entire perimetre.

Besides longitudinal oscillations in the direction of air pressure the resonance transversal oscillations were also considered which occur through periodical cessations of wind vortexes.

The critical velocity of air which leads to a resonance of the vortex cessation and proper oscillations of the structure can be determined by the formula:

$$V = \frac{5D}{t}$$

where D is the diametre of the tower

t - period of oscillation

The amplitude of the transversal aerodynamic force is determined by the formula

$$F = \frac{V^2 D}{80}$$

When determining the full resonance amplitude the damping of oscillations on account of friction is taken into consideration. The logarithmic decrement is assumed: for steel structures 0.10 and for the reinforced concrete structures 0.30. The mixed structure is being calculated through the interpolation similar to the design of frontal oscillations.

In connection with the very large period of fluctuation of transversal oscillation for the tower the latter ones were found to be considerably less than frontal oscillations although the

resonance was considered to appear along the entire height of the tower.

The Dynamic Design

When making the dynamic design the tower was modeled in the form of a cantilever rod with the 24 concentrated loads (masses) and 24 elastic hinges in the same points where the concentrated loads were applied. By means of consecutive approach method the forms of free oscillations were determined together with the amplitude of acceleration at the top level of the tower which was equal to the acceleration of the gravity force further called unity oscillations.

In this case the inertia forces at the time of maximum deviations are determined by the formula:

$$T = G \frac{Y}{f} = G\lambda$$

where G is concentrated mass; Y - deviation of the mass;
f - deflection of the upper point of the rod.

Having assumed in the first approximation the diagram of deflections in form of a parabola the inertia forces T are determined and on the basis of these diagrams we determine the diagram of deflections. By means of the following procedure we gradually approach the diagram of deflections. After the fourth attempt we have come to a satisfactory precision.

After the unit form of oscillation has been determined the period of fluctuations can be determined by the formula:

$$t = \sqrt{\frac{4\pi^2 f}{g}} = 0.2\sqrt{f}$$

where f is in cm.

When determining the second harmonic the basic curve was reduced to orthogonal position with the first one.

$$Y_1^{I} = Y_o^{I} - a\lambda^{II}$$

where

$$a = \frac{\Sigma T^{I} Y_o^{II}}{\Sigma T_1^{II} \lambda^{I}}$$

When determining the third harmonic the original curve was reduced to the orthogonal position with the two first ones

$$Y_1^{III} = Y_o^{III} - a_1\lambda^{I} - a_2\lambda^{II}$$

where

$$a_1 = \frac{\xi T^I Y_o^{III}}{\xi T^I \lambda^I} ; \quad a_2 = \frac{\xi T^{II} Y_o^{III}}{\xi T^{II} \lambda^{II}}$$

The amplitude of oscillations and the accompanying stresses can be determined by the formula:

$$K^n = \eta \beta k^n$$

where K^n is deviations and stresses according to harmonic n-power, k^n - the same deviations and stresses in the singular harmonic; β - the mentioned above dynamic coefficient; η - the influence coefficient

$$\eta^n = \frac{\xi P^n \lambda^n}{\xi T \lambda^n}$$

where P^n - the load applied at the point n; λ^n - relative deviation at the singular harmonic n.

Summing up of all the amplitudes of all harmonics is done by means of the square root:

$$K = \sqrt{(K^I)^2 + (K^{II})^2 + (K^{III})^2}$$

The Static Design

The static design was carried out on the basis of deformed scheme, i.e., all bending moments from the vertical loads were taken into consideration, bending moments which appear on account of deflection of the shaft. The deflection of the shaft taken into consideration gives us increase of the bending moments up to 10-15%.

Since the design was carried out on the basis of the deformed scheme separate design for stability was not performed.

A special design for the season fluctuations of the temperature was performed. It was assumed that the foundation has permanent temperature but the cone and supports can be heated up to + 30°(C) and cooled up to -30°(C). This design led us to the necessity to make the supports of the tower flexible in the radial direction.

Strength, Stability and Crack Resistance Design

The strength design of any usual structure is being carried out by means of comparison of stresses caused by the designing

loads having considerably small probability together with the limit stresses which the structure can receive. In this case a reduced stress compared to the nominal strength of materials of the structure is taken into consideration.

For the tower such an approach was found to be nonconvincing. There is a definite assurance as far as the size of the normal stress is concerned, stress which is caused to 95% by the weight of the entire structure. The quality of building materials were under a very thorough observation and there is no doubt in total reliability of the concrete and reinforcement's strength. Still doubtful is the correct choice of the designing wind load as well as the correct determination of breaking stress in the ring section. In connection with this the following condition of the rigidity of the shaft was adopted: the breaking bending moment in each section was determined under the given permanent normal force, must be twice the size of the bending moment caused by the wind load. The breaking bending moment in the section of the shaft of the tower is determined under the assumption that in the part of the ring section the concrete is stressed and these stresses reached the prismatic strength; and in the reinforcement they reached the ultimate compression strength in concrete (0.2%) $R^1a = 4000$ kg/cm^2.

In the tensile zone the concrete resistance was not taken into consideration and the reinforcement was considered to have the yield point at $R_a = 4600$ kg/cm^2. This conventional yield limit somewhat exceeds the reject minimum (4000 kg/cm^2) and approaches the average statical. It is assumed that the following distribution of stresses will take place along the cross section (Fig.5). In the compressed zone (φ) the stresses in concrete and in the reinforcement are uniform (the orthogonal diagram); in the tensile zone (ψ) as well. Between the compressed and tensile zones it is assumed that a neutral zone is located in which neither concrete nor reinforcement are stressed.

It is assumed that the strends in the tensile zone have a stress limit that is $R_H = 19200$ kg/cm^2; and in the compressed zone

$$\sigma_c^1 = 19200 - 4000 \frac{1.5 \times 10^6}{2.0 \times 10^6} = 6200 \text{ kg/cm}^2$$

and in the neutral zone the stress in strends is assumed to be equal to original minus the losses $\sigma_c = 11050$ kg/cm^2.

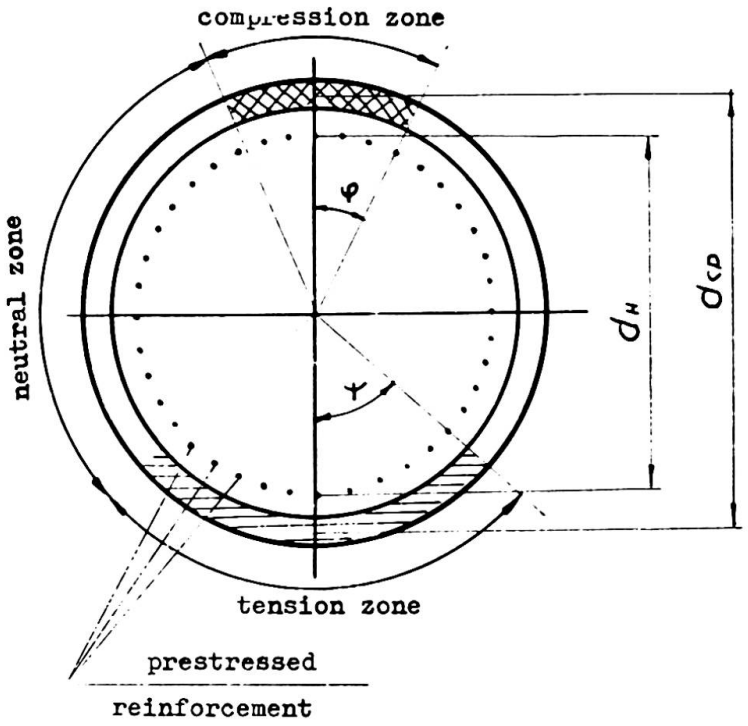

FIG.5

The size of the tensile zone is selected in such a way that it must satisfy the following conditions: $S_\delta = 0.8\, S_o$, where S_δ - the statical moment of compressed zone calculated in relation to the centre of gravity of tensile zone, S_o - the statical moment of the entire area of concrete situated above the centre of gravity of the tensile zone, related to this centre.

From this condition we receive an equation to determine the size of the tensile zone depending on the size of the compressed zone

$$\varphi\left(\frac{\operatorname{Sin}\varphi}{\varphi} + \frac{\operatorname{Sin}\Psi}{\Psi}\right) = 0.8\ \left(\frac{\operatorname{Sin}\theta}{\theta} + \frac{\operatorname{Sin}\Psi}{\Psi}\right)$$

This equation is invariant to the reinforcement of the normal force/diametre.

Solving this equation we can compile the following table which gives us the values of the compressed and tensile zones:

φ	<1.28	1.29	1.31	1.33	1.35	1.37	1.39	1.41	1.43
Ψ	1.55	1.46	1.37	1.28	1.19	1.10	1.00	0.89	0.77

The size of the compressed zone can be determined from the condition of equilibrium of all stresses acting in the cross section:

$$\varphi = \frac{N + d_{cp} f_a R_a \Psi + d_H f_n \left[\pi\sigma_o + \Psi(R_H - \sigma_o)\right]}{d_{cp}\delta R_{np} + a_{cp} f_a R'_a + d_H f_H (\sigma_c - \sigma'_c)}$$

After this the breaking moment

$$M_p = \tfrac{1}{2} d^2_{cp}\delta R_{np} \operatorname{Sin}\varphi + \tfrac{1}{2} d_{cp} f_a (R_a \operatorname{Sin}\Psi + R'_a \operatorname{Sin}\varphi) + \tfrac{1}{2} d^2_n f_n \times$$
$$\times \left[(R_H - \sigma_c)\operatorname{Sin}\Psi + (\sigma_c - \sigma'_a)\operatorname{Sin}\varphi\right]$$

where N is normal force in the cross section; f_a, f_n - the cross section area of unstressed and stressed reinforcement related to

the unity of the perimetre. The crack resistance design was carried out in the elastic state. At the wind load equal to 0.75 of assumed there was no tensile stresses allowed in the concrete.

The Design Data and Observations

For the three forms of harmonic oscillations the periods of the fluctuations were determined at 13.1 seconds, 4.6 seconds and 2.7 seconds.

Actually the period of fluctuations was found to be 11.3 sec in the main form. This fact shows that the rigidity of the shaft was 1.35 times underestimated. When designing the fluctuations the module of deformation of concrete was also reduced; it should have been taken considering the age of concrete at the impact load equal to 390000 kg/cm^2, actually was taken 300000 kg/cm^2. Evidently all numerous elements filling the tower inside as well as external constructions participated in the total work.

As a nominal wind load it is assumed by the norms such a probable wind load which is equal to 1/7300, i.e., such a load which would be surpassed on the average during 1/7300 of the considered period of time, for instance, during 1.2 hours a year. At this wind velocity according to the design the statical deflection of the upper part of the tower will be equal to 5.8 m, the amplitude of fluctuations according to the first form 1.4 m, the second - 1.1 m and the third 0.2 m.

It can be expected that the actual deflections of the tower will be less than mentioned above since the rigidity of the entire structure was not taken into account in design.

A one-sided heating by the sun was also taken into consideration. According to design the deformation must reach 3.3 m. The small amount of observations carried so far give somewhat smaller value.

During the 24 hours the upper part of the tower moves along a very complicated closed curve with a maximum diametre of 2.5 m.

There were apprehensions that the visitors of the tower would experience large and unpleasant fluctuations of the tower. The experience showed that visitors do not feel any of those fluctuations.

A very vast program of observation of the condition of the structure was organized. The wind velocity is being measured at various heights. Deformations, oscillations of the tower, conditions of the concrete, lightning discharges, the status of the

prestressed strends as well as sedimentation and deformation of the soil under the structure are also being observed and measured.

SUMMARY

In the design of the Moscow prestressed r.c. 533 m TV tower both static and dynamic effects of the wind load were taken into consideration. Three forms of harmonic oscillations were determined. The amplitudes of frontal and transversal fluctuations were also found. The design was based on the deformed scheme. The s strength computation was performed at the failure stage. Crack resistance and rigidity were determined at the elastic stage.

RÉSUMÉ

Pour le calcul de la tour de télévision a Moscou, 533 m haute et construite en béton armé précontraint, les effects statiques et dynamiques de la force du vent ont été pris en consideration. Trois formes des oscillations harmoniques et les amplitudes des divergences frontales et transversales ont été déterminées. Le schéma déformé a été adopté pour les calculs. La résistance de la structure a été calculée pour l'état de destruction, la résistance à la fissuration ainsi que la rigidite pour l'état d'élasticité.

ZUSAMMENFASSUNG

Bei der Projektierung des 533 m hohen Turmes aus vorgespanntem Stahlbeton in Moskau wurden die statischen und dynamischen Wirkungen der Windbelastung in Betracht gezogen. Es wurden drei Formen von harmonischen Schwingungen festgelegt und die Amplituden der Frontal- und Querschwingungen bestimmt. Die Berechnungen wurden auf Grund eines deformierten Schemas vorgenommen. Die Widerstandsfestigkeit wurde auf dem Stadium der Zerstörung, die Rissfestigkeit und Steifigkeit auf dem Stadium der Elastizität berechnet.

Leere Seite
Blank page
Page vide

DISCUSSION LIBRE / FREIE DISKUSSION / FREE DISCUSSION

Contreventement des structures spatiales raidies

Windverband in versteiften Raumtragwerken

Wind-Bracing in Spatial Structures

M.A. BOUDAKIAN
Ingénieur des Arts et Manufactures
(S.N.C.T. et S.N.E.F.R. – FRANCE)

Le très intéressant exposé présenté par M. NELSON sur la méthode de MM. COULL et IRWIN pour la détermination de l'effet des charges horizontales sur les structures étagées me donne l'occasion de vous faire part de mes propres recherches concernant ces questions.

J'ai été amené à aborder ce problème lors de la conception et de la construction par les Etablissements FOURRE & RHODES, de la Tour Aquitaine près de Paris. Cet immeuble, qui a 116 mètres de hauteur depuis sa fondation, a été achevé en 1966, en ce qui concerne le gros-oeuvre. C'est le premier ouvrage de cette hauteur construit en France entièrement en béton armé.

Ce type de construction devenant de plus en plus fréquent, j'ai été amené, depuis, à développer la théorie initialement ébauchée, de façon à permettre d'aborder le problème du contreventement des tours en béton armé avec plus de généralité.

Il est permis de cette façon de considérer, non plus seulement des ossatures constituées par des voiles parallèles, mais plus généralement des structures comportant des voiles porteurs dont le profil en section horizontale peut épouser n'importe quelle forme, aussi bien rectiligne que courbe ou brisée, ces profils pouvant d'ailleurs être ouverts ou fermés.

De plus, ces voiles peuvent être reliés entre eux par des linteaux dont la disposition en projection horizontale est quelconque.

On voit qu'une telle généralisation est nécessaire si l'on veut laisser une certaine souplesse au plan d'architecte et profiter pleinement des possibilités plastiques du béton armé (l'adjectif étant ici pris dans son sens esthétique).

La solution du problème ainsi posé n'est pas très différente de celle qui a été présentée par MM. COULL et IRWIN, ou de celle qui est connue en France sous le nom de "Méthode de MM. ALBIGES et GOULET". On aboutit en effet dans toutes ces méthodes à une équation différentielle, dont le premier membre comporte deux termes (le terme d'inertie et le terme de raideur) et dont le second membre correspond à la loi de distribution des forces horizontales données sur la hauteur de la Tour.

Le terme d' inertie du premier membre est relatif à la torsion-flexion des voiles (ou groupes de voiles adjacents), en l'absence de linteaux de liaison.

Le terme de raideur du premier membre est dû à la présence de ces linteaux, ainsi que de profils fermés éventuels constitués par les voiles.

Dans le cas le plus général, le nombre des équations différentielles est de trois. Elles correspondent respectivement aux deux composantes de l'effort tranchant d'ensemble dû aux forces horizontales extérieures, et au moment de torsion dû à ces mêmes forces.

La résolution de ce système de trois équations différentielles s'effectue aisément, lorsque l'on choisit un système d'axes de référence approprié.

Nous espérons publier très prochainement l'étude dont je viens de vous entretenir. Je suis à la disposition des personnes ici présentes qui pourraient souhaiter obtenir des précisions complémentaires sur ce sujet.

Remarques sur le fluage dans les ossatures en béton armé

Bemerkungen über das Kriechen in Eisenbeton-Stockwerkrahmen

Observations Related to Creep in Reinforced Concrete Framed Structures

AUREL A. BELES
Professeur-Ingénieur
Membre de l'Académie des Sciences de
Roumanie

Le problème du fluage peut revêtir des aspects intéressants surtout dans les bâtiments de grande hauteur à ossature en béton armé qui se manifeste dans les piliers soumis à de fortes charges permanentes.

C'est à l'occasion de l'anniversaire de 50 ans de la fondation du " DEUTSCHER BETON-VEREIN " que le Professeur Emil Mörsch a mis en évidence l'effet du fluage sur la redistribution des efforts dans les piliers en béton armé.

Ayant mis sous charge 2 piliers en béton armé , l'un ayant 2,7% d'armature et une charge de 70 tonnes, l'autre 5,5% et une charge de 100 tonnes, il put constater, après trois années, que le premier marqua une réduction des contraintes du béton qui tombèrent de 54 kg/cm^2 à 14,3 kg/cm^2 et une augmentation dans l'acier de 1155 kg/cm^2 à 2565 kg/cm^2. Le second pilier indiqua de même une réduction des contraintes du béton de 54,5 kg/cm^2 à 0,5 kg/cm^2 et en échange l'augmentation des contraintes dans les armatures qui passa de 1170 kg/cm^2 à 2100 kg/cm^2.

Evidemment une redistribution des contraintes se produit effectivement dans les éléments des constructions, mais , à ma connaissance, une pareille constatation vérifiée en pratique n'est pas mentionnée dans la littérature de spécialité.

Je voudrais en donner un exemple intéressant. Un bâtiment ayant rez-de-chaussée et 8 étages avait au rez-de-chaussée des piliers en béton armé, recouverts de placage en travertin, qui étaient exposés aux intempéries.

Construit vers 1935, le bâtiment se comporta très bien quoiqu'il subit en 1940 l'action d'un tremblement de terre qui causa de nombreux dégats dans la ville et en outre il fut incendié aux étages supérieurs pendant la dernière guerre mondiale.

Approximativement 30 années après son éxécution, on con-

stata une dislocation du placage due à la corrosion des armatures des piliers et on décida d'enlever le placage de tous les piliers. Tandis que j'assistais à cet enlèvement j'aperçus que les barres longitudinales, au fur et à mesure qu'elles étaient mises au jour prenaient une légère courbure entre les étriers. Cette courbure était d'autant plus prononcée que la corrosion était plus accentuée et que la distance entre les étriers était plus grande.

Pour l'une des barres, dont la corrosion était plus accentuée, c'est à dire le diamètre plus réduit, la courbure se produisit après l'enlèvement du placage et atteignit une flèche d' approximativement 1 cm. en plusieures secondes pour s'arrêter ensuite définitivement.

En tenant compte de l'ensemble des faits il semble évident que pendant les 30 années de charge, par suite du fluage, une redistribution des efforts entre le béton et les armatures s' était produite et les contraintes dans les barres longitudinales des piliers avaient dépassées les valeurs initiales qui étaient de l' ordre de 1000 kg/cm^2. Le fait que les barres commençaient à flamber dès qu'elles étaient mises au jour et la déformation latérale était d'autant plus grande que la section était plus réduite par suite de la corrosion et la longueur de flambement plus grande par suite de l'espacement plus grand des étriers, est une indication que les contraintes dans les barres avaient dépassées la valeur critique de flambement ce qui a été confirmé par un calvul.

Je voudrais remarquer que lors de certaines réparations effectuées sur des piliers ayant un certain âge, j'ai pu constater des fissures dans le béton recouvrant les armatures qui se trouvaient dans la région ou l'espacement entre les étriers était plus grande et qui étaient dues aux déformations transversales des barres.

Pour les bâtiments de grande hauteur à ossature en béton armé il faudrait tenir compte de l'accroissement des contraintes dans les armatures des piliers et de fixer la distance entre les étriers fontion du diamètre des barres qui devraient être assurées au flambement pour des contraintes atteignant la limite élastique de l'acier.

Remarques de l'auteur du rapport introductif
Bemerkungen des Verfassers des Einführungsberichtes
Comments by the author of the introductory report

R.C. REESE

The various contributions and discussions indicate the interest in, and importance of, high-rise structures in reinforced concrete. Such structures are being built in a great many parts of the world, perhaps even more frequently than their economic profitability would seem to dictate.

Flat plate construction is most popular, possibly beam-and-slab second, with precast or composite (job-cast with precast) having considerable popularity.

In addition to the stress problems involved, the physiological and psychological effects upon the occupants are being considered. The accommodation of mechanical trades and architectural features and the serviceability of the design from the viewpoints of tolerable deflections of flexural members, tolerable lateral drift of the structure as a whole, minimization of cracked partitions, or exterior cladding, watertightness, low maintenance, and similar features are all carefully thought about.

In ultra-high-rise construction, the differential creep between various stands of columns and shear walls needs to be taken into consideration.

Leere Seite
Blank page
Page vide

Vb

Béton léger considéré comme matériau porteur (technologie du béton léger, calcul des ouvrages)

Leichtbeton als tragender Baustoff (Technologie des Leichtbetons, Berechnung von Tragwerken)

Structural Lightweight Aggregate Concrete (Concrete Technology, Structural Design)

Leere Seite
Blank page
Page vide

DISCUSSION PRÉPARÉE / VORBEREITETE DISKUSSION / PREPARED DISCUSSION

Improvement of Structural Lightweight Aggregate Concrete by Synthesis of Gap Grading with Shrinkage-Compensating Matrix (Concrete Technology)

Amélioration d'agrégats de béton légers par synthèse de la classification avec la matrice de compensation du retrait (technologie du béton)

Verbesserung von Leichtbetonaggregaten durch Synthese aus Klassierung mit Schwindausgleichformen (Betontechnologie)

SHU-T'IEN LI
FASCE, Professor of Civil Engineering
South Dakota School of Mines and Technology
Rapid City, S. Dak.

1. Introduction

Professor Adrian Pauw has ably and pertinently summarized the state-of-the-knowledge in structural lightweight aggregate concrete. As compared with normal-weight concrete, lightweight concrete is more affected by the moisture condition, has lower strength and modulus of elasticity, suffers more creep and shrinkage, requires slightly more cement, attains somewhat higher accelerated strengths and less creep and shrinkage by steam curing, can be improved in tensile splitting strength, bond strength, creep and shrinkage by partial sand replacement of the fines, and costs more because of more costly aggregate and more cement.

Lightweight aggregates, being mostly rotary-kiln manufactured, can be easily produced in rounded and smooth pebbles by presizing the feed and controlling the burning process. It is thus more adapted to gap grading than normal-weight aggregates. Inherently, gap-graded concrete has less specific surface, is less affected by the moisture condition, requires much less cement paste and hence much less cement and also water for the same water-cement ratio, attains higher strength and higher modulus of elasticity, suffers much less creep and shrinkage, and costs less than continuously-graded concrete. The much reduced cement requirement even permits the blending of the higher-premium shrinkage-compensating cement to produce shrinkage-compensating gap-graded concrete at less cost than conventional concrete.

It is, therefore, both technologically sound and economically feasible to synthesize gap-graded lightweight-aggregate shrinkage-compensating structural concrete by partial sand replacement of the fines and steam-cured. It can be competitive with normal-weight concrete of comparable strength.

2. Some Unique Properties of Structural Lightweight Aggregates That Can Be Improved by Gap Grading

To exploit the full potential of structural lightweight aggregates, the writer fully agrees with Professor Pauw in the under-

standing of their unique properties. Some of these unique properties can, however, be improved by gap grading. Gap grading is distinguished from continuous grading of aggregates by using only one size or a narrow range of size for both coarse and fine aggregates. A parallel exhibit is given below, using Professor Pauw's statements of some unique properties of structural lightweight aggregates as a basis, and the writer's observations that gap grading would improve such unique properties.

Unique Properties of Structural Lightweight Aggregates	Feasible and Adaptable Improvements from Gap Grading
(1) More rounded aggregate can be produced by presizing or pelletizing the raw material feed and controlling burning to prevent or minimize agglomeration.	(1) Manufactured lightweight aggregates would realize advantages of gap grading without any alleged sacrifice of other sizes resulting from crushing natural aggregate material.
(2) Finer fractions generally have a somewhat greater unit weight due to the fact that they tend to include fractions of material which have bloated least.	(2) Gap grading generally results in less mortar requirement which would counterbalance the greater unit weight of finer fractions of lightweight aggregates and/or the increased weight of sand replacement.
(3) Difference in density between aggregate fractions results in somewhat greater tendency for segregation in stockpiles.	(3) Being only one size or within a narrow range of size in gap grading, the tendency for segregation in both coarse and fine-aggregate stockpiles would be eliminated.
(4) Consistent aggregate gradation is more critical for lightweight aggregate because changes in gradation can cause fluctuation in both the unit weight and other properties of the concrete.	(4) By virtue of only one size or within a narrow range of size, gap grading would ensure more uniform unit weight and other properties of the concrete.
(5) Maximum size (1-2.5 cm) of lightweight aggregates is generally smaller than most normal-weight concrete aggregates.	(5) Maximum size of gap grading is limited by the spacing of reinforcing steel or prestressing strands. The smaller maximum size of lightweight aggregates fits well with stress-carrying members of reinforced or prestressed concrete.
(6) Since the expanded particles contain voids or dead air spaces, the apparent speci-	(6) With gap grading, smaller particles in the coarse aggregate would be eliminated,

fic gravity is difficult to determine (especially in the fine fraction because of variable absorption), and it has lower values with the larger pieces.	more uniform apparent specific gravity obtained, and more accurate unit weight of concrete predicted.
(7) Most lightweight aggregates can absorb 5 to 20% water by weight of dry material, and this does not normally occur during mixing and before placing. Hence allowance must be made for the aggregate's water demand to prevent stiffening of the mixture during the interval between mixing and placement. But it is difficult to account for this variable rate of absorption in maintaining uniform consistency in successive batches.	(7) The use of gap grading will confine to one maximum size or within a narrow range of the maximum size whose rate of absorption would be more uniform and whose water demand could be more easily determined for maintaining a uniform consistency in successive batches.
(8) The absorbed water is not available to the cement paste in the mix during the hydration process. The net effective water-cement ratio for lightweight concrete is, however, essentially the same, at comparable strengths, as that of normal-weight concrete.	(8) The less water requirement for gap-graded concrete of equal consistency and strength narrows down the gross difference between the greater water requirement for lightweight concrete and the smaller one for normal-weight concrete.

3. Some Physical Properties of Lightweight Aggregate Concrete That Can Be Improved by Gap Grading

As compared with normal-weight concrete, the properties of lightweight aggregate concrete are more affected by the moisture conditions. The lighter concretes require slightly more cement content, have a lower modulus of elasticity, and suffer more creep and shrinkage. The beneficial use of steam curing and sand replacement of the fines have been well covered by Professor Pauw. The following will confine to certain physical properties of lightweight concrete that can be improved by gap grading.

(1) The lighter unit weight of lightweight structural concrete has made it an economical structural material in spite of the higher cost of the lightweight aggregate.	(1) The much less cement requirement of gap grading would make gap-graded lightweight concrete less costly than continuously-graded and still more competitive with normal-weight concrete.
(2) Compressive strengths of lightweight aggregate concrete up to a practical max-	(2) The much less cement requirement of gap grading could make gap-graded light-

imum of about 400 kg/cm^2 can be obtained with minor increases in cement content compared with normal-weight concrete of equivalent gradation and strength.	weight aggregate concrete having comparable strength as normal-weight concrete, without increase in cement content.
(3) The modulus of elasticity of both normal and lightweight concretes varies with the 1/2th power of f'_c (compressive strength) and 3/2th power of w (unit weight), and hence it is lower for lightweight concrete.	(3) The generally higher compressive strength of gap-graded concrete would make the modulus of elasticity of gap-graded lightweight concrete higher than that of continuously-graded lightweight concrete. Tests have also shown that gap-graded concrete has higher modulus of elasticity.
(4) On the average, both creep and shrinkage are considerably greater for lightweight concrete than for normal-weight concrete.	(4) Both creep and shrinkage are much lower for gap-graded concrete. Thus, gap grading is especially beneficial to lightweight prestressed concrete.
(5) In general, the properties of lightweight aggregate concrete are more affected by the moisture condition because of its porosity and especially the variable porosities from the coarse to the fine fractions of its aggregates.	(5) Gap grading would limit the coarse aggregate to one size only or within a narrow range of size which would keep the porosity more uniform, moisture absorption less variable, and physical properties of the concrete less affected by the moisture condition.

4. Technological Synthesis of Gap-Graded Lightweight Aggregates and Shrinkage-Compensating Matrix

It is seen from the above comparisons that some of the major shortcomings of lightweight aggregate concrete are just counterbalanced or eliminated by the use of gap grading, and the drying shrinkage of concrete could be further nullified with shrinkage-compensating matrix using shrinkage-compensating cement. This concept has proven to be economically feasible because of the much less cement requirement in gap-graded concrete.

Technological developments of shrinkage-compensating expansive cements, their successful applications to producing shrinkage-compensating concrete, retrospect on gap grading, advantages and avoidable disadvantages of gap grading, size relation between coarse and fine aggregates, typical gap-graded aggregates in practice, technological synthesis of gap-graded aggregates, previous applications of gap-graded concrete, optimum matrix percentage, optimum slump and Vebe time, sample example of physical and mechanical properties of gap-graded concretes, gap-graded shrinkage-

compensating concrete and its economics, have been treated in more detail with available authentic data in the writer's previous papers, namely:

1. "Expansive Cements and concretes," AREA Committee 25-Waterways and Harbors, Report on Assignment 7, AREA-Bulletin, Proc., Vol. 66, No. 588, November 1964, pp. 177-182.

2. Discussion of Paper by George W. Washa and Richard L. Fedell on "Carbonation and Shrinkage Studies of Non-plastic, Expanded Slag Concrete Containing Fly Ash," ACI Journal, Proc., Vol. 62, No. 3, March 1965, pp. 1767-1768.

3. "Expansive-Cement Concrete Construction," Concrete Construction, Vol. 10, No. 6, June 1965, pp. 207-209.

4. "Expansive-Cement Concretes--A Review," ACI Journal, Proc., Vol. 62, No. 6, June 1965, Title No. 62-43, pp. 689-706.

5. Closure of "Expansive Cement Concretes--A Review," ACI Journal, Proc., Vol. 62, No. 12, December 1965, Disc. 62-43, pp. 1683-1692.

6. "Proposed Synthesis of Gap-Graded Shrinkage-Compensating Concrete," ACI Journal, Proc., Vol. 64, No. 10, October 1967, Title No. 64-56, pp. 654-661.

7. Closure of "Proposed Synthesis of Gap-Graded Shrinkage Compensating Concrete," ACI Journal, Proc., Vol. 65, No. 4, April 1968, Disc, 64-56, pp. 343-345.

8. "Non-Shrinking Gap-Graded Concrete--Its Synthetic Technology," Paper presented to the Inter-American Conference on Materials Technology, 20-24 May 1968, San Antonio, Texas; ASME Transactions of Inter-American Conference on Materials Technology, 1968.

9. "Gap-Graded Shrinkage-Compensating Concrete Vs. Conventional Concrete," Paper presented to AREA Committee 25-Waterways and Harbors, Publication pending.

Additionally, in the above-said Paper No. 8, there are listed chronologically 61 references relevant to gap-graded aggregate concrete, shrinkage-compensating concrete, and gap-graded shrinkage-compensating concrete. Being restricted in space herein, the writer is obliged to refer those who are further interested in this discussion to the above cited publications.

The writer has initiated, since May 1968, a comprehensive series of investigations to determine the laws of variations of basic parameters to facilitate optimum job-mix proportioning, concreting, restraining, and curing of gap-graded shrinkage-compensating concretes of normal-weight and lightweight aggregates, with a view of translating the envisaged technological synthesis into actual engineering practice.

It is believed that gap-graded shrinkage-compensating structural concrete with partial sand replacement of the fines and steam cured should be more economically competitive with normal-weight concrete of comparable strengths than the heretofore continuously-graded lightweight concrete. This proposed synthetic lightweight concrete will be best suited for prestressed precast structural members by virtue of higher strength, higher modulus of elasticity, less shrinkage, less creep, and lower cost than conventional lightweight concrete.

SUMMARY

Mostly rotary-kiln manufactured, lightweight aggregates can be easily produced in rounded pebbles by presizing the feed and controlling the burning process. They are more adapted to gap grading than normal-weight aggregates. When gap-graded, the advantages of reduction in specific surface, moisture variation, cement paste and water (for the same water-cement ratio), creep and shrinkage, and of increase in strength and modulus of elasticity, all contribute to eliminate corresponding shortcomings of conventional lightweight concrete. The lower cement requirement alone permits blending of higher-premium shrinkage-compensating cement to produce shrinkage-compensating gap-graded lightweight concrete at competitive cost.

RÉSUMÉ

Les agrégats légers, manufacturés le plus souvent dans le four rotatoire, peuvent être produits aisément dans des caillous ronds en classifiant les matériaux d'avance et en contrôlant le procédé de brûlage. Ils sont plus adaptés à la granulométrie discontinue que les agrégats à poids normal. Le béton léger à granulométrie discontinue a les avantages de la réduction de la surface spécifique, de la variation d'humidité, de la pâte de ciment et eau (pour le même rapport ciment-eau), du fluage et du retrait, de l'augmentation de la force de résistance et du module d'élasticité, éliminant ainsi les défauts du béton léger conventionnel. Le besoin en ciment diminué en lui seul permet d'utiliser un mélange de ciment à retrait diminué pour produire du béton léger à retrait compensé à un prix compétitif.

ZUSAMMENFASSUNG

Meist können in Drehöfen hergestellte Leichtaggregate sehr einfach in abgerundeten Steinen produziert werden, wenn Brennmaterial und Brennprozess kontrolliert werden. Sie sind für die Klassierung besser geeignet denn normalgewichtige Aggregate. Der Vorteil in der geringeren spezifischen Oberfläche, in der Aenderung des Feuchtigkeitgehaltes, in Zementmischung und Wasser (bei derselben Zement-Wasser-Rate), in Kriechen und Schrumpfen (Schwinden) als auch in der Erhöhung der Druckfestigkeit und des Elastizitätsmoduls trägt dazu bei, die entsprechenden Nachteile des herkömmlichen Leichtbetons aufzuwiegen. Der geringere Zementverbrauch allein erlaubt das Beimischen teureren schrumpfausgleichenden Zementes, um schrumpfausgleichenden Leichtbeton zu vergleichbaren Kosten herzustellen.

Incremental Loading of Reinforced Lightweight Concrete Columns

Accroissement différentiel de la charge dans les colonnes en béton armé léger

Differentieller Lastzuwachs bei Leichtstahlbetonsäulen

DONALD W. PFEIFER
Manager, Concrete
Products Research Section
Portland Cement Association
Skokie, Illinois

EIVIND HOGNESTAD
Director of
Engineering Research
Member, U.S. Council, IABSE
Portland Cement Association
Skokie, Illinois

INTRODUCTION

A recent experimental investigation[1] has shown that high quality structural lightweight aggregate concrete can safely be used in reinforced concrete columns, including ultra-highrise buildings. Their creep and shrinkage characteristics differ little from those of columns containing normal weight concrete. In both cases, elastic and time-dependent column shortenings were found to be governed primarily by reinforcing steel percentage, the influence of concrete type was relatively minor.

The previous study involved the typical laboratory procedure of moist curing the specimen for 28 days and then applying the full design load at that age. This loading technique bears little semblance to the actual incremental loading of concrete columns as construction of a tall structure proceeds. At the suggestion of Dr. Fazlur Khan of Skidmore, Owings and Merrill, laboratory tests dealing with incremental loadings were therefore undertaken. The main objective being comparison with the shortening characteristics of columns loaded in the typical laboratory manner.

DESCRIPTION OF LABORATORY INVESTIGATION

General -- These tests were made to determine the elastic and time-dependent shortenings of reinforced lightweight concrete columns which were fabricated and loaded to simulate conditions encountered in a 50-story concrete building 714 ft. (218 m) tall. The investigation primarily concerns columns loaded in weekly increments to simulate the actual construction schedule. These columns required 50 equal weekly increments, each 2 percent of full load. Companion reinforced columns were also instantaneously loaded to full load when the columns were 1, 4, 35, and 50 weeks old.

Tests were also undertaken on non-reinforced concretes to determine compressive strength, elastic deformation, creep, and drying shrinkage characteristics as functions of time.

Materials -- The coarse lightweight aggregate, No. 14 in the PCA numbering series, is an expanded shale produced in a rotary kiln that has been studied extensively in previous investigations.(1) Normal weight Elgin, Illinois sand was used as all the fine aggregate. The concrete was proportioned to produce a nominal compressive strength of 6000 psi (422 kg/cm²) at 28 days. Lightweight concrete of this strength and containing 100 percent normal weight sand fines has a nominal modulus of elasticity of 3.0 million psi (211,000 kg/cm²) at 28 days. The slump and air contents were maintained at approximately 3 in. (7.5 cm) and 4 percent, respectively. The laboratory mix data are presented in Table 1; accompanying measured physical properties of this concrete are presented in Table 2.

TABLE 1 -- LABORATORY CONCRETE MIX PROPORTIONS

Fine Aggregate, percent by vol.	Quantities per cu. yd. (m^3) of concrete				Percent Air, Roll-A-Meter	Plastic Unit Weight, lb./ft.³ (kg/m³)	Slump, in. (cm)
	Water, lbs. (kg)	Cement, lbs. (kg)	Air-Dry Aggregates Coarse,* lbs. (kg)	Sand,** lbs. (kg)			
44	315 (187)	623 (370)	900 (534)	1245 (739)	3.8	114.2 (1830)	2.8 (7)

* $^3/_4$" maximum size lightweight aggregate
** Normal weight Elgin, Illinois sand

TABLE 2 -- PHYSICAL PROPERTIES OF CONCRETE *

Compressive Strength,** psi (kg/cm²)				Modulus of Elasticity,** 10^6 psi (10^5 kg/cm²)			
7 da.	28 da.	90 da.	1 yr.	7 da.	28 da.	90 da.	1 yr.
5220 (367)	6360 (447)	6990 (491)	7230 (508)	3.07 (2.16)	3.34 (2.35)	3.60 (2.53)	3.82 (2.69)

* All cylinders were continuously moist cured
** An average of four specimens.

The reinforced columns contained $^5/_8$-in. (16-mm) diameter high strength deformed bars, which conform to the ASTM A431 specification and have a nominal yield point of 75,000 psi (53 kg/mm^2).

Fabrication, Curing and Instrumentation of Specimens -- The study involved fabrication and long-time testing of eight 6-in. (15 cm) square by 36-in. (91 cm) long reinforced columns and 32 non-reinforced 6 by 12-in. (15 by 30-cm) cylinders.

The reinforcing was fabricated into tied column assemblies each containing four deformed bars. Lateral tie reinforcement consisted of $^1/_4$-in. (6 mm) bars spaced at 6 in. (15 cm). The symmetrical longitudinal reinforcement was positioned to provide 1-in. (2.5 cm) concrete cover over the lateral tie reinforcement. The longitudinal bars were welded to 1-in. (2.5 cm) thick steel bearing plates.[1]

The columns were cast in a horizontal position and consolidation of concrete was by table vibration. The columns were moist cured for three days; they were then sealed in 0.003-in. (0.08 mm) thick copper foil to simulate idealized moisture conditions in the large prototype columns of the structure.

The elastic and time-dependent deformations were observed by a mechanical strain gage. At midheight of the columns, brass plugs were glued directly to the concrete on 10-in. (25-cm) centers on three of the four sides of the column. The deformation of the reinforcing steel and concrete have previously been measured to be equal[1], and measurements directly on steel were therefore not made during this study. More detailed description of fabrication and instrumentation procedures reported previously[1] are similar to those used in this study.

The 6x12-in. (15x30-cm) cylinders were cast in the vertical position and consolidation of concrete was by internal vibration. All cylinders including those wrapped in copper foil were continuously moist cured until time of test.

TEST PROGRAM

All eight reinforced columns were eventually loaded to 70,000 lbs. (31,780 kg). Two were loaded in 50 increments of 1400 lbs. (636 kg) over a 50-week period, starting when concrete was one week old. The remaining six were loaded instantaneously to 70,000 lbs. (31,780 kg), two at a concrete age of 1 week, two at 4 weeks, one at 35 weeks, and one at 50 weeks.

The 6x12-in. (15x30 cm) plain concrete cylinders were subjected to strength and modulus of elasticity testing at ages 7, 28, 90, and 365 days. Creep and drying shrinkage tests on unsealed cylinders began at ages 1 and

4 weeks and those specimens were then stored at 73°F (23 C) and 50 percent relative humidity. Creep tests on copper-foil wrapped cylinders began at ages 1, 4, 35, and 50 weeks. All creep specimens were loaded to 1500 psi (105 kg/cm²). The later-age sealed creep specimens (plain and reinforced) were initially observed to verify the lack of drying shrinkage in the copper-wrapped specimens.

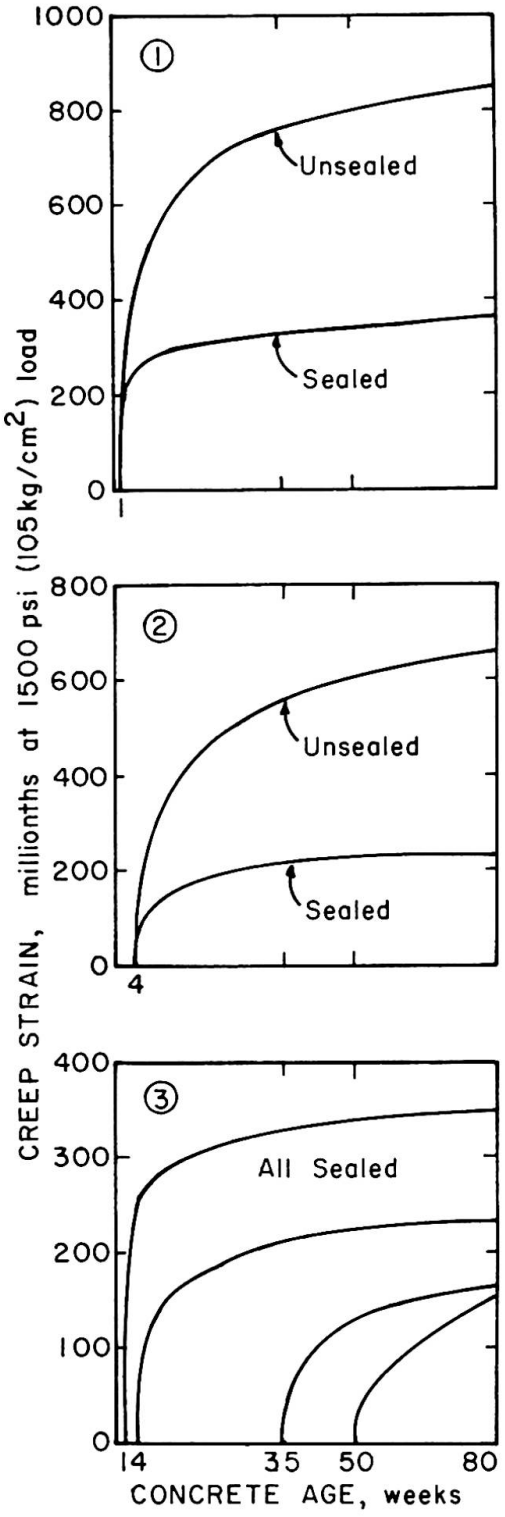

Figs. 1,2,3 – Creep of Plain Concrete – Effect of Age of Concrete at Loading and Drying Shrinkage.

TEST RESULTS

Strength and Elastic Properties -- The properties of the plain concrete presented in Table 2 indicate that substantial increases in strength and stiffness of the concrete occurred as a function of curing time.

Creep Properties of Plain Concrete -- The measured creep of these sealed and unsealed concretes are shown in Figs. 1 to 3.

Fig. 1 shows the creep of concretes loaded at an age of 1 week. After 79 weeks of loading, the measured creep of the sealed and unsealed cylinders was 370 and 850 millionths, respectively. The drying shrinkage of the companion unsealed concrete was 570 millionths at that same time. It is noted that the presence of drying shrinkage has the significant effect of approximately doubling the measured creep at age 50 weeks.

Fig. 2 shows the creep of concretes loaded at 4 weeks. After 76 weeks of loading, the measured creep of the sealed and unsealed cylinders was 230 and 650 millionths, respectively. The drying shrinkage of the companion unsealed concrete was 510 millionths at that same time. With this loading age the creep at age 50 weeks is almost tripled when drying shrinkage is allowed.

Fig. 3 shows the measured creep of the sealed cylinders which were loaded at ages 1, 4, 35 and 50 weeks. These data show the well-known influence of age of concrete at loading, and illustrate low creep characteristics of these sealed lightweight concretes.

The measured creep coefficients (creep strain per unit load) at age 50 weeks range from 0.08 to 0.25 millionths/psi (1 to 4 millionths/kg/cm^2) for the sealed concretes. The data shown in Fig. 4 relate this measured creep coefficient occurring from the time of loading to the 50-week age versus the concrete age at loading. These data will be used later in the application of the theoretical prediction equation to the incrementally loaded sealed reinforced columns.

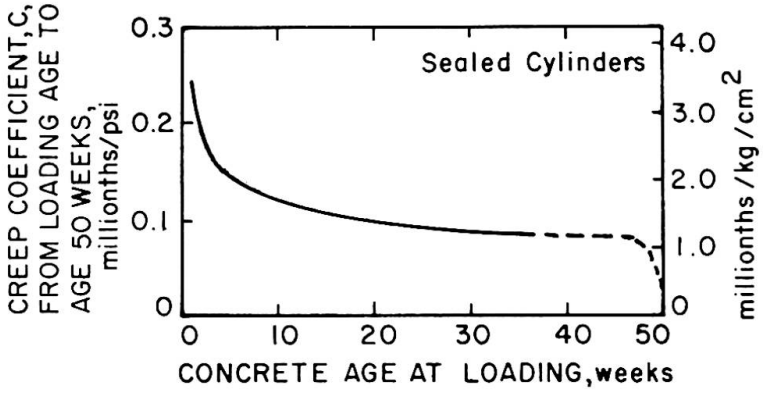

Fig. 4—MEASURED CREEP COEFFICIENT OF PLAIN CONCRETE VERSUS CONCRETE AGE AT LOADING

Elastic and Creep Properties of Instantaneously Loaded Columns -- The measured data from the instantaneously loaded columns are shown in Fig. 5. The elastic response to load is in accord with elastic theory, and the significant increase in modulus of elasticity of concrete as a function of curing time is quite evident in the measured elastic response of these reinforced columns. The measured

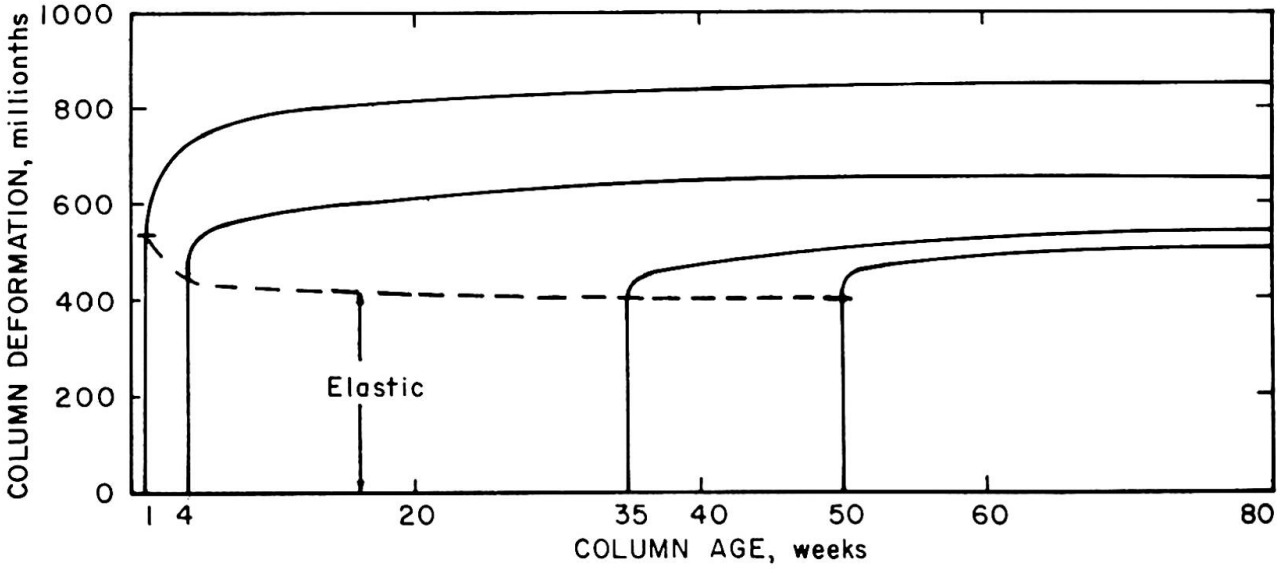

Fig. 5 — ELASTIC AND TIME-DEPENDENT CREEP DEFORMATION OF INSTANTANEOUSLY LOADED REINFORCED COLUMNS

time-dependent creep characteristics also reflect the influence of age of concrete at loading on the time-dependent behavior of reinforced columns. At age 50 weeks the ratio of creep strain to elastic strain ranges from 0.57 with the 1-week loading to 0.25 with the 35-week loading.

Elastic and Creep Properties of Incrementally Loaded Columns -- The measured data from the incrementally loaded columns are shown in Fig. 6. It is quite evident that the non-linear creep behavior was small as observed by the measured linear response during the incremental loading period. Creep is being further observed after the 50th and last load was applied. Since this last load application, the columns have shortened only about 20 millionths during the 30-week period following the last loading.

The computed elastic shortening, taking into account the increased modulus of elasticity of the concrete, is also shown in Fig. 6. It is seen

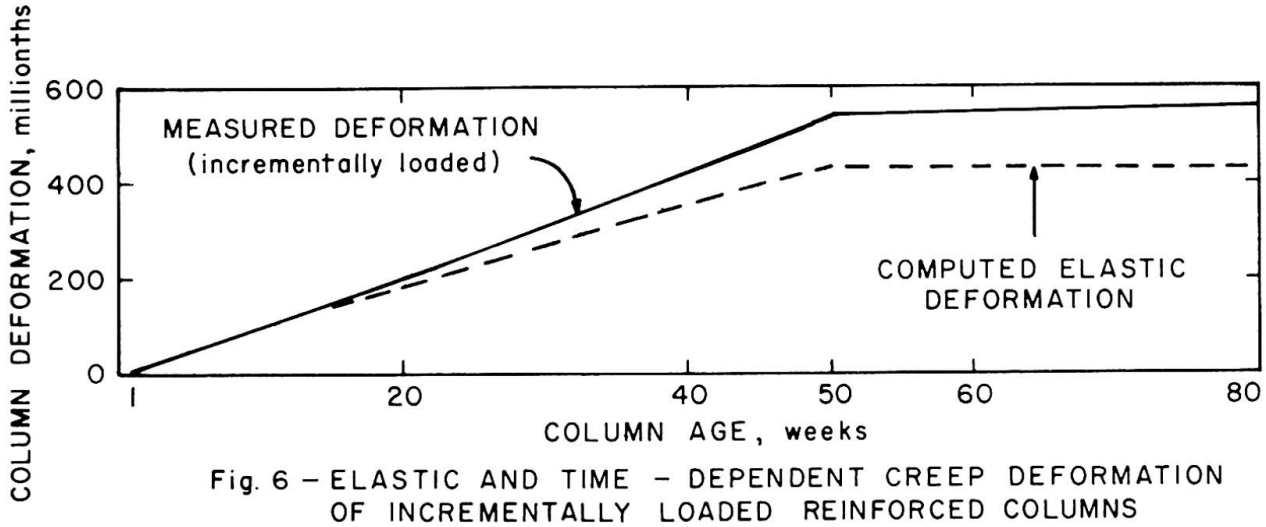

Fig. 6 – ELASTIC AND TIME – DEPENDENT CREEP DEFORMATION OF INCREMENTALLY LOADED REINFORCED COLUMNS

that the influence of creep is small when sealed reinforced columns are incrementally loaded during a long-time period. At an age of 50 weeks the ratio of measured creep strain to computed cumulative elastic strain was 0.25.

ANALYSES OF DATA

The analyses of data are presented in a condensed form due to the IABSE manuscript length limitation. More significant details and data analyses will be provided in future extensions of this investigation.

Elastic Analysis -- The elastic response of these reinforced lightweight concrete columns was found to be in accord with elastic theory. The measured elastic shortenings for the 5 conditions of loading were as follows:

Instantaneous Load at	1 week	=	540 millionths	elastic	shortening
" "	4 weeks	=	434 "	"	"
" "	35 weeks	=	400 "	"	"
" "	50 weeks	=	400 "	"	"
Incrementally Loaded during	50 weeks	=	433 "	"	"

Creep Analysis -- Theoretical analyses as discussed by Leonhardt[2,3] have been shown[1] to adequately predict the time-dependent strain in reinforced columns caused by creep and drying shrinkage. The following equation[1] was used to predict the time-dependent steel stresses in the reinforced columns of this study caused by creep:

$$\Delta f_s = \frac{f_o}{p_g}\left[1 - e^{-\alpha C E_c}\right] \qquad \ldots\ldots (1)$$

Eq. (1) can be converted to time-dependent reinforced column strain by applying the measured creep values (C) obtained from the unreinforced copper-wrapped cylinders and then by calculating the resulting change of steel strain which also equals change of column strain.

Application of Eq. (1) to the sealed reinforced columns which were instantaneously loaded at 1, 4, and 35 weeks results in single-step solutions which underestimate the measured time-dependent shortenings at 50 weeks of age by 13 to 27 percent. This underestimate may result because the use of the singular creep coefficient determined at a particular loading age does not take into account the change in creep characteristics as a function of time.

However, when Eq. (1) is applied to the incrementally-loaded columns in a 50-step solution, using the data in Fig. 4 to account for changing creep coefficients and the assumptions of superposition, much better results are obtained. The cumulative creep of the incrementally loaded columns was predicted to be 113 millionths and the measured creep was 106 millionths. The multi-step solution, which takes account of changing concrete properties results in a ratio of Δf_s(meas.)/ Δf_s(calc.) of 0.94.

CONCLUDING REMARKS

Data obtained from the incrementally loaded reinforced columns show that little creep takes place when the load is applied at a realistic rate and when the drying shrinkage influence on creep is eliminated. The creep that was measured during this 50-week loading period was only 25 percent of the elastic response, and the time-dependent creep phenomena essentially stopped after the 50th and final load was applied.

Theoretical time-dependent strains[2] compared well with the test data, so that theoretical analyses may be used to estimate such time-dependent movements.

REFERENCES

1. Pfeifer, Donald W., "Reinforced Lightweight Concrete Columns" to be published in the Journal of the Structural Division, ASCE.
2. Leonhardt, F., Prestressed Concrete Design and Construction, Wilhelm Ernst and Son, Berlin, 1964.
3. Illston, J.M., Leonhardt, F., Soboyejo, A.B.O., Wang, C.H., and Authors, Discussion of the paper "Time-Dependent Load Transfer in Reinforced Lightweight Concrete Columns," by T.A. Holm and J. Pistrang, ACI Journal, Proceedings V. 64, No. 6, June 1967, pp. 1587-1592.

NOTATION

A_s = cross-sectional area of longitudinal reinforcement
A_g = gross cross-sectional area of concrete column
C = unit creep coefficient of plain concrete
e = base of natural logarithms
E_c = modulus of elasticity of concrete
E_s = modulus of elasticity of reinforcement
f_o = initial elastic stress in concrete
n = modular ratio E_s/E_c
p_g = percentage of reinforcement A_s/A_g
$\alpha = \dfrac{p_g n}{1 + p_g n}$
Δf_s = change in steel stress due to creep

SUMMARY

Tests were made at the Portland Cement Association Laboratories regarding the elastic and time-dependent shortening of reinforced lightweight concrete columns which were fabricated and loaded to simulate construction conditions encountered in a 50-story concrete building 714 ft. (218 m) tall. The measured data from these incrementally loaded columns show low creep when the load is applied at a realistic rate. A 3-year field investigation of the actual structure will be undertaken and comparison between laboratory and field data will be made. Such comparison will provide data toward developing improved design concepts for ultra-highrise concrete buildings.

RÉSUMÉ

Aux laboratoires de l'association du Portland Cement on a fait des tests concernant le raccourcissement élastique et celui en fonction du temps sur des colonnes en béton armé léger, fabriquées et chargées de façon à simuler les conditions rencontrées dans une construction en béton de 50 étages et de 218 m de haut. Les valeurs mesurées sur ces colonnes chargées différentiellement montrent peu de fluage tant que les charges appliquées restent dans une limite raisonnable. Il sera procédé à des essais sur nature pendant 3 années, et des comparaisons seront faites entre les résultats de laboratoire et ceux obtenus sur le bâtiment. On profitera de ces comparaisons pour améliorer la projection de constructions en béton d'extrême hauteur.

ZUSAMMENFASSUNG

Die Portland Cement Association hatte Versuche zwecks Bestimmung der elastischen und zeitabhängigen Verkürzung an Leicht-Stahlbetonsäulen durchgeführt, die unter den Bedingungen eines fünfzigstöckigen und 218 m hohen Betongebäudes hergestellt und belastet wurden. Die Messergebnisse zeigen, dass die mit differentiellem Lastzuwachs belasteten Säulen geringes Kriechen zeigen, wenn die Lasten mit einer vernünftigen Geschwindigkeit aufgebracht werden. Eine Dreijahresuntersuchung dieses Gebäudes wird unternommen und Vergleiche zwischen Laboratoriums- und Felddaten werden angestellt. Solche Vergleiche sollen Angaben zur Entwicklung derartig hoher Massivbauten liefern.

Leere Seite
Blank page
Page vide

Experiment on Lightweight-Concrete Composite Girder Bridges

Expériences sur des poutres métalliques composées avec du béton léger

Versuch über Leichtbeton-Verbundbrücken

Y. TACHIBANA
Dr.-Eng., Prof. of Osaka City University
Japan

1. Introduction

Recently in Japan, due to the shortage of natural aggregate and to growing requirement of lightweight structure, inquiry and application of lightweight concrete have greatly been promoted. In case of a steel bridge with lightweight-concrete slab, a composite girder is found to be a reasonable and economical construction.

From such standpoint, after model tests were carried out, the first lightweight-concrete composite girder bridge in Japan was successfully constructed by the Hanshin Expressway Public Corporation.

Following experiments are conducted always in comparison with a lightweight concrete composite girder and a normal-weight-concrete composite girder.

2. Model test of shear connector and composite beam

2.1. Specimens

As shown in Figs.1 and 2, push-out test specimens, and composite beams with reinforced concrete slab and shear connectors were prepared.

Push-out test specimens contain various types with different pitches of shear connectors. Back surface of H-beam is oiled, and concrete placing

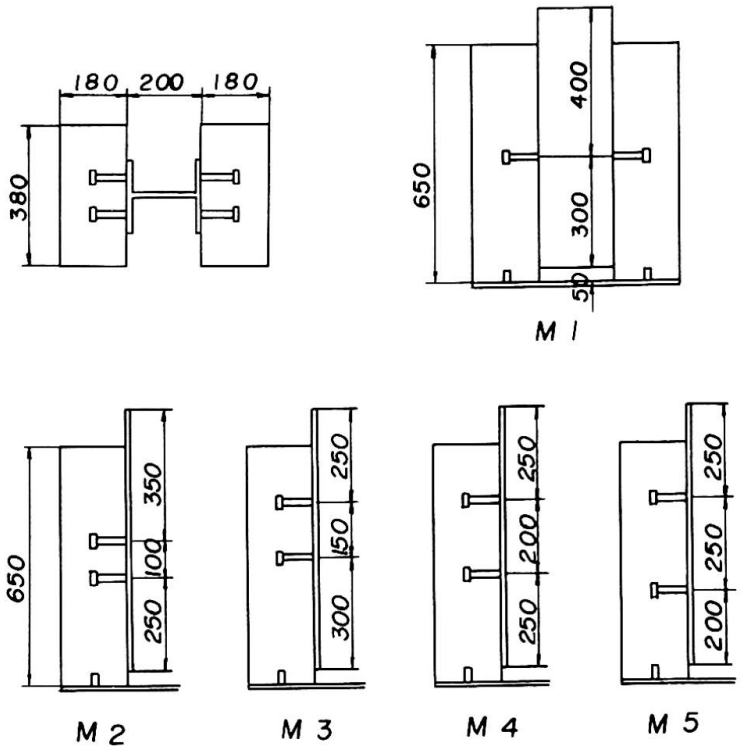

Fig. 1. Push-out specimens

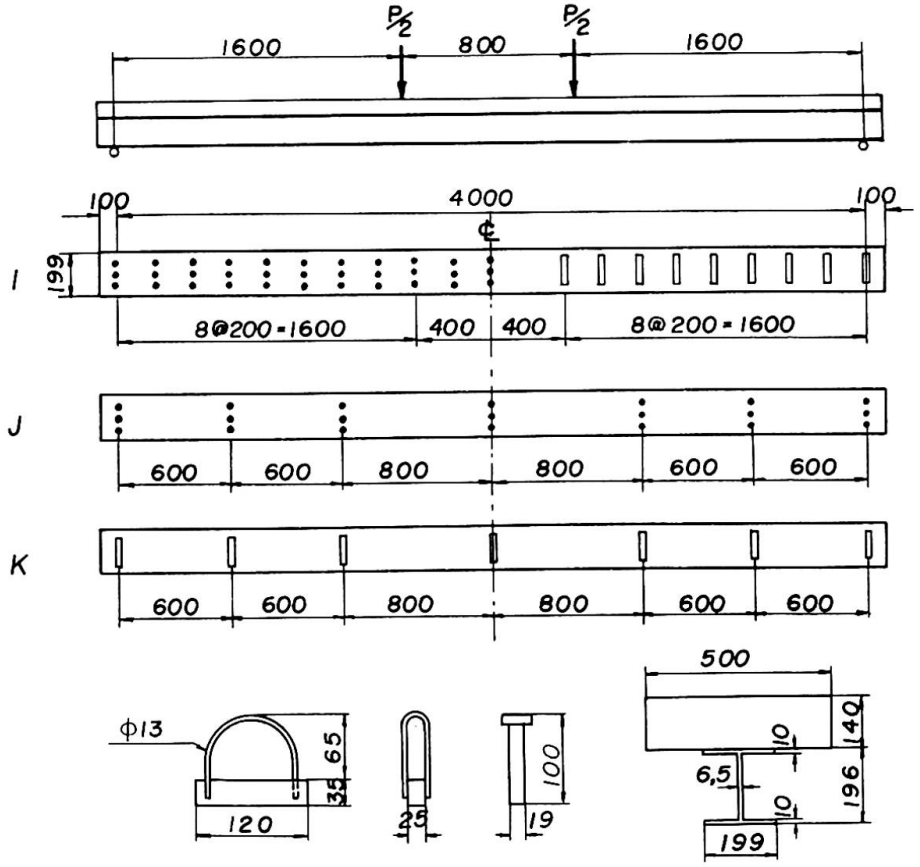

Fig. 2. Beam specimens

is executed from the lateral side, so that the bearing strength of shear connectors may not be influenced by bleeding of the concrete at the lower surface of the reinforcing bars.

Beam I has stud shear connectors and block shear connectors whose strength are quite equal as the preliminary test shows. Beams J and K are made to only few shear connectors, so that breaking strength of shear connectors as well as ultimate strength of beams may also be examined.

Table 1 shows the number of specimens, and Table 2 strength and Young's modulus of concrete on the 28th day in contrast with normal-weight concrete beam and lightweight-concrete beam. Mean value of yielding stress of steel is about 2700 kg/cm^2.

Table 1. Number of specimens

Specimen	Name	Number		Kind of shear connector
		NC	LC	
Push out	L	4	4	Block
	M	12	12	Stud
Composite beam	I	1	1	Block and stud
	J	1	1	Stud
	K	1	1	Block
Sum		19	19	

Table 2. Strength and Young's modulus of concrete (kg/cm^2)

Concrete	Compressive strength	Tensile strength	Bending strength	Young's modulus, $E_{0.3}$	n at $E_{0.3}$
NC	285	25.5	41.3	276,000	7.6
LC	313	24.1	30.6	194,000	10.8
NC/LC	0.91	1.05	1.35	1.42	

2.2. Push-out test

The load corresponding to useful capacity (residual slip = 0.08mm) [1] per one shear connector are shown in Table 3. Capacity of LC is larger than NC, even if in consideration of the difference of their compressive strength in Table 2.

Table 3. Useful capacity of shear connector

Concrete	M1	M2	M3	M4	M5
NC	4.1 ton	3.4	4.3	3.8	3.5
LC	5.5 ton	4.5	4.5	4.8	5.0
NC / LC	0.75	0.75	0.96	0.79	0.70

The pitch of stud shear connector has a slight influence upon its capacity, and ultimate strength of LC is a little lower than NC.

2.3. Beam test

Deflection and stress of LC beam are somewhat larger than those of NC beam. The deflection of beams are shown in Fig.3. where the calculated values are described as n = 7 for NC beam, and n = 10 for LC beam. As compared with these results, the theoretical values coincide well with the measured ones.

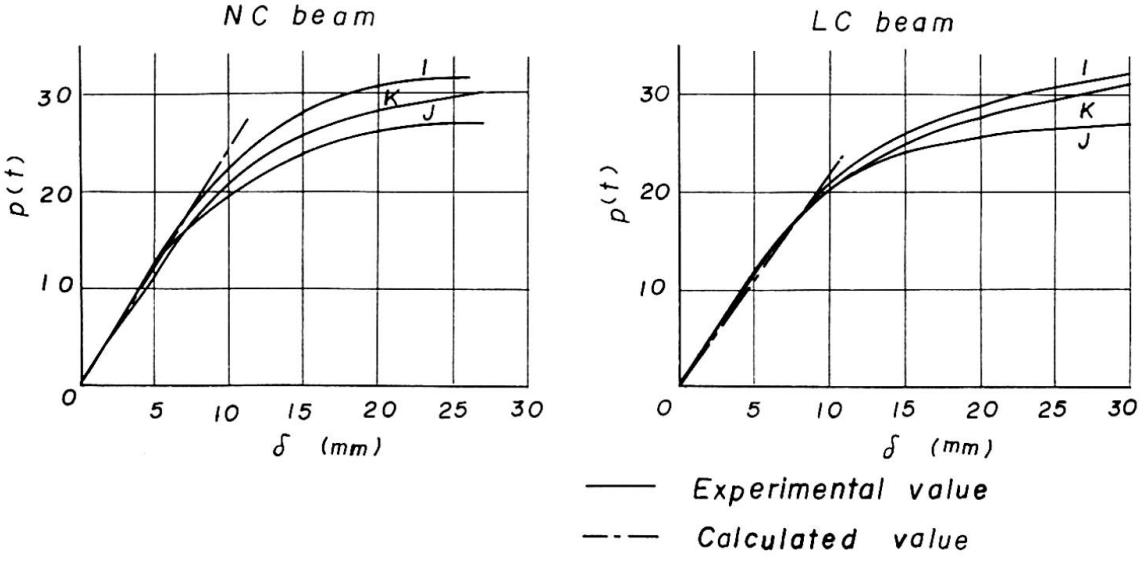

Fig.3. Deflection of beamsat center

Breaking state of NC beams as in LC beams are due to bending. The calculation method of breaking moment can be classified into 3 cases (Fig. 4), according to the strength of concrete and shear connector [2].

In both NC and LC beams, beam I corresponds to case II , beams J and K correspond to case III . By comparing the calculated breaking load

with the experimental one in Table 4, we can see that they agree quite well.

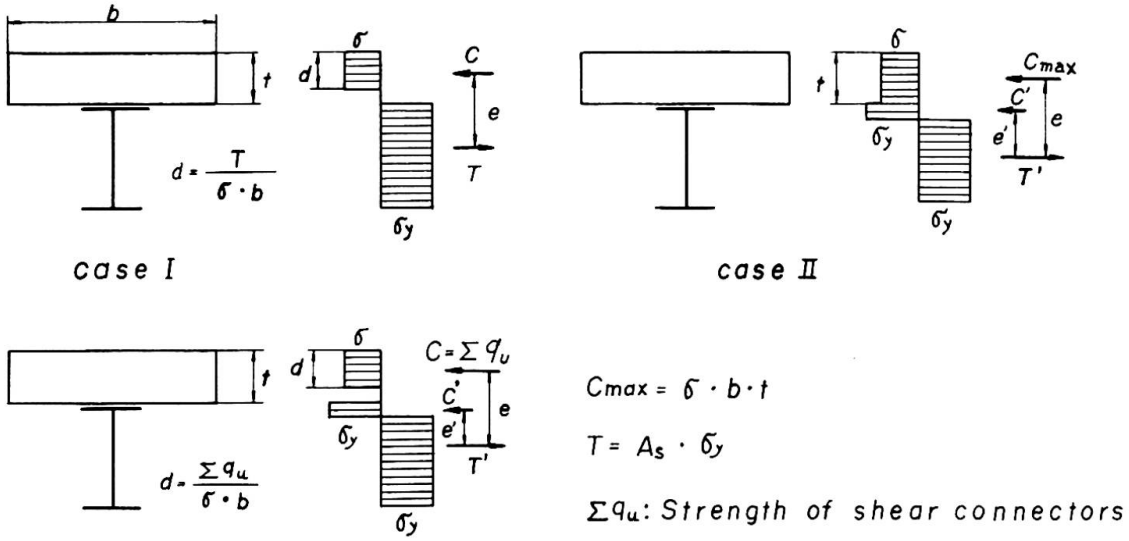

Fig. 4. Calculation method of breaking moment

Table 4. Breaking load of beams

Beam	NC			LC		
	I	J	K	I	J	K
Experimental value (ton)	33.8	29.4	31.0	35.2	30.2	33.0
Calculated value (ton)	33.3	29.3	31.0	34.2	29.1	30.6
Ex./ Cal.	1.02	1.00	1.00	1.03	1.04	1.08

3. Field experiment of two test bridges

3.1. Test bridges

Statical and dynamical tests were conducted in two multiple plate girder bridges in the Hanshin Expressway. One is a composite girder bridge built of the normal concrete (NC girder) and the other a bridge of the lightweight concrete (LC girder).

Table 5. Value of concrete

Concrete	Measured value		Value used in calculation	
	σ_c (kg/cm^2)	E_c (kg/cm^2)	E_c (kg/cm^2)	γ_c (kg/cm^3)
NC	302	2.47×10^5 (n=8.5)	3.00×10^5 (n=7)	2.5×10^{-3}
LC	331	1.71×10^5 (n=12.3)	1.75×10^5 (n=12)	1.8×10^{-3}

Table 5 shows 28th-day compressive strength σ_c, Young's modulus E_c and density γ_c for two concrete materials used in these bridges.

Besides, the shape and dimension of the two bridges are designed in the same way as shown in Fig. 5. Total steel weight of NC girder is 41.5 ton, that of LC girder being 39.6ton. In this case, weight of steel material is slightly saved. If the span length is longer, however, we shall be able to expect more economical design of a girder and substructure.

By the way, the pavement, hand-rail and curbs were not equipped during the tests to avoid the errors involved in the experimental results owing to their uncertain stiffness.

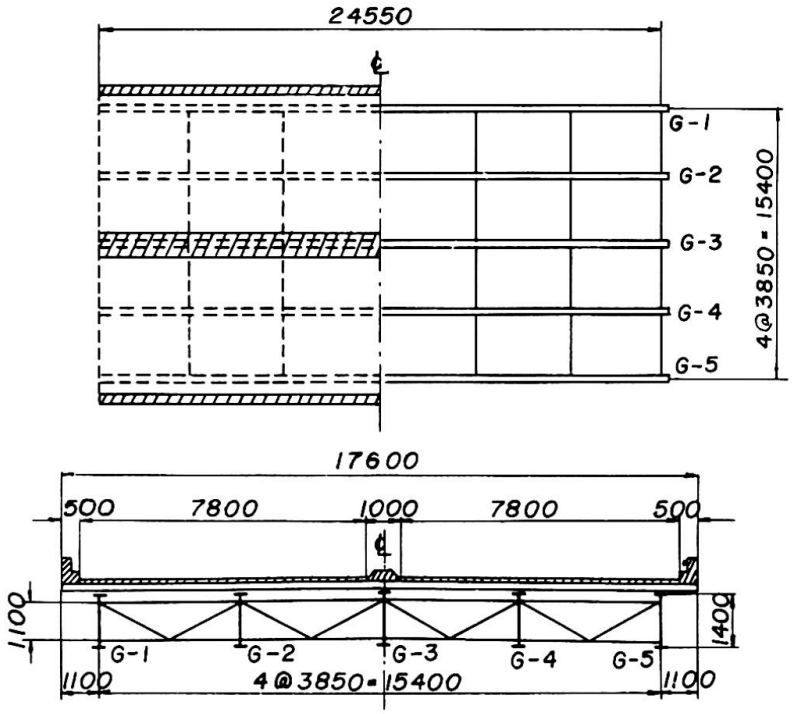

Fig. 5. General view of test bridges

3.2. Theoretical study

As the width of these bridges is greater compared with their span length, the vibration should be analyzed by regarding these bridges as two dimensional structures. Accordingly, the dynamical response of the multiple plate girder bridge has been developed in reference to the

literatures [4] and [5].

The outline of analysis is as follows; First, the bridge is idealized in an orthotropic plate as is seen in the theory of Guyon and Massonnet[6]. Next, by assuming the mode of vibration in the transverse direction and by applying the Lagrange's equation, the fundamental differential equation of motion can be obtained. From this equation, simple and practical formula for determining the natural frequency, and a method of analyzing the response due to dynamical forces are derived. Finally, an approximate method to estimate deflection and stress-resultants under statical forces has also been proposed by the above theory.

3.3. Statical loading test

The statical loading tests were made by loading four 12tons vehicles with tire rollers. These vehicles were loaded upon the bridge, back to back, symmetrical with respect to the middle point of span under three loading conditions. Values of deflection for two typical loading conditions are plotted in Fig. 6.

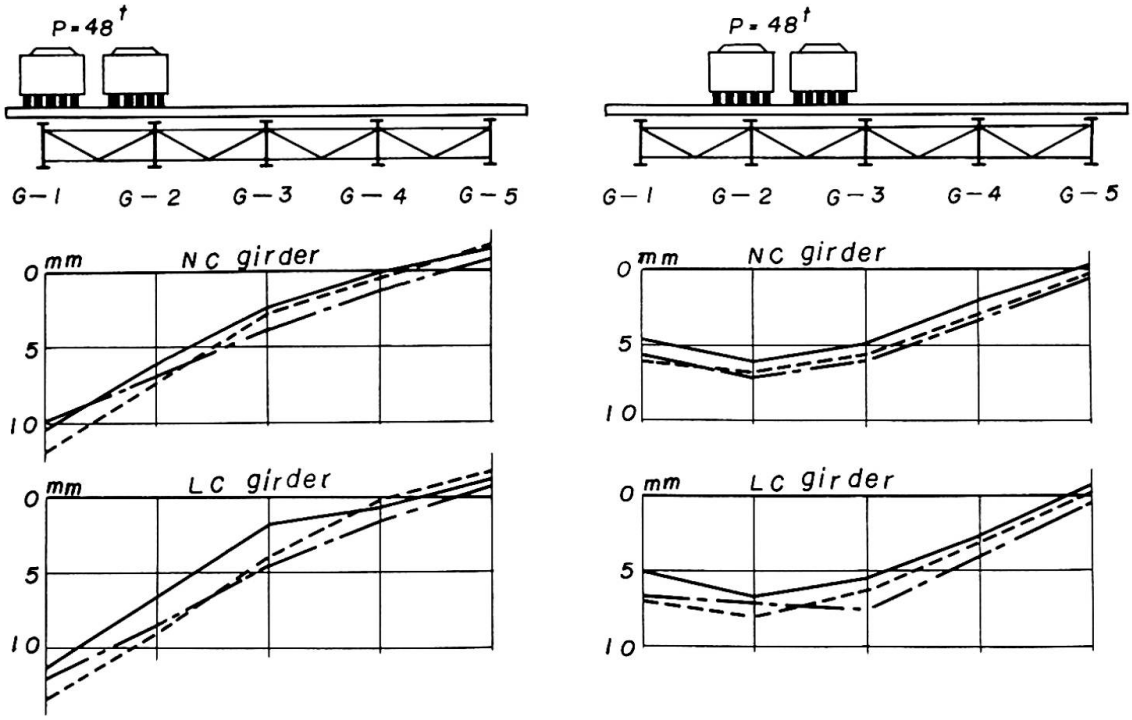

Fig.6. Deflection of girder

By comparing these results, the theoretical values are found to coincide well with the measured ones.

Thus we can see that the weakness of low Young's modulus of light-weight concrete can be made up for by making use of a composite girder.

3.4. Dynamical loading test

The dynamical tests were conducted by pulsating the bridges with an oscillator and by recording the dynamical deflection and stress with the oscillograph. From these data, resonance curves are drawn and three resonant frequencies are clearly obtained.

The vibration patterns are shown in Fig. 7 and experimental values together with the theoretical ones are summarized in Table 6, and we can see quite complete agreement between them.

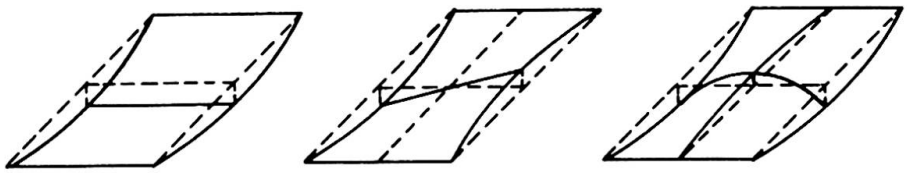

Fig. 7. Vibration pattern

Table 6. Natural frequencies (cycle/sec.)

Girder	Vibration mode	1st mode 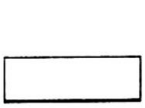	2nd mode 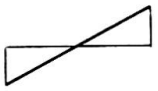	3rd mode 
NC	Experimental value	4.55	5.03	8.77
	Theoretical value	4.59	5.35	8.66
	Th./Ex.	1.01	1.06	0.99
LC	Experimental value	4.71	5.66	9.77
	Theoretical value	4.82	5.67	9.49
	Th./Ex.	1.02	1.00	0.97

Then, by the drop test of wheel of tire roller, we obtained logarithmic damping coefficient, Δ =0.33 for LC girder, Δ =0.20 for NC girder.

References

1. VIEST, I. M.: Investigation of Stud Shear Connector for Composite Concrete and Steel I-Beams, Proceedings of A.C.I., 1956, No. 8.
2. ROGER G. SLUTTER: Flexual Strength of Steel-Concrete Composite Beams, Journal of Structural Division, Proceedings of the A.S.C.E., Apr., 1965.
3. M. NARUOKA and H. YONEZAWA: A Study on the Period of the Free Lateral Vibration of the Beam Bridge by the Theory of the Orthotropic Rectangular Plate, Ingenieur Archiv, 26 Band, Heft 1, 1958.
4. I. HIRAI: Dynamic Responses of Orthotropic Plates with Two Opposite Free Edges and Other Two Simply Supported Edges under the Action of a Constant Moving Force, Trans. of J.S.C.E., Vol. 92, 1963.
5. I. HIRAI: Dynamic Analysis of Gridworks by the Method of Composition, Trans. of J.S.C.E., Vol. 101, 1964.
6. Massonnet C.: Méthode de calcul des points a poutres multiples tenant compte de leur résistance a la torsion, Publication of I.A.B.S.E., Vol. 10, 1950.

SUMMARY

In consequence of (1) the push-out test and the beam test, and of (2) the experiment of two test bridges equivalently designed, we can recognize that the lightweight-concrete composite girder brige is a quite useful type, as compared with a normal-weight-concrete composite girder bridge.

RÉSUMÉ

Suite au test des goujons (1) et au test de la poutre, ainsi qu'aux expériences (2) sur deux ponts dimensionnés identiquement, nous concluons que le pont en action combinée acier-béton léger constitue un type tout-à-fait acceptable, comparé au pont acier-béton normal.

ZUSAMMENFASSUNG

In Folgerung des Dübel- und Balkenversuchs (1) sowie der Untersuchung zweier gleichwertiger Brücken (2), können wir erkennen, dass die Leichtbetonverbundbrücke, verglichen mit der Normalbeton-Verbundbrücke, durchaus brauchbar ist.

Leere Seite
Blank page
Page vide

Remarques de l'auteur du rapport introductif
Bemerkungen des Verfassers des Einführungsberichtes
Comments by the author of the introductory report

A. PAUW

The application of lightweight aggregate concrete in the construction of such structures as No. 1 Shell Plaza in Houston, Texas is evidence that lightweight concrete has "come of age" as an acceptable and, for many applications, superior structural material. The successful use of lightweight concrete in the columns of the above structure as described in the contribution by D. W. Pfeifer and E. Hognestad is especially noteworthy. While the success in this application was due, in part, to extreme care in the proportioning and placing of a specially developed sanded lightweight aggregate mix, this report demonstrates that the creep and shrinkage characteristics of lightweight aggregate concrete columns differ little from those of columns containing normal weight concrete. In both cases, elastic and time-dependent column shortening are governed primarily by the reinforcing steel percentage. Two factors contribute to this result, namely the shrinkage and creep characteristics of the concrete.

Shrinkage causes an internal stress balance which increases the compressive stress in the reinforcement and reduces the net compressive stress in the concrete. Creep causes an internal redistribution of stress which also increases the stress in the reinforcement and decreases the stress in the concrete. Because lightweight aggregate concrete has a lower elastic modulus, the instantaneous or elastic stress in the reinforcement of a lightweight concrete column (with equal reinforcement and subjected to the same load) will be considerably higher and the concrete stress correspondingly lower, than the corresponding stresses in a normal weight concrete column. As a result, for highly reinforced columns, while the instantaneous or elastic strain is larger for the lightweight concrete column, the time-dependent strain may actually be smaller, with the total elastic and time-dependent strain being only slightly greater than that for the normal weight concrete column. Both instantaneous and time-dependent strains are markedly affected by the age of the concrete at time of loading and hence these deformations are significantly smaller if the column is loaded incrementally over a prolonged period of time.

The contribution of Dr. Shu-t'ien Li opens up the possibility of even greater reduction of elastic and time-dependent strains through the application of gap grading. The advantages to be gained by gap grading are probably economically more justifiable for lightweight aggregate because aggregate gradation and shape can be more readily controlled in a manufactured aggregate. The potential advantages of gap grading have also been investigated by Dr. F. Leonhardt.

The contribution of Prof. Y. Tachibana confirms the fact that lightweight aggregate concrete can be substituted for normal weight concrete in composite concrete slab and steel stringer construction with no appreciable change in strength or behavior.

His test results show that in push-out specimens stud shear connectors actually develop a somewhat greater useful capacity (based on residual slip) in lightweight concrete and that the ultimate load capacity of composite beams is essentially the same for either type concrete.

While the load deflection of the lightweight concrete composite beams, in the elastic range, was about ten to fifteen percent greater, the natural frequencies obtained in the dynamic tests were slightly higher. This result indicates that the reduction in structural stiffness was more than compensated for by the reduced weight.

These contributions confirm the fact that with proper design and field control the primary requirements of structural safety and behavior can be assured. The comparative cost analysis in the contribution by Mr. A. A. Yee further demonstrates that considerable overall economy can be achieved in spite of a considerable premium on the lightweight aggregate concrete.

Vc

Comportement dynamique des bâtiments de grande hauteur, en béton armé ou en béton précontraint, soumis à des efforts horizontaux (vent, séismes, explosions). Conception des joints

Dynamisches Verhalten von bewehrten und vorgespannten Beton-Hochhäusern unter horizontalen Kräften (einschließlich Wind-, Erdbeben- und Explosionskräfte) und zweckentsprechende Ausbildung der Verbindungen

Dynamic Behaviour of Reinforced and Prestressed Concrete Buildings under Horizontal Forces and the Design of Joints (Incl. Wind, Earthquake, Blast Effects)

Leere Seite
Blank page
Page vide

DISCUSSION PRÉPARÉE / VORBEREITETE DISKUSSION / PREPARED DISCUSSION

Earthquake Response Analysis of a Reinforced Concrete Building having Four Box Columns

Analyse de la réponse aux séismes d'un bâtiment en béton armé avec quatre poteaux en caissons

Berechnung der Erdbebenreaktion eines Stahlbetongebäudes mit vier Kastensäulen

TSUKASA AOYAGI HIDEYUKI TADA
Eng.D., Struc.Engrs.
Nikken Sekkei Komu Co., Ltd.
Japan

In an attempt to ascertain the earthquake response characteristics of medium-rise (30 to 45 meters in height) reinforced concrete buildings having shear walls, the authors have made analytical studies on a number of buildings of the type described above. The building (shown in Fig. 1), whose response characteristics are discussed in this paper, represents such buildings.

It is a common practice in Japan that the analysis of external vibrational force as well as the structural design of buildings is based on the loads prescribed in the national building code. Then, the structural response to the external vibrational force is analized to verify the appropriateness of the design. Methods of analysing such a structural response have been remarkably improved in these past years. Among them, non-linear earthquake response analysis of bending-shear type mass system seems to be favorably accepted by the increasing number of structural engineers in Japan recently.

It, however, is important for practising engineers that they should have some means to make fairly accurate assessment of a building's response to vibrational forces at the preliminary design stage so that a rational design will result thereby insuring a reasonably earthquake-resistant structure.

In this paper, an attempt will be made to deduce some earthquake response characteristics of the buildings of the type previously described from a variety of response analyses conducted by the authors while they were designing the building shown in Fig. 1. It is hoped that the results of such analyses may serve in future as a source of some useful information for preliminary structural design of similar buildings.

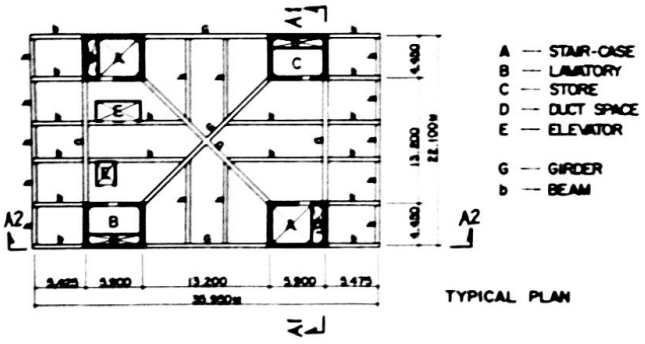

Designed in Nov. 1966

Fig. 1 CASE A

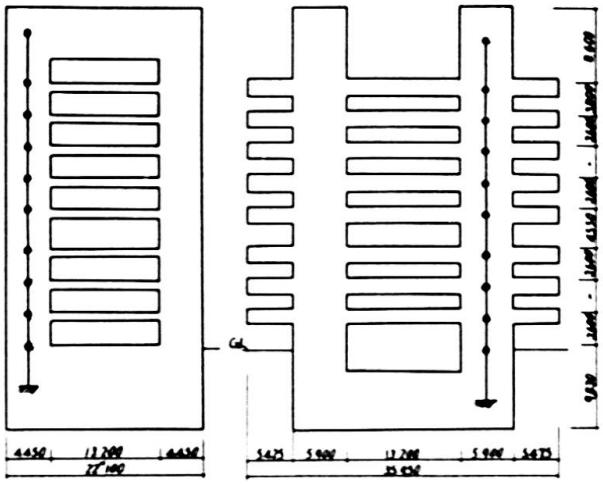

SECTION A1 SECTION A2

1. Earthquake Motions and Method of Analysis.

a. Earthquake Motions used in the Analysis.

As shown in Table 1, two ground motions, which were selected from among a number of typical earthquake motions recorded in Japan, were used for the purpose of this analysis. Of these two, the ground motion recorded in Akita represented typical earthquake motion in the soft ground while that recorded in Sendai represented one in the hard ground. Further, the N-S component of El Centro earthquake which is often used for this sort of analysis was also included so as to make possible a comparative study.

As indicated in the table, the maximum acceleration of these earthquakes were all different from one another; therefore, they were converted into the motions having a maximum acceleration of loo gals. Fig. 2 shows the spectrum of each earthquake motion used for the analysis.

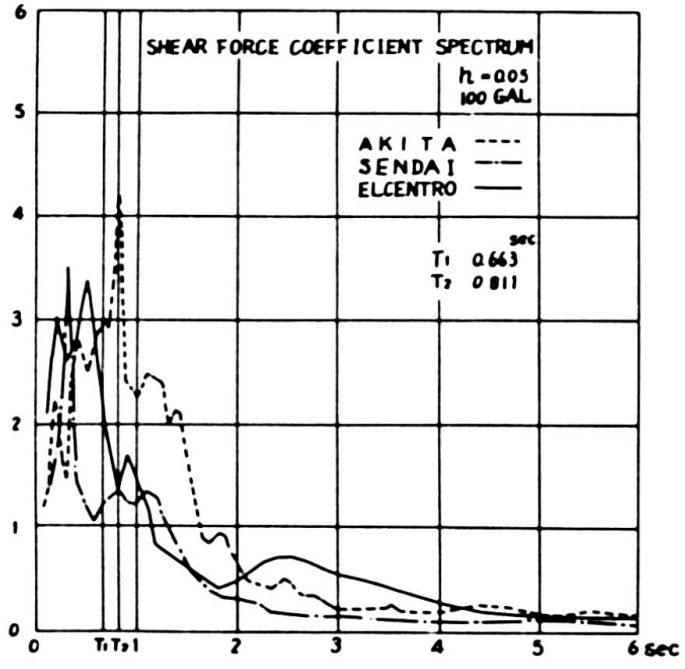

Fig. 2 LINEAR RESPONSE SPECTRUM OF ONE MASS SYSTEM

Table 1

Earthquake Names	Date	Max. Accel.	Symbols
Akita 502 NS	Jun. 16 '64	90 gals	--------
Sendai 501 EW	Apr. 30 '62	45 gals	— — —
El Centro Calif. NS	May 18 '40	319 gals	———

b. Method of Analysis.

Response Analysis for Bending-Shear Type Vibrational System.

For the purpose of making a non-linear earthquake response analysis of bending-shear type multi-mass point system, the following differential equation was used.

$$m_i\ddot{y}_i + \sum_{j=1}^{n}(1+r_I\frac{d}{dt})K_{ij}\cdot y_i = -m_i\ddot{y}_0$$

where, m_i : mass at the mass point i

y_i : displacement of mass point i relative to the ground in cm

r_I : coefficient of internal friction

k_{ij} : elastic coefficient matrix (the reaction which occurs in the direction of vibratory motion at mass point i when a unit elastic deflection is caused at point j)

$\ddot{y}_0$: acceleration of ground motion

The modes (the first to the fourth) were computed by the above formula, and the responses at a specific time were amalgamated. To do this, the responses at various given times were computed by means of numerical integration using Runge-Kutta's approximation formula. For damping coefficient (h_n), the value h_1=0.05 was used, and it was related to frequency (ω_n) as follows:

$$h_n/\omega_n = r_I/2 = \text{constant}$$

where, n = number of modes

Response Analysis for Shear-Type Vibrational System.

The linear earthquake response analysis for shear-type multi-mass point system was made by the use of the following differential equation.

$$m_i\ddot{y}_i + (1+r_I\frac{d}{dt})\{K_i(y_i-y_{i-1})+K_{i+1}(y_i-y_{i+1})\} = -m_i\ddot{y}_0$$

where, m_i : mass at the mass point i

y_i : displacement of mass point i relative to the ground in cm

r_I : coefficient of internal friction

k_i : spring constant of story i

$\ddot{y}_0$: acceleration of ground motion

The values of responses were computed by applying a series of numerical integrations to this differential equation by using linear acceleration method. Further, the damping coefficient was determined based on the same assumption as used for bending-shear type system previously discussed. As for the spring constant, the value as computed on the basis of design lateral loads was used.

Table 2 Natural Periods for 1st Mode to 4th Mode

	1st	2nd	3rd	4th
Direction A1	0.663	0.147	0.069	0.043
Direction A2	0.811	0.173	0.073	0.043

2. Response Analysis

The building now being discussed was of simple framing design which gave no particular problem for its structural studies. In view of this, it was decided to have each story of the building represented by one mass point in both A_1 and A_2 directions by the use of the slope-deflection method in which deformation due to shear and axial force as well as rigid zone are taken into consideration, and the elastic coefficient matrix was computed accordingly. Then, the linear response analysis of bending-shear type vibrational system was conducted.

The periods are as shown in Table 2, and the exitation functions for Frame A_1 and Frame A_2 are as shown in Fig. 3 and Fig. 4 respectively.

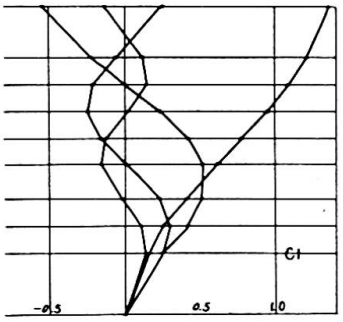

Fig. 3

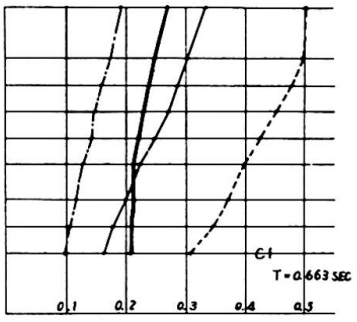

Fig. 5

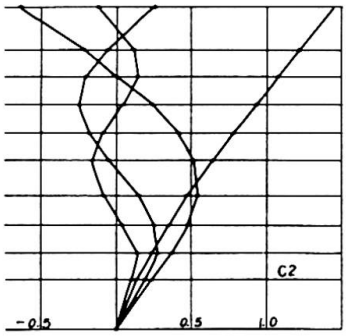

Fig. 4

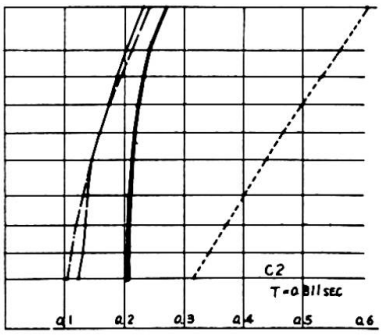

Fig. 6

AKITA ------
SENDAI —·—
EL CENTRO ———

The response values were expressed as shear force coefficient or by symbol Qf. These are shown in Fig. 5 and Fig. 6 for Frame A_1 and Frame A_2 respectively. (The term "shear force coefficient" as used here demotes the shear force acting on the i-th story divided by the summation of individual weight from the top down to the i-th story in question.) In Fig. 5 and Fig. 6, the shear force coefficient corresponding to the lateral loads adopted for the design of this building are shown in bold lines.

Considerations

Actually, the building now being discussed stands on a con-

tinuous layer of firm sandy gravelly soil; therefore, its behaviour under an earthquake will be assessed on the basis of response values computed for the ground motions recorded in Sendai (or El Centro). Figs. 5 and 6 indicates the response values corresponding with the maximum acceleration of ground motion which was taken as 100 gals. From these figures, it can be known that at the base of the building, the response to the acceleration of ground motion of 200 gals corresponds with the design lateral loads set out in the code; and at the top of the building, the response to the acceleration of 150 gals corresponds with the design lateral loads actually used for this building. Buildings of this type have, as shown by the studies in the past, a general tendency to give fairly larger earthquake response values at the top than at the bottom when considered in relation with the distribution of design lateral loads in the structure, so this phenomenon should be duly taken into account by the structural designer.

3. Evaluating the Method of Analysis.

Under strong earthquake motions with acceleration of 200 gals or over, most of structural members usually enter the plastic range as was the case with this building. It, therefore, is necessary to make non-linear response analysis of bending shear type vibrational system if the structural response characteristics under very severe earthquakes are to be assessed with high accuracy. Such an analysis, however, is too complicated and time-consuming for practising engineers to make in the course of actual design for which both labor and time are almost always restricted. For this reason, engineers in practice usually proceed with the structural response from linear response with the aid of the research accomplishments in the past. Since quite a variety of linear analysis methods, some intended for precise computation and others for approximation, are now available, an attempt will be made here to evaluate some of these methods on a comparative basis by applying them to the structural problems of the subject building, and on the basis of such an evaluation, some adequate method for approximate analysis that may prove a handy tool for preliminary structural design will be proposed.

For the purpose of the present comparative appraisal, the following methods of analysis will be discussed.

For precise analysis: Response analysis of the 1st to the 4th mode of bending-shear type vibrational system (expressed by symbol BS)

For approximate analysis:

(1) Response analysis of shear type system (expressed by Symbol S)
(2) Response analysis of the 1st mode only of bending-shear type system (expressed by Symbol BS 1st)
(3) Response analysis of the 1st mode only to be computed from design lateral loads (expressed by Symbol S 1st), which is the method proposed by the authors.

a) Comparison of Factors in Bending-Shear Type System with Those in Shear Type System.

The difference in modes of these two systems are shown in

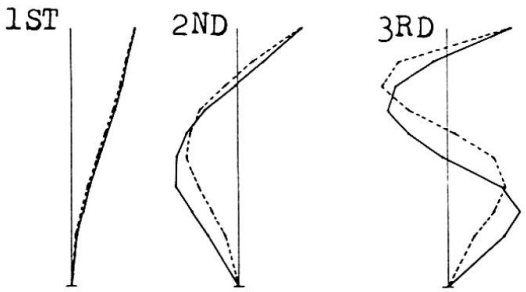

Fig. 7 Mode at Sec. A1

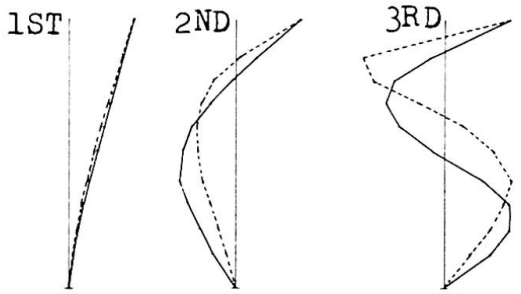

Fig. 8 Mode at Sec. A2

BS ———

S --------

Fig. 7 and Fig. 8 for Frame A1 and Frame A2 respectively. Natural periods and damping coefficients for the 1st to the 4th mode are indicated in Fig. 9. These diagrams indicate that there existed a large difference between the values for bending-shear type system and those for shear type system as to all factors that were analyzed, especially at the modes of higher order. It is believed that this substantial difference is due largely to the deformation of shear walls caused by bending, which gave greater influence in the vibrational modes of higher order.

b) Comparison of Response Values (Shear Force Coefficient).

To begin with, the results obtained by analysis of the 1st mode of bending-shear type system and those of shear type system will be studied. As shown in Fig. 10, no substantial difference was observed in the analysis results of these two systems. This is only too natural because the modes of these two systems were fairly alike as can be known from Fig. 7 and Fig. 8. The results of analyses (BS) 1st/BS and S/BS are shown in Fig. 11.

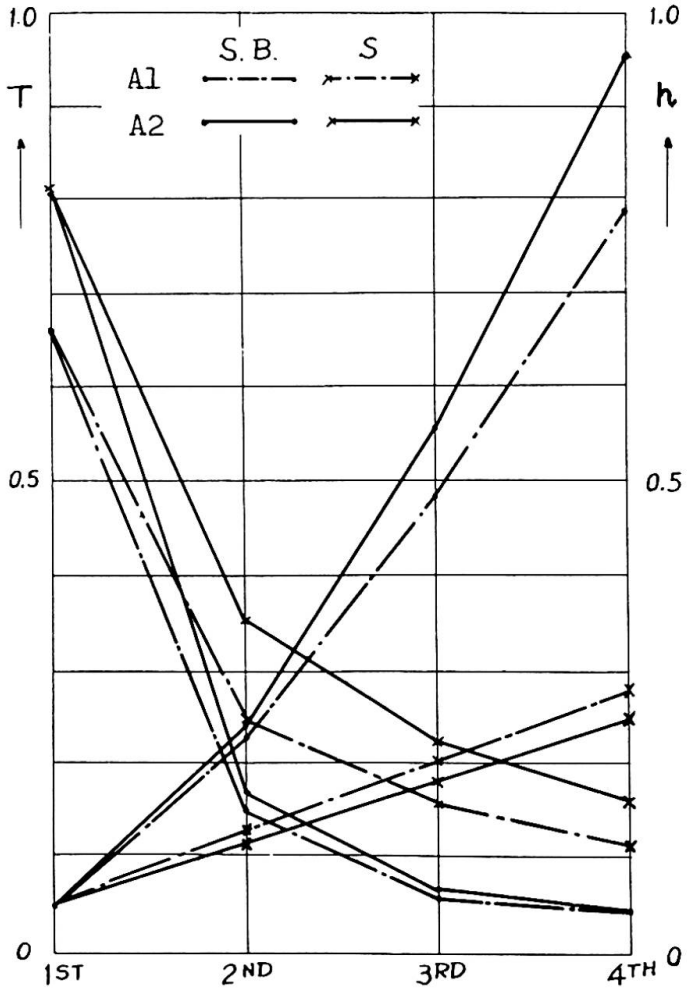

Fig. 9

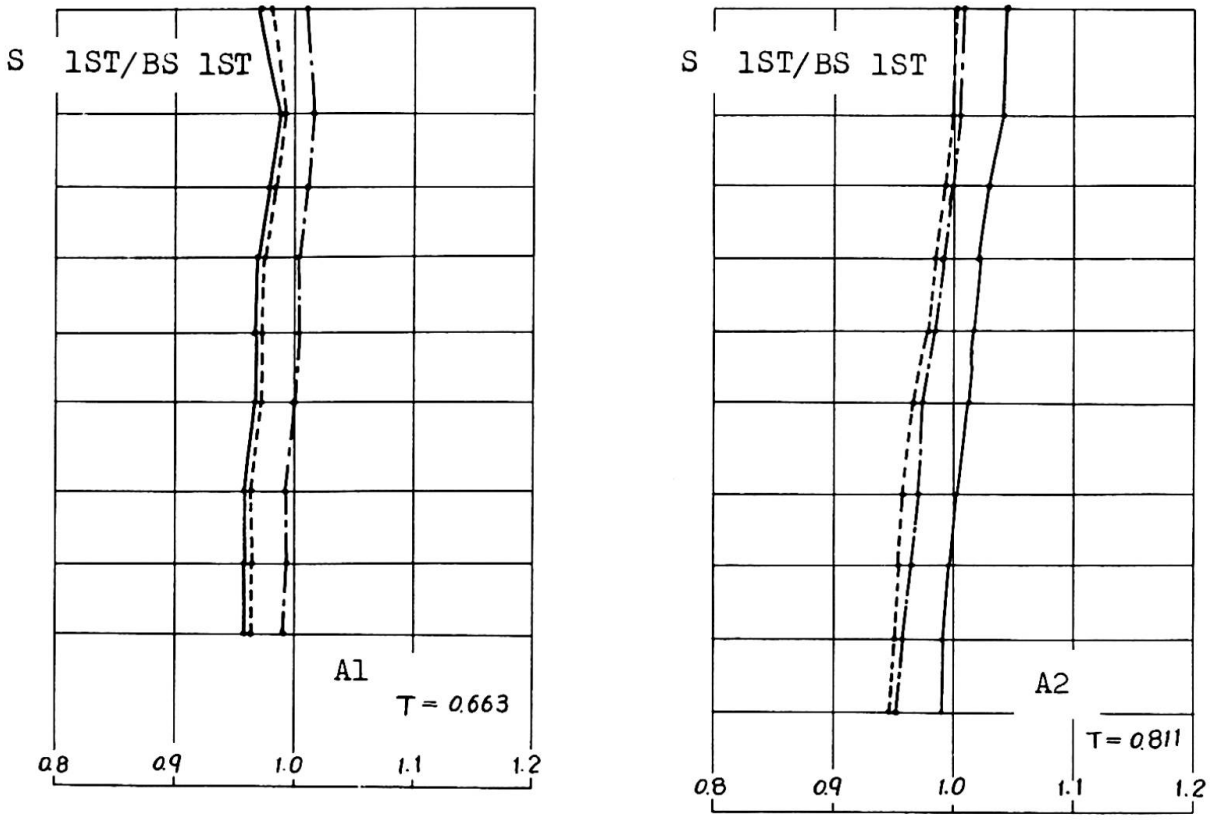

Fig. 10

Considerations.

For the purpose of these analyses, the damping coefficient, h, was determined on the assumption that there existed a relation h_n/ω_n = constant. Because of this assumption, rather high damping coefficients resulted for the mode of high order in case of the bending-shear type system, and this in turn led to the response values which were little affected by the modes of high order. Thus, the response values for the 1st mode turned out to be only slightly different from those for the modes of higher orders.

In the analysis of the shear type system, however, the effects of different vibration modes (Figs. 7 and 8) gave significant effects on the response values (see Fig. 9), and thus some complicated difference was observed due to the variation of modes.

An approximate method of analysis should always be used with caution especially when such a method is intended to deduce the structural response to all types of vibrational modes from only one mode of lower degree, because in some buildings (for instance a building in Example B), their structural responses will be greatly affected by the modes of higher orders.

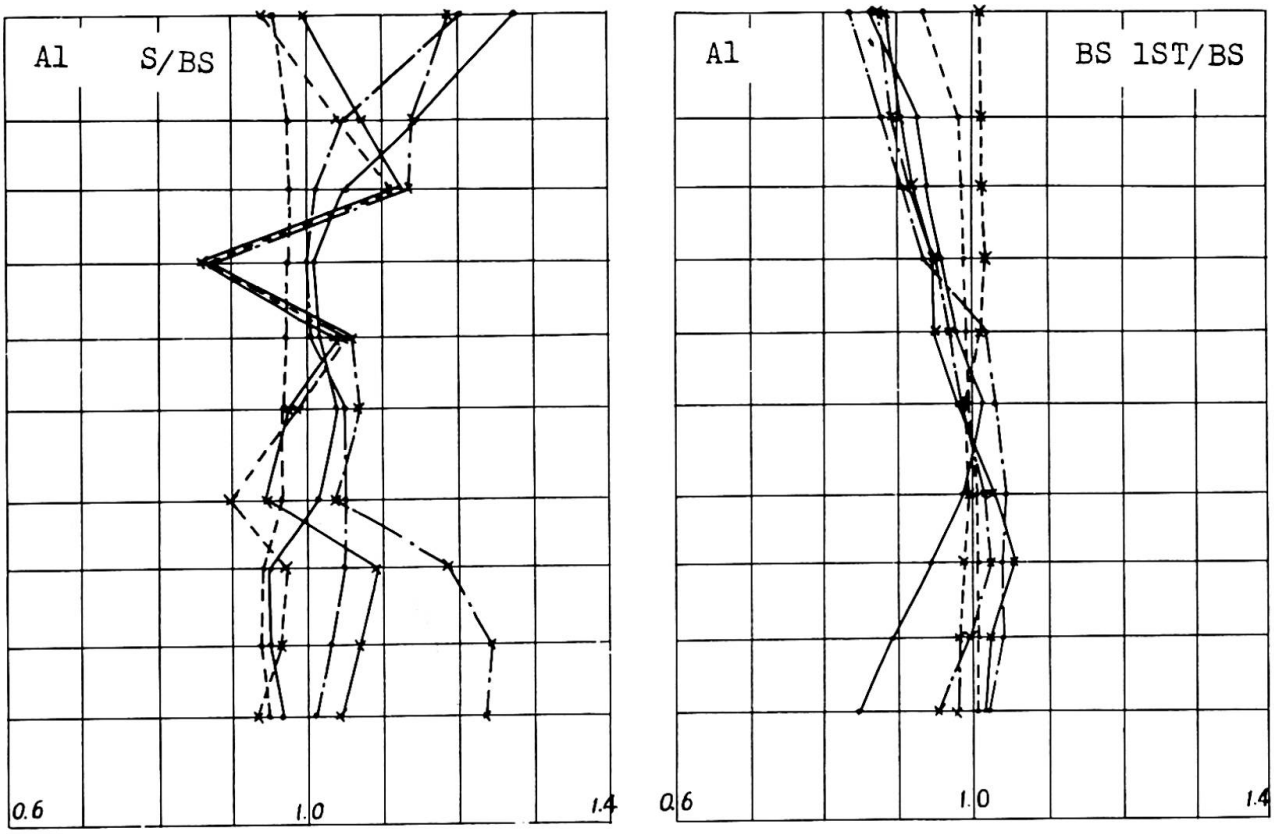
A1 S/BS
0.6
1.0
1.4
A1 BS 1ST/BS
0.6
1.0
1.4
T_1 - 0.663 sec
T_2 - 0.811
AKITA
SENDAI
EL CENTRO

Fig. 11

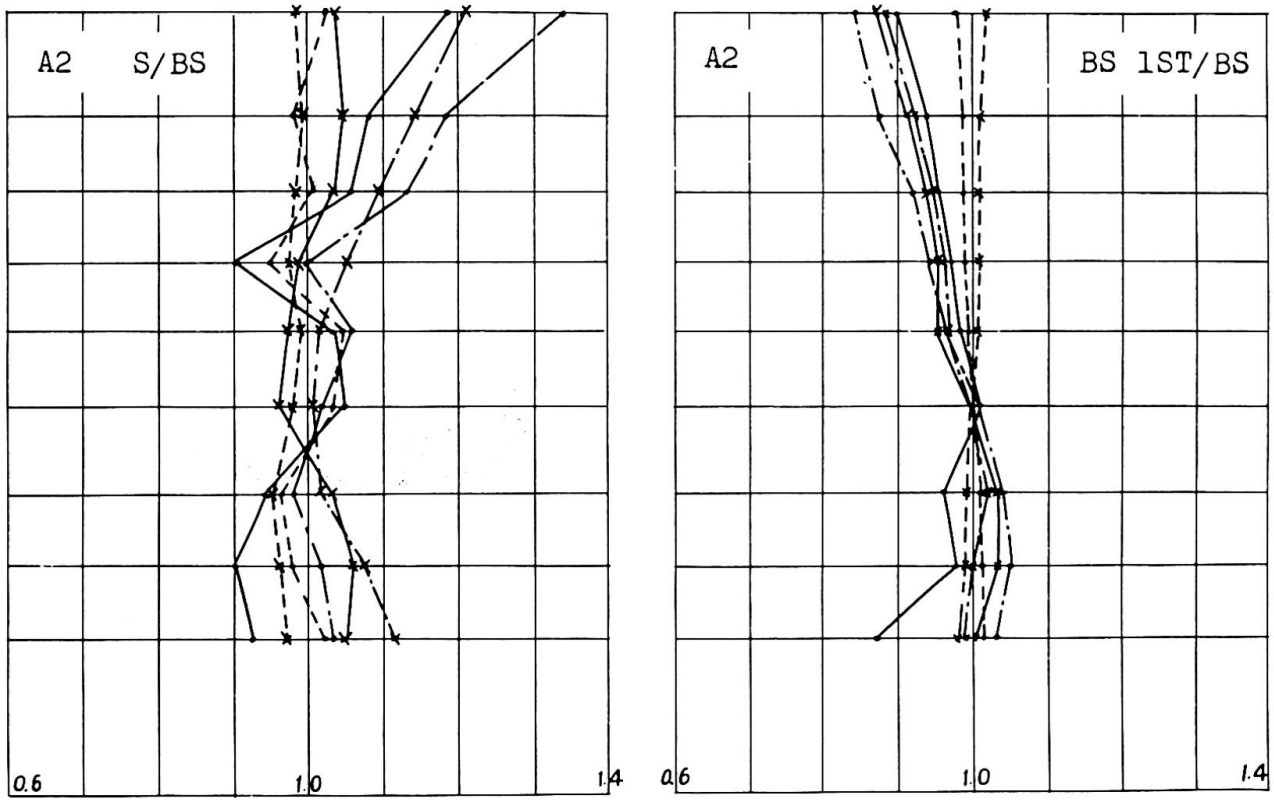
A2 S/BS
0.6
1.0
1.4
A2 BS 1ST/BS
0.6
1.0
1.4

4. Variation of Response due to Different Modes.

Since the building heretofore discussed (i.e., Example A) is somewhat unusual in Japan in terms of the structural features, two buildings of more common structural design will be discussed as a matter of comparison. These are shown in Fig. 14 and Fig. 15 as Examples B and C respectively, and their responses have been analyzed by assuming an equivalent 5-mass point system of shear type.

In order to enable to investigate the characteristic of response to vibration of different modes on a comparative basis, the natural periods were taken at 0.663 second which was the period for the 1st mode of Frame A_1 and at 0.811 second which was the period for the 1st mode of Frame A_2.

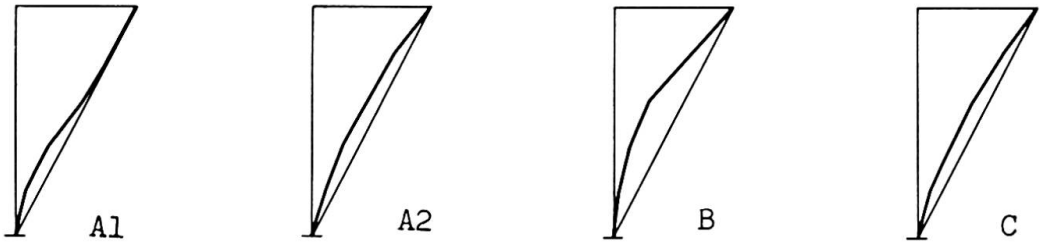

Fig. 12 FIRST MODE OF FOUR CASES

The modes of vibration obtained for the Frames A_1, A_2, B and C are shown in Fig. 12, and the response values in terms of shear force coefficient are shown in Fig. 13.

Considerations.

The comparative analysis has revealed that Frame B has the response characteristic which is quite different from other three cases evidently due to the effects of the higher mode vibration. The reason for this is presumed to be attributable to the fact that the 1st mode of vibration of Frame B is not linear. Japanese structural engineers should bear in mind that a building with this type of response characteristics often results if the building is designed faithfully in accordance with the lateral loads set forth in the Japanese national building code but in disregard of the building's vibration characteristics. The shear force coefficients widely vary with the types of earthquakes adopted for the analysis. This means that the difference in the spectra of the earthquakes shown in Fig. 2 has been directly reflected in the vibration characteristics. The results of these analyses seem to indicate that there are two "problem areas": one is a design problem which concerns the determination of the natural period of a building; and the other, the analysis problem which concerns the types of earthquakes to be used for the earthquake response analysis.

Acknowledgment.

The authors are gratefully indebted to Dr. H. Umemura, professor of structural engineering at Tokyo University for the guidance and help he extended to the authors both during the design of the building discussed here and during the preparation of this present paper.

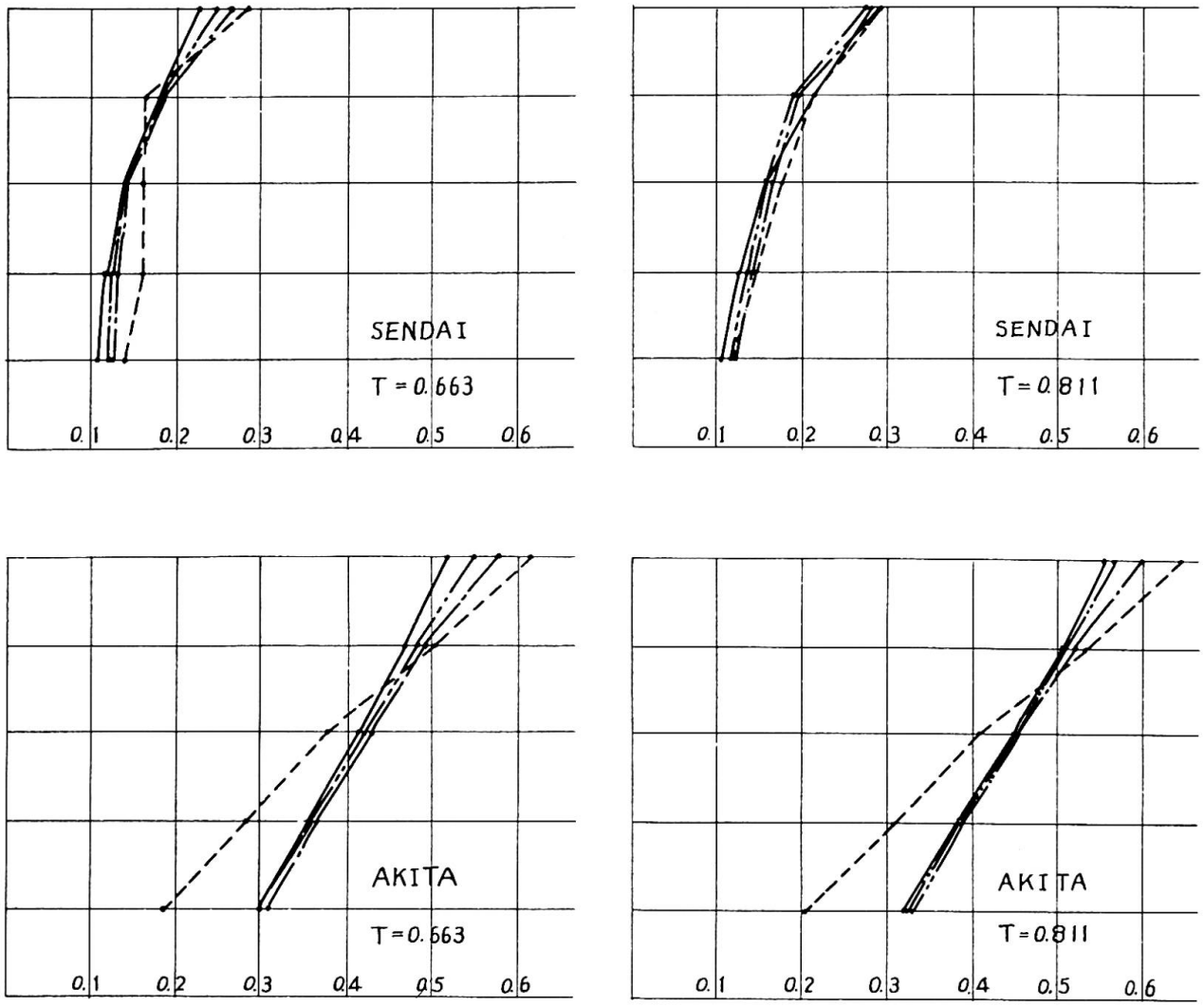

Fig. 13

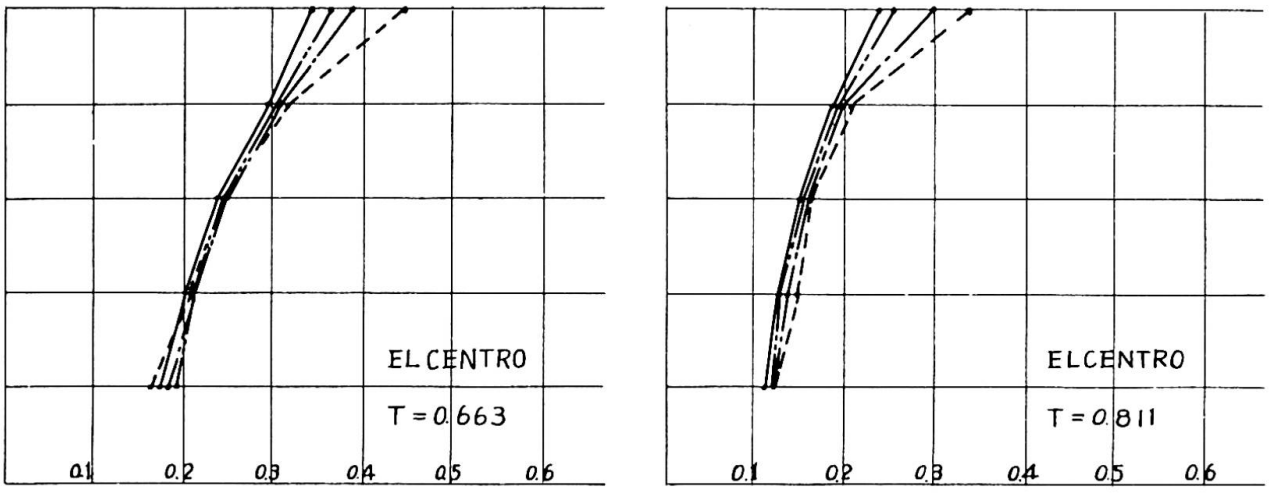

A1 ———— B ----------

A2 —·—·—·— C —··—··—

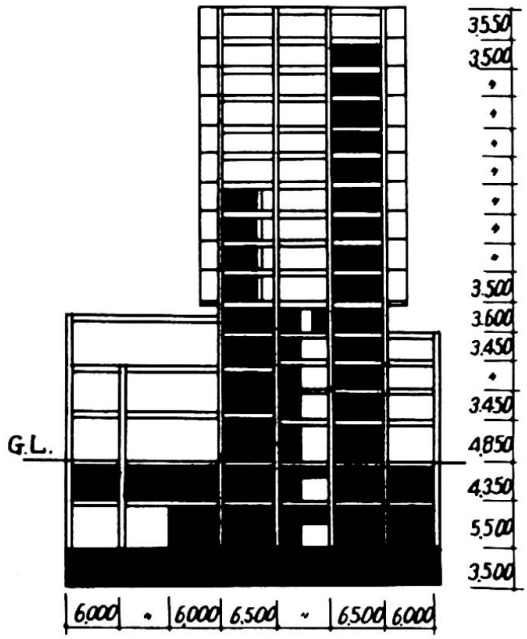

SECTION

Designed in 1963

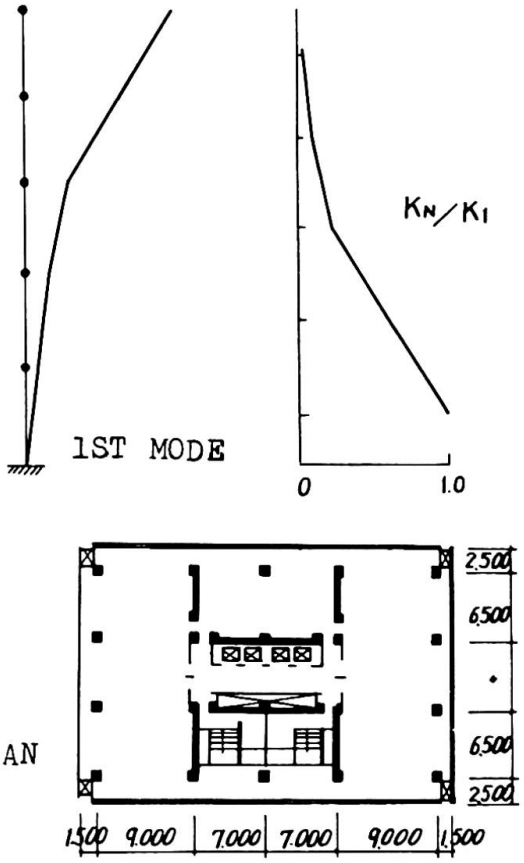

Fig. 14 CASE B

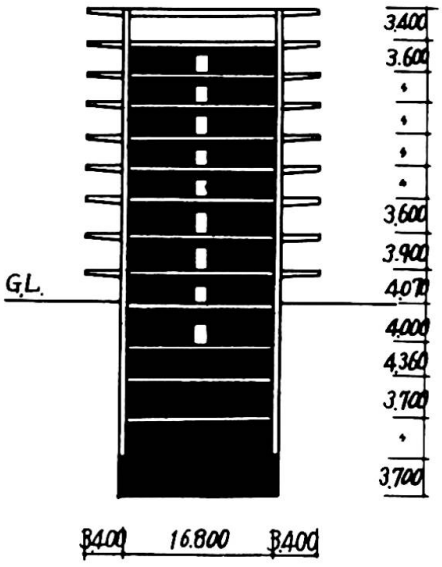

SECTION

Designed in 1964

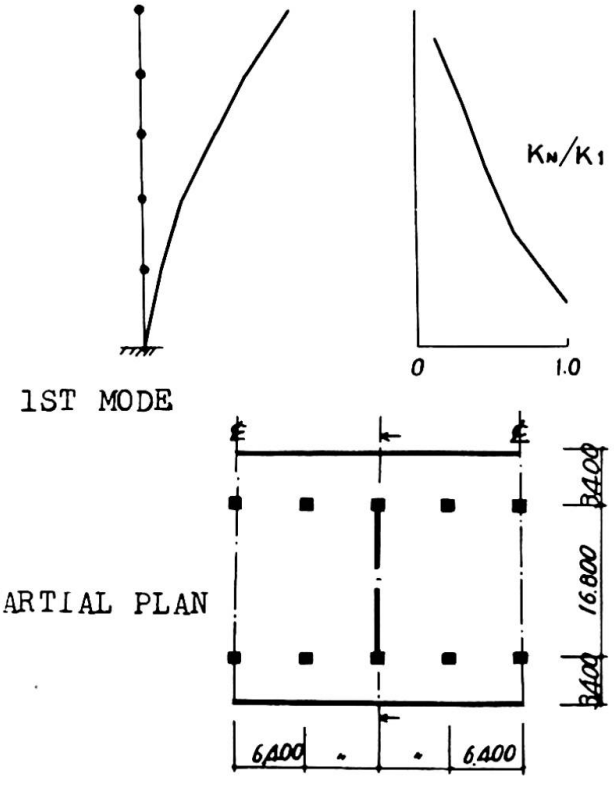

Fig. 15 CASE C

SUMMARY

In an attempt to ascertain the earthquake response characteristics of medium-rise (30 to 45 meters in height) reinforced concrete buildings having shear wall, the authors have made analytical studies on a number of buildings of the type described above. It is hoped that the results of such analyses may serve in future as a source of some useful information for preliminary structural design of similar buildings.

RÉSUMÉ

Pour obtenir des caractéristiques de secousses sismiques dans des constructions de hauteur moyenne (30 - 45 m) en béton armé avec murs de cisaillement, l'auteur a procédé à plusieurs réflections analytiques. Il espère que les résultats de cette analyse servent à pré-dimensionner des constructions simples.

ZUSAMMENFASSUNG

Der Verfasser hat, in der Absicht Erdbebencharakteristiken an mittelhohen Stahlbetongebäuden von 30 bis 45 Meter mit Schubwänden zu erhalten, einige analytische Ueberlegungen angestellt, hoffend, dass die Ergebnisse dieser Analyse in Zukunft als eine Quelle dienlicher Angaben für den vorläufigen Entwurf einfacher Bauten Verwendung finde.

Shear Resistance and Explosive Cleavage Failure of Reinforced Concrete Members Subjected to Axial Load

Résistance au cisaillement et rupture cassante explosive d'éléments en béton armé sous charge axiale

Schubwiderstand und explosiver Sprödbruch der Stahlbetonsäulen unter Achsiallast

MINORU YAMADA
Professor Dr.-Ing.

SHIGEZO FURUI
Dipl.-Ing.

Department of Architecture, Faculty of Engineering
Kobe University, Kobe / Japan

1. INTRODUCTION

As one of the most essential problem for the ductility requirement of the dynamic behaviour of reinforced concrete buildings, it is discussed here the shear resistance and explosive cleavage failure of reinforced concrete members subjected to axial load. Tests were carried out mainly to make clear the influences of axial load level ratios, shear span ratios and web reinforcement ratios upon their shear resistances and fracture modes. An analytical approach is presented here and compared with test results. By this research, the behaviours of brittle fracture and the causes of the lack of ductility of reinforced concrete members become clear and it will be possible to avoid the explosive cleavage failure, which had caused very often heavy damage of reinforced concrete buildings under strong earthquakes, and to establish the design methods how to give them sufficient ductility.

2. OBJECTIVES and SCOPE

The importance of ductility of members or connections for the dynamic resistance of reinforced concrete structures was emphasized by professors Newmark and Hall [1] in the preliminary publication. The lack of ductility of reinforced concrete members is caused mainly by the presence of high axial load or by the presence of high shearing force.

The former problem was discussed by several researchers [2] or by the author [3][4][5] at the 7th. congress of IABSE. Under higher axial load ($\frac{N}{\sigma_B bD} > 0.5$) [6], the deformation energy of reinforced concrete beam-column is dissipated mainly by concrete and not by longitudinal reinforcement. Therefore it shows the lack of ductility. On the contrary, under lower axial load ($\frac{N}{\sigma_B bD} < 0.5$), the deformation energy is dissipated mainly by longitudinal reinforcement and so it shows sufficient ductility. The only

way to improve it, is to use sufficient web reinforcement in order to increase the ductility of concrete. There exists not so sufficient ductility by the presence of axial load but the fracture mode is always mild and not so brittle as shear fracture.

On the latter problem there are not yet sufficient knowledge[7][8]. Moreovere this problem is more essential for ductility requirements, because the fracture mode under higher shearing force shows a very brittle nature, and that it shows often even explosive fracture, especially in the presence of axial compression (see Photo. 1). There exists no ductility and yet such a fracture mode were found very often in heavily damaged reinforced concrete buildings under strong earthquake motion. They had caused often the collapse of whole structures at earthquake (see Photo. 2).

This paper deals on the fracture mode of reinforced concrete members subjected to high shearing force under axial compression and on the contribution of web reinforcements for this explosive cleavage failure. Tests were carried out to make clear the influences of axial load level ratios, shear span ratios and web reinforcement ratios of reinforced concrete members upon the shear resistance and shear fracture modes of them. An analytical treatment, which is based upon the biaxial fracture criteria of concrete, is presented here and compared with test results.

3. TESTS

3-1. Test Procedures and Measuring Devices

Tests were carried out by loading frames, which were specially installed in testing machine as shown in Fig. 1. The constant axial compression load N $(=X \cdot N_0)$ was introduced by testing machine through roller and maintained steady at constant value throughout the test. The transverse load P was applied by oil jack with electric load cell at its head, which was installed in loading frames.

There were two loading systems for shear tests as shown in Fig. 2, i.e. type C with single curvature in uniform shear span "a" at the both ends of the specimen and type Z with double curvature in uniform shear span "2a" at the central part of the specimen. Type C is ordinary shear mechanism for beam test and it has a merit of ordinary case as beam but has a demerit of the influences of additional bending through axial load by deflection for column test. Type Z is a special mechanism for shear test and it has a merit for the case of column test to avoid the influences of additional bending through deflection and to make possible the tests under higher shear span ratios. This loading system simulate often the loading condition of columns, beams or beam to column connections under earthquake motion.

Longitudinal and transverse displacements between main points or diagonal displacements between diagonal points in test span were measured by 1/100 mm dial gauges, which were set in measuring frame, that was fixed at one end on one loading line. Wire strain gauges were pasted upon surfaces in test span or several other deformation measuring techniques like checkerboard printing on the testing surfaces were applied them too.

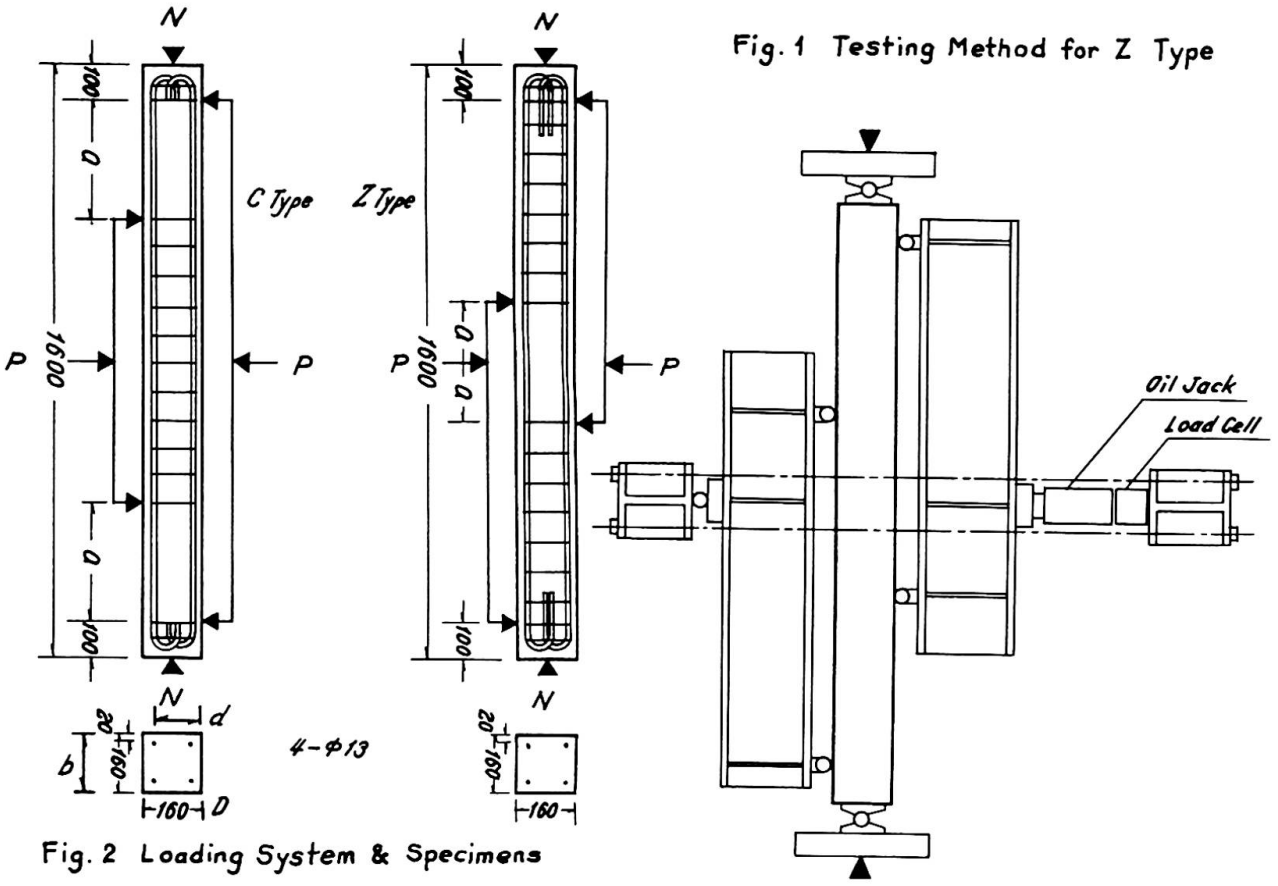

Fig. 1 Testing Method for Z Type

Fig. 2 Loading System & Specimens

3-2. Test Specimens and Test Series

Specimens had a length of 160 cm with a square cross section of width and depth of 16 cm x 16 cm and reinforced with 4 ordinary round steel bars of 13 mm diameter for longitudinal reinforcement, i.e.longitudinal gross reinforcement ratio $p_g = 1{,}04\%$. Test spans were reinforced with or without web reinforcement according to test series. Other spans were reinforced with web reinforcement of square type hoop of ordinary round steel bars of 6 mm diameter with 8 cm pitchs (see Fig. 2). Both ends of web reinforcement were welded together.

Concrete mix is 1 : 2,55 : 3,34 and $W/C = 60\%$, the approximate concrete compressive strength $\sigma_P \cong 200$ kg/cm², the approximate concrete tensile strength $\sigma_z \cong 20$ kg/cm², the approximate yield point of longitudinal reinforcement of ϕ 13, $\sigma_y \cong 2800$ kg/cm² or 3045 kg/cm² and of web reinforcement of ϕ 6, $\sigma_{yw} \cong 2144$ kg/cm². The mechanical properties of materials are shown in Table 1.

Tests were carried out in three series:

Series I : For the research of the influence of shear span ratios upon shear behaviour, comparison between test mechanisms C type and Z type. The shear span ratio of Z type is defined here a/d. In this project the shear span ratios were varied 0,6 1,2 1,8 2,4 for Z type and 1,2 2,4 3,6 4,8 for C type. Test spans were not reinforced with web reinforcement.

Series II : For the research of the influences of the axial load level ratios upon shear behaviour. The axial

load level ratio $X(=\frac{N}{N_0})$ is defined here as the ratio of acting constant axial compression N versus ultimate strength of centrally loaded column N_0. There were varied 0(beam), 1/6 and 1/3. Test spans were not reinforced with web reinforcement.

Series III : For the research of the contribution of web reinforcement. As web reinforcement it was applied here a square type hoop of round steel bar with 6 mm diameter. The hoop spacings were varied 0, 16 cm, 8 cm, 4 cm, i.e. web reinforcement ratios $\eta = 0,\ 0{,}22,\ 0{,}44,\ 0{,}88\%$. It is defined here as the ratio of the area of longitudinal cross section of concrete versus the area of web reinforcement. contained in that cross section (see Fig. 4).

Series I and II were tested together. They are shown in Table 1.

3-3. Test Results

Test results are summarized in Table 1. Numerals following to B in the specimen notation of the table indicate the hoop spacing in cm and C or Z with numerals indicate the test mechanism and the ratio of the shear span versus the depth of specimen.

The fracture mode S in the table indicates cleavage shear explosion, B → S indicates initially bending and finally shear crack opening and B indicates bending crack deformation.

The deformation process and fracture modes under various shear span ratios and various axial load level ratios are shown in Fig. 3, as the relation between relative displacements of both ends of shear span "2a" for Z type and lateral load P.

Table 1 Test Series & Test Results

Specimen	a/d	Steel σ_y kg/cm²	Concrete Comp. σ_p	Concrete Tens. σ_z	Const Axial Load	Max. Bending Moment	Max. Shear Force	Fracture Mode
RC:C1:B0:C1:1/3N0Q	1.2	2800	291	24.7	30t	1.95 t·m	12.2 t	S
RC:C1:B0:C2:1/3N0Q	2.4	2800	360	27.7	36	2.24	7.00	B
RC:C1:B0:C3:1/3N0Q	3.6	2800	360	27.7	36	2.30	4.79	B
RC:C1:B0:C4:1/3N0Q	4.8	2800	360	27.7	36	2.40	3.75	B
RC:C1:B0:C3:1/6N0Q	3.6	2800	360	27.7	18	1.96	4.10	B
RC:C1:B0:C3: 0N0Q	3.6	2800	360	27.7	0	1.00	2.09	B
RC:C1:B0:Z1:1/3N0Q	0.6	2800	291	24.7	30	1.05	12.7	S
RC:C1:B0:Z2:1/3N0Q	1.2	2800	291	24.7	30	1.60	9.40	S
RC:C1:B0:Z3:1/3N0Q	1.8	2800	291	24.7	30	2.29	9.50	S
RC:C1:B0:Z4:1/3N0Q	2.4	2820	218	19.7	24	1.97	6.17	B→S
RC:C1:B0:Z1:1/6N0Q	0.6	3045	213	19.7	12	0.73	9.10	S
RC:C1:B0:Z2:1/6N0Q	1.2	3045	213	19.7	12	1.12	7.00	S
RC:C1:B0:Z3:1/6N0Q	1.8	3045	213	19.7	12	1.70	7.10	S
RC:C1:B0:Z4:1/6N0Q	2.4	3045	213	19.7	12	1.92	6.00	B→S
RC:C1:B0:Z1: 0N0Q	0.6	3045	197	19.4	0	0.53	6.60	B→S
RC:C1:B0:Z2: 0N0Q	1.2	3045	197	19.4	0	1.04	6.50	B→S
RC:C1:B0:Z3: 0N0Q	1.8	3045	197	19.4	0	0.91	3.80	B→S
RC:C1:B0:Z4: 0N0Q	2.4	3045	197	19.4	0	1.25	3.90	B
RC:C1:B0:Z3: 0N0Q	1.8	2800	291	24.7	0	1.15	4.80	B→S
RC:C1:B4:Z2:1/3N0Q	1.2	2800	202	20.2	23	1.81	11.3	B→S
RC:C1:B8:Z2:1/3N0Q	1.2	2800	202	20.2	23	1.51	9.42	S
RC:C1:B16:Z2:1/3N0Q	1.2	2800	202	20.2	23	1.38	8.66	S
RC:C1:B0:Z2:1/3N0Q	1.2	2800	202	20.2	23	1.13	7.06	S

B: Bending Fracture
S: Cleavag Shear Fracture (Explosion)
B–S: Bending — Shear Crack Opening

Z.R. in the figures of deformation characteristics indicates the formation of tensile crack, S.R. the formation of shear crack opening, L.R. the formation of a diagonal tension crack between loading points and X-mark the explosive cleavage shear

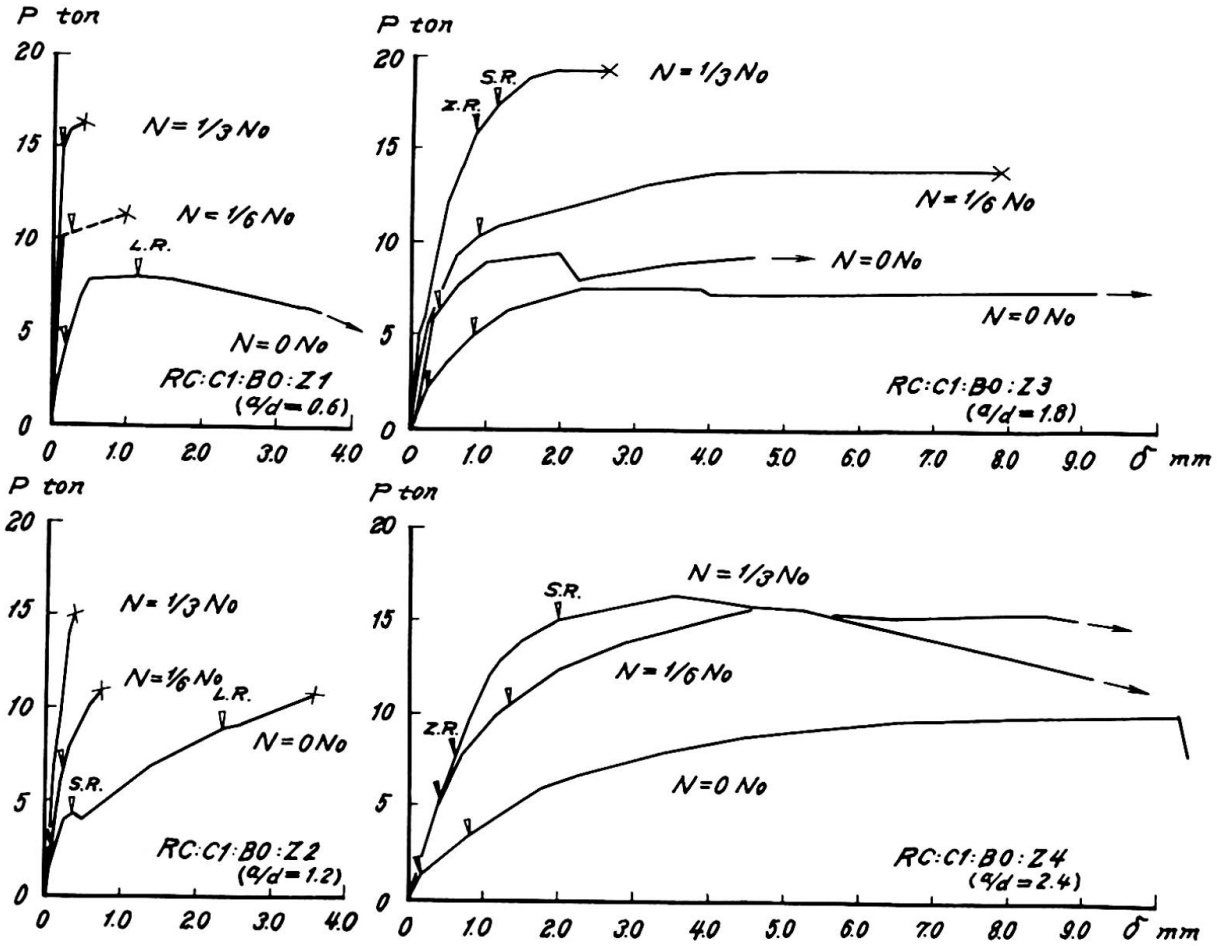

Fig. 3 Deformation Characteristics

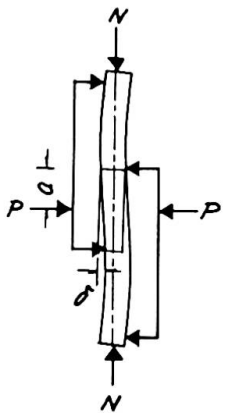

failure.

Under higher shear span ratios it appears at first bending crack Z.R. at the tension side of the loaded cross section and the deformation occurs mainly by the opening of this tensile crack, then this tensile crack shows inclination or it appears several shear cracks S.R. and finally the compression side of the loaded cross section is crushed down.

Under intermediate shear span ratios it appears initially tensile crack Z.R. by bending at the tensile side of the loaded cross section, then on the side surfaces of shear span it appears short diagonal cracks and its opening becomes larger.

Under lower shear span ratios it appears initially several short shear cracks on the side surfaces of shear span and gradually it increases their number accompanied by the increase of transverse load, then suddenly but in several seconds it occurs explosion by a large diagonal tension crack opening directly between loading points independently from formerly formed short shear cracks. This behaviour is intensiver, the higher the axial load ratios (see Photo.1).

The deformation process and fracture modes, for the case of a shear span ratio of 1,2 and an axial load level ratio of 1/3 with various web reinforcement ratios are shown in Figs. 4 and 12.

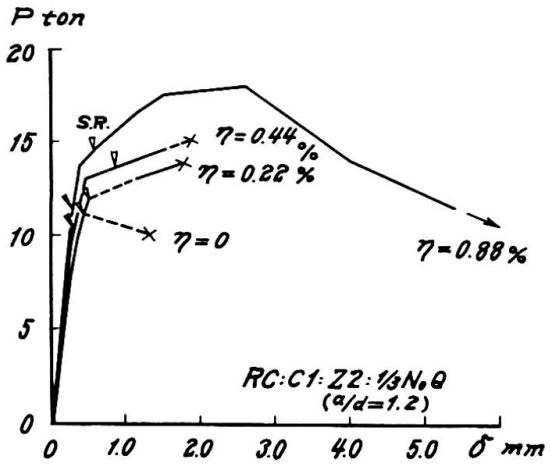

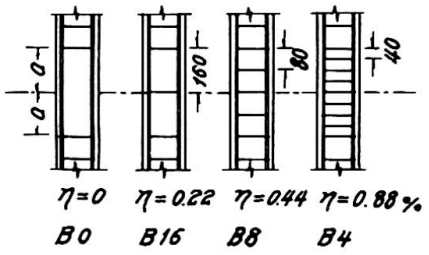

Fig.4 Contribution of Web Reinforcement for Shear Deformation & Fracture

4. ANALYTICAL APPROACH

4-1. General Description

For the analysis, the reinforced concrete member is devided into finite small rectangular elements with a central point (i,j) as their co-ordinates. The stresses and displacements of each element are represented by this cross point. Following to the increase of external load, the stresses and displacements are calculated and the fracture of each element is checked by critical fracture condition of concrete. If the stress condition of one element reaches the critical condition, the element is destroyed and it bears no more stresses and the stresses, which were born by the failed element, will be redistributed to another elements proportional to their stiffness. After the redistribution of stresses, it proceeds to next loading stage. So by repeating this procedure step by step, the elasto-plastic deformation behaviour of this member is able to followed. Through the decrease of the number of load bearing elements, finally it will bear no more increase of external load and it will reach the ultimate state. Fracture mode and ultimate strength will be so clarified.

4-2. Elements and their Fracture Condition

For the stresses and displacements of an element, it is assumed that:

(1) As the element, there are two kinds of elements,i.e. concrete element with reinforcing steel and concrete element without reinforcing steel. Reinforcing steel is estimated by equivalent cross section for normal stresses.

(2) The external forces are distributed to each elements proportional to their stiffness. They are represented with their central point. As the stresses of each element, it is considered σ_{ij} and τ_{ij} but it is neglected here the normal stresses perpendicular to the member axis.

(3) The shearing stress τ_{ij} is decided by normal stress and for the element with reinforcing steel it is considered the

increment of shearing stress by the difference of stresses in reinforcing steel.

The displacements of each cross point are: (see Fig. 5)

$$V_{ij+1} = -\beta\cdot\alpha\left[\frac{\sigma_{ij}+\sigma_{ij+1}}{2}\cdot\frac{1}{E_c}\right]+V_{ij} \quad (1),$$

$$V_{i+1j+1} = -\beta\cdot\alpha\left[\frac{\sigma_{i+1j}+\sigma_{i+1j+1}}{2}\cdot\frac{1}{E_c}\right]+V_{i+1j} \quad (2),$$

$$\sigma_{ij} = \frac{\tau_{ij}+\tau_{i+1j}+\tau_{ij+1}+\tau_{i+1j+1}}{4}\cdot\frac{1}{G_c} \quad (3),$$

$$\varphi_{ij} = \frac{V_{i+1j}-V_{ij}}{\alpha\cdot D} \quad (4),$$

$$\theta_{ij} = -(\gamma_{ij}+\varphi_{ij}) = \theta_{i+1j} \quad (5),$$

$$u_{ij+1} = \beta\cdot\alpha\cdot\theta_{ij}+u_{ij} \quad (6).$$

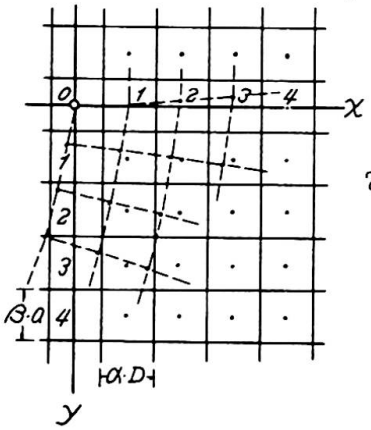

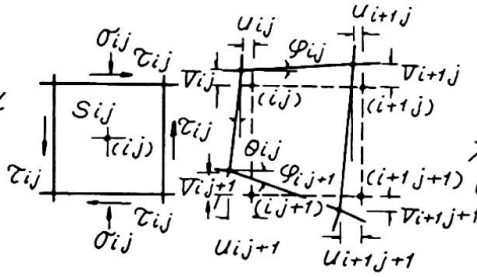

Fig.5 Finite Element

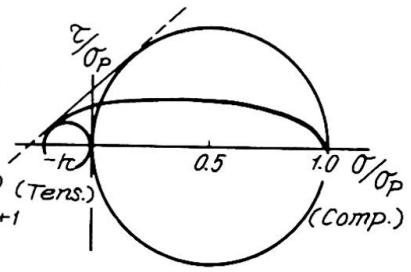

Fig.6 Fracture Condition of Concrete

The critical fracture condition of each element is assumed to occur under the following combined biaxial fracture condition of concrete by Mohr (see Fig. 6):

$$\frac{(1+K)^2}{K}\cdot\tau^2+\left[\sigma-\frac{(1-K)}{2}\sigma_p\right]^2=\frac{(1+K)^2}{4}\cdot\sigma_p^2 \quad (7),$$

here, $K=\sigma_t/\sigma_p$, σ_t and σ_p tensile and compressive strength of concrete respectively.

The normal stress σ and the shearing stress τ for the estimation of the critical condition of the element, which are influenced by redistribution of stresses from neighbouring elements, are calculated as follows:

$$\sigma = \frac{\sigma_{ij-1}+2\sigma_{ij}+\sigma_{ij+1}}{4} \quad (8),$$

$$\tau = \frac{\tau_{i-1j}+2\tau_{ij}+\tau_{i+1j}}{4} \quad (9).$$

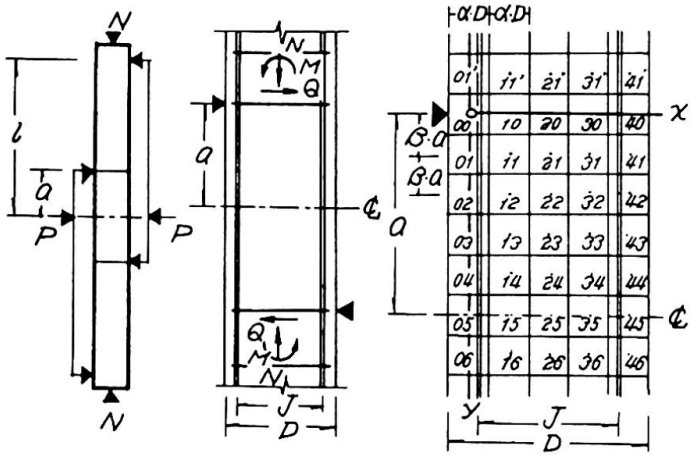

Fig.7 Reinforced Concrete Member

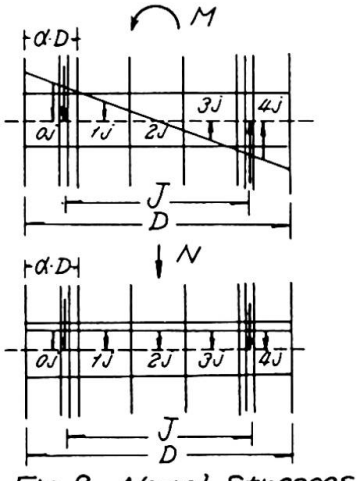

Fig.8. Nomal Stresses

4-3. Application for Reinforced Concrete Columns loaded by Bending Moment, Shearing Force and Axial Compression

Normal stress of each element is calculated as the sum of normal stresses ${}_M\sigma_{ij}$ through bending moment and ${}_N\sigma_{ij}$ through axial

load. Within each element the stress is assumed to distribute uniformely. The steel stress is calculated by the concrete normal stress σ_{ij}, in which element the reinforcing steel is contained (S_{0j}, S_{4j} in Fig. 8), and if the reinforcing steel is placed excentrically to the center of the cross point, it is modified by the equivalent ratio of moduli of elasticity n' as follows:

$$\sigma_{sij} = n' \cdot \sigma_{ij} \quad , \quad \left(n = E_s/E_c \, , \; n' = \frac{j/2}{2\alpha \cdot D} \cdot n \right) \tag{10}$$

So the normal stress through bending moment is calculated by the equilibrium condition as follows:

$$ {}_M\sigma_{0j} \cdot (\alpha \cdot D \cdot b + n' \cdot A_s) + {}_M\sigma_{1j} \cdot \alpha \cdot D \cdot b + {}_M\sigma_{2j} \cdot \alpha \cdot D \cdot b + {}_M\sigma_{3j} \cdot \alpha \cdot D \cdot b + {}_M\sigma_{4j} (\alpha \cdot D \cdot b + n' A_s) = 0 \tag{11}$$

$$ {}_M\sigma_{0j} (2\alpha^2 D^2 b + n' \cdot A_s \cdot j/2) + {}_M\sigma_{1j} \cdot \alpha^2 D^2 b - {}_M\sigma_{3j} \cdot \alpha^2 D^2 b - {}_M\sigma_{4j} (2\alpha^2 D^2 b + n' \cdot A_s \cdot j/2) = M_j \tag{12}$$

Normal stress ${}_N\sigma_{ij}$ by axial compression is calculated by the ratio of moduli of elasticity n as follows:

$$ {}_N\sigma_{ij} \cdot \alpha \cdot D \cdot b = \frac{\alpha \cdot D \cdot b \cdot E_c}{(5 \cdot \alpha \cdot D \cdot b + 2n \cdot A_s) E_c} \cdot N \tag{13}$$

Shearing stress τ_{ij} is calculated for the element without longitudinal reinforcement:

$$\tau_{ij} = \frac{1}{2} \left[\frac{({}_M\sigma_{ij-1} + {}_N\sigma_{ij-1}) - ({}_M\sigma_{ij+1} + {}_N\sigma_{ij+1})}{2} + \frac{({}_M\sigma_{i-1,j-1} + {}_N\sigma_{i-1,j-1}) - ({}_M\sigma_{i-1,j+1} + {}_N\sigma_{i-1,j+1})}{2} \right] \cdot \frac{\alpha \cdot b \cdot D}{\beta \cdot a \cdot b} + \tau_{i-1,j} \tag{14}$$

and for the element with longitudinal reinforcement:

$$\tau_{ij} = \frac{1}{2} \left[\frac{{}_M\sigma_{ij-1} - {}_M\sigma_{ij+1}}{2} + \frac{{}_M\sigma_{i-1,j-1} - {}_M\sigma_{i-1,j+1}}{2} \right] \cdot \frac{\alpha \cdot b \cdot D + n' A_s}{\beta \cdot a \cdot b} + \frac{1}{2} \left[\frac{{}_N\sigma_{ij-1} - {}_N\sigma_{ij+1}}{2} + \frac{{}_N\sigma_{i-1,j-1} - {}_N\sigma_{i-1,j+1}}{2} \right] \cdot \frac{\alpha \cdot b \cdot D + n A_s}{\beta \cdot a \cdot b} + \tau_{i-1,j} \tag{15}$$

Through the fracture of each element, the stresses are re-distributed. If the element S_{4j} in Fig. 9 is destroyed, the element S_{4j} bears now only by longitudinal steel and therefore the stiffness of S_{4j} for normal stress decreases. Then the neutral axis removes towards the compression side and through the equilibrium condition the new normal stress σ_{ij} is decided. Shearing stresses in S_{ij-1} and S_{ij+1} are redistributed by (14) and (15).

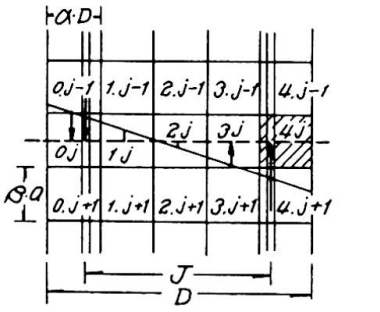

Fig. 9 Destroyed Element

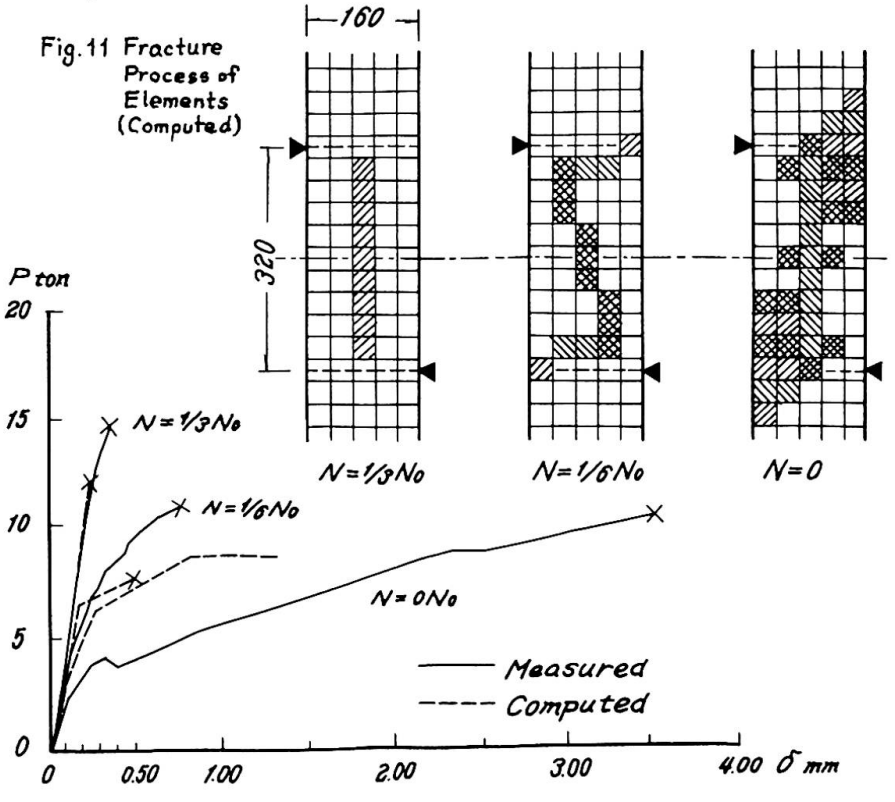

Fig. 11 Fracture Process of Elements (Computed)

Fig. 10 Fracture Process of RC:C1:B0:Z2 (Measured & Computed).

Fig. 10 shows the test results with solid lines and corresponding calculated values of foregoing deformation analysis for the case of a shear span ratio $a/d = 1,2$ and axial load level ratios of 0, 1/6 and 1/3 with dotted lines.

Fig. 11 shows the fracture process of foregoing analysis. For the case of $N=\frac{1}{3}N_0$, the elements in the central part of the member is destroyed through compressive shear and the redistributed stresses destroyed another elements one after another and it increases no more load bearing capacity. For the case of $N=\frac{1}{6}N_0$, at first the extreme tension side element reaches the critical condition at the maximum moment section and then, following to the increase of external load, the inside elements are destroyed gradually and final state is decided. For the case of $N = 0N_0$, at first the tensile crack occures and it penetrates into inside and, even when the central elements are destroyed by tensile shear, it shows the more increase of load carrying capacity.

5. DISCUSSIONS

5-1. Interaction between Shear Span Ratios and Axial Load Ratios

Table 2 shows the interaction between shear span ratios (a/d) and axial load level ratios ($X=\frac{N}{N_0}$) upon the fracture behaviours of reinforced concrete members very clearly. The lower the shear span ratios and the higher the axial load ratios becomes the explosiver the fracture mode. On the contrary, the higher the shear span ratios and the lower the axial load ratios, the milder the fracture mode. The ductility of members is influenced and decided by this fracture mode. Ductility requirement of reinforced concrete members is satisfied under the condition of lower axial load ratios and higher shear span ratios.

It is a remarkable fact that there exists a very clear difference of fracture modes at a value of (a/d) between 1,8 and 2,4 for every axial load ratios. (See Photo. 3)

Bending resistance decreases under lower shear span ratios for columns as it was pointed out for beams by prof. Kani [9].

Table 2. Interaction a/d - X

a/d	Constant Axial Load Ratio		
	$N=0N_0$	$N=\frac{1}{6}N_0$	$N=\frac{1}{3}N_0$
0.6	B→S	S	S
1.2	B→S	S	S
1.8	B→S	S	S
2.4	B	B→S	B→S

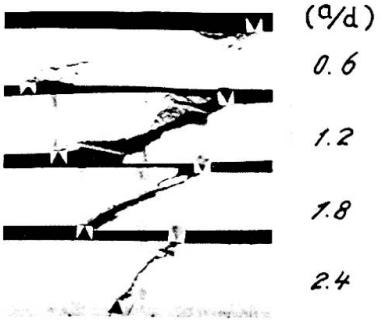

Photo. 3 Influences of Shear Span Ratios (a/d) upon the Fracture Modes ($\eta = 0$, $N=\frac{1}{3}N_0$)

5-2. Effect of Web Reinforcement

Ductility requirement under higher axial load ratios with lower shear span ratios is improved by web reinforcement. The effects are shown in Fig. 4 under an axial load level ratio of 1/3 and a shear span ratio of 1,2. It is a very severe condition, but it happens often in actual case, for the case of without web reinforcement $\eta = 0$, it shows a typical explosive shear fracture. For the case with lower web reinforcement ratios $\eta = 0,22$ and $0,44\%$, they showed a little ductility even with a little increase of resistance, but finally explosive cleavage failure. However for the case with fairly higher web reinforcement ratio $\eta = 0,88\%$, it shows no more shear fracture but

sufficient ductility.

5-3. Damage of Reinforced Concrete Buildings under Strong Earthquakes

Photo. 2 shows one of the typical cleavage shear fracture of a reinforced concrete column of the gymnasium of Niigata high school, at the strong earthquake on the 16th. June 1964, Niigata/ Japan. Photos 1 and 2 , i.e. test specimen and real case show a very good similarity of their fracture mode. Test specimen shows the cause of damage of reinforced concrete columns under earthquake very clearly. Such a explosive cleavage shear failure of column caused very often heavy damage of whole buildings under strong earthquakes. These photographs of damage under earthquake show very clearly the importance of the problem of shear resistance under axial compression for the dynamic behaviour of reinforced concrete buildings.

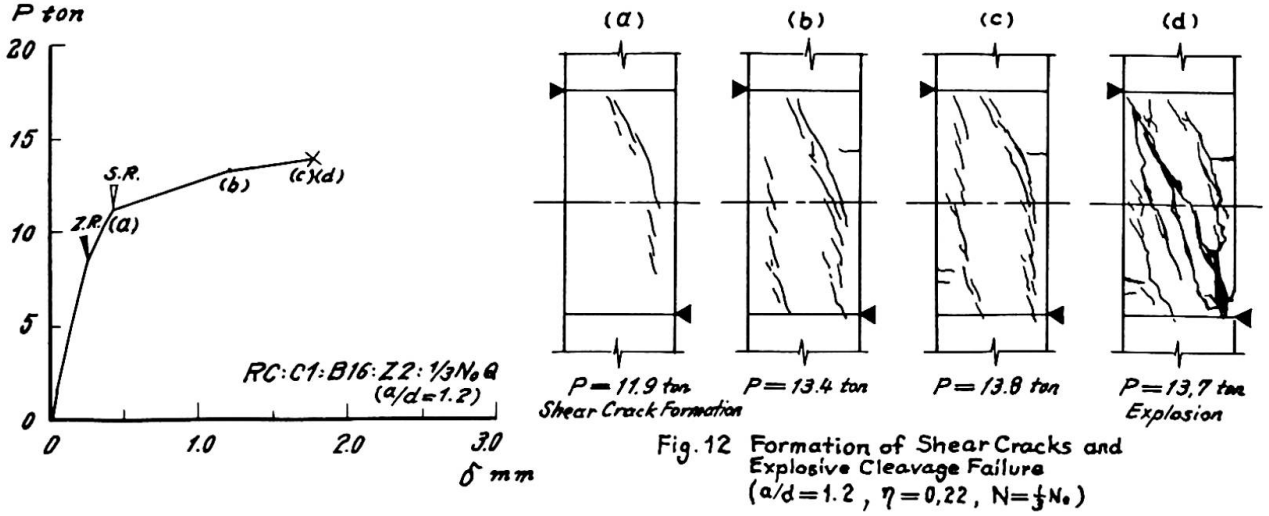

Fig. 12 Formation of Shear Cracks and Explosive Cleavage Failure
($a/d=1.2$, $\eta=0,22$, $N=\frac{1}{3}N_0$)

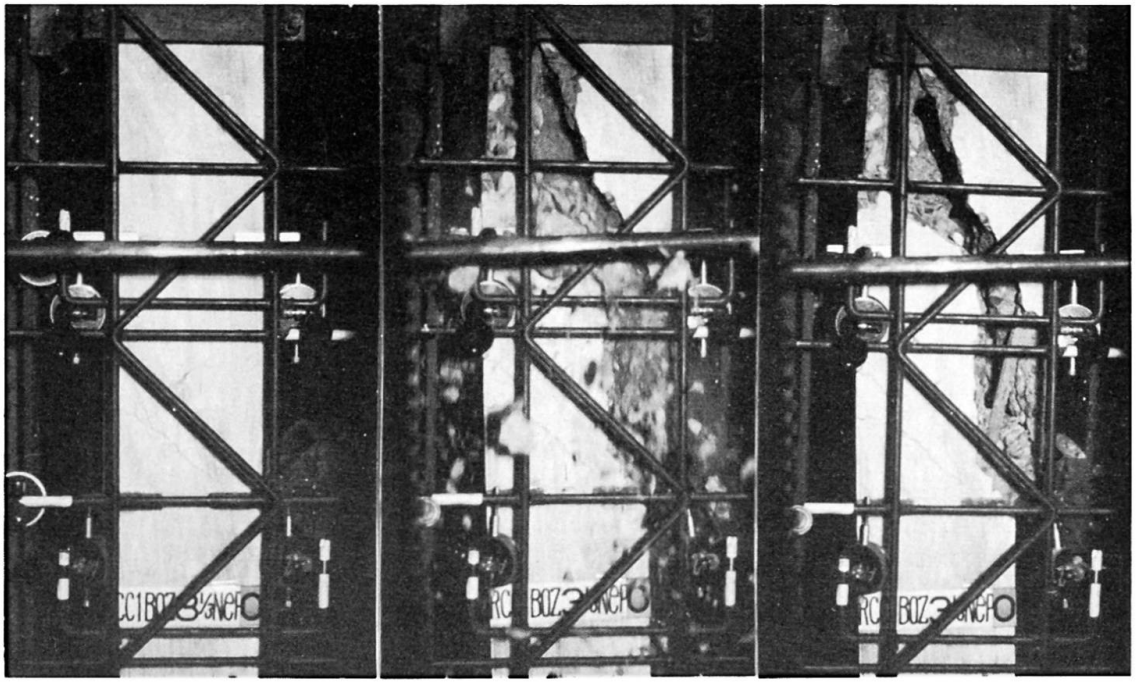

Photo. 1 Cleavage Explosive Shear Fracture of Reinforced Concrete Columns.
($a/d \fallingdotseq 1.8$, $\eta=0$, $N=\frac{1}{3}N_0$)

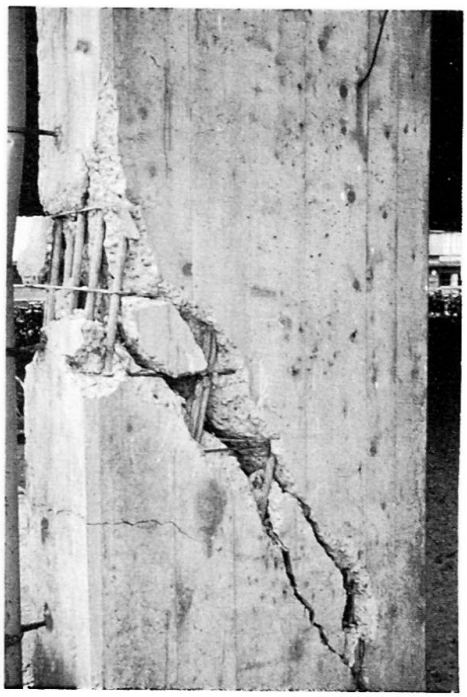

Photo. 2 Cleavage Shear Fracture of a Reinforced Concrete Column of Gymnasium in Niigata High School / Japan, by the Earthquake on the 16th. June, 1964.
(Photo.: Courtesy of ass.Prof. Mizuhata)

6. CONCLUDING REMARKS

The lack of ductility of reinforced concrete member is caused by high axial compression and high shear force. The simultaneous action of both forces had caused very often heavy damage of whole structures under strong earthquakes (see Photo. 2).

This paper intends to make clear the shear resistance and explosive cleavage failure of reinforced concrete members subjected to axial load as one of the most essential cause of the lack of ductility. Three series of tests were carried out to make clear the influences of axial load level ratios, shear span ratios and web reinforcement ratios upon deformation characteristics and fracture modes. Test results are shown in Figs. 3 and 4 and summerized in Tables 1 and 2. They show the fact that the higher the axial load level ratios, the lower the shear span ratios and the lower the web reinforcement ratios, the ductility of the member will be lost and it causes often explosive cleavage failure (see Photo. 1). Test specimens show a very good simulation with actual case under earthquake.

An analytical approach gives a fairly good agreement with the behaviours of test results (Figs. 10, 11).

7. REFERENCES

[1] Newmark, N.M., Hall, W.J.: Dynamic Behaviour of Reinforced and Prestressed Concrete Buildings under Horizontal Forces and the Design of Joints, Prel. Publ., 8th. Congress, IABSE, pp.585/613.

[2] Flexural Mechanics of Reinforced Concrete, Proc., Internl. Symposium, Miami, Fla./Nov. 1964, ASCE-ACI.

[3] Yamada, M.: Drehfähigkeit Plastischer Gelenke in Stahlbeton balken, Beton- u. Stahlbetonbau, H.4. Apr. 1958, pp.85/91.

[4] Yamada, M.: Verhalten Plastischer Gelenke in Stahlbetonbalken, Prel. Publ.,7th. Congress, IABSE, 1964, pp.963/970.
[5] Yamada, M.: Verhalten Plastischer Gelenke in Stahlbetonsäulen, Finl. Publ.,7th. Congress, IABSE, 1964, pp.481/488.
[6] Yamada, M., Kawamura, H.: Elasto-Plastische Biegeformänderungen der Stahlbetonsäulen und-balken, Abh., IVBH, Bd. 28/I.
[7] Morrow, J., Viest, I.M.: Shear Strength of Reinforced Concrete Frame Members Without Web Reinforcement, J., ACI., Mar. 1957, pp.833/869.
[8] Baldwin, J.M.Jr., Viest, I.M.: Effect of Axial Compression on Shear Strength of Reinforced Concrete Frame Members, J., ACI, Nov. 1958, pp.635/654.
[9] Kani, G.N.J.: The Riddle of Shear Failure and Its Solution, J., ACI., Apr. 1964, pp.441/467.
[10] Leonhardt, F., Walter, R.: Beiträge zur Behandlung der Schubprobleme in Stahlbetonbau, Beton- u. Stahlbetonbau.
[11] Thürlimann, B.: General Report, IVa, Shear Strength, Reinforced and Prestressed Concrete, Prel. Publ., pp.747/750, Finl. Publ., pp.311/315, 7th. Congress, IABSE, 1964.
[12] Rüsch, H.: Über eine Erweiterung der Mörschschen Fachwerkanalogie, Finl. Publ., 7th. Congress, IABSE,1964,pp.353/369.
[13] Wästlund, G.: A Theory of Combined Action of Bending Moment and Shear in Reinforced and Prestressed Concrete Beams, Finl. Publ., 7th. Congress, IABSE, 1964, pp.371/377.

SUMMARY

As one of the most essential problem for the ductility requirement of the dynamic behaviour of reinforced concrete buildings, theoretical and experimental researches were carried out to make clear the influences of axial load ratios, shear span ratios and the contribution of web reinforcement ratios upon the shear resistance and fracture modes. It becomes clear one of the most important cause of the heavy damage of reinforced concrete buildings by the lack of ductility (Photos. 1 and 2).

RÉSUMÉ

Des recherches théoriques et expérimentales ont été faites concernant la ténacité et son influence dans le comportement dynamique de bâtiments en béton armé, pour déterminer l'influence de la charge axiale, de la répartition des forces de cisaillement, et la contribution du réseau d'armature sur la résistance de cisaillement et sur le comportement à la rupture. On voit que le manque de ténacité est une des causes les plus importantes des lourds domages dans les bâtiments en béton armé. (Fig. 1 et 2)

ZUSAMMENFASSUNG

Als eines der wichtigsten Probleme für die Zähigkeitsforderung des dynamischen Verhaltens von Stahlbetongebäuden wurden theoretische und experimentelle Untersuchungen angestellt, um den Einfluss der Achsialkraft, der Querkraftverteilung sowie des Bewehrungsnetzes auf den Schubwiderstand und das Bruchverhalten aufzuklären. Es wird klar, dass dies einer der hauptsächlichsten Gründe für den schweren Schaden bei Stahlbetongebäuden ist, wenn diese der Zähigkeit ermangeln. (Fig. 1 und 2)

Vc

DISCUSSION LIBRE / FREIE DISKUSSION / FREE DISCUSSION

The Impact Resistance of Prestressed Concrete

Résistance aux chocs du béton précontraint

Der Stoßwiderstand des vorgespannten Betons

P.W. ABELES

The contribution by Professors Newmark and Hall shows clearly the ductility of under-reinforced concrete members. It is remarkable that even without a favourable compressive reinforcement "the removal and re-application of load had little or no effect on either the load carrying capacity or the ultimate ductility". The title of the paper covers the "dynamic behavior of reinforced and prestressed concrete". Mr. Rogers in his contribution stated that prestressed concrete should not be used for earthquake frame structures. However, I should like to point out that the conditions with prestressed concrete may vary to a great extent dependent on the degree of prestress. In the figure below comparative bending moment deflection curves of under-reinforced rectangular prestressed concrete beams are shown in which all steel members are tensioned. Curve (a) presents a case at which cracking and failure occur simultaneously. This would be only obtained if the steel were over-prestressed and an effective prestress of 85% of the maximum were available which is not permitted in most countries. However, type (b) shows the limit case of fully prestressed concrete at which under service load which is supposed to be 55% of the failure load no tensile stresses occur. Curve (c) refers to a partially prestressed construction Class II of FIP-CEB at which the effective prestress is 40% of the maximum steel stress and under service load the first cracks just become visible, whereas type (d) relates to the limit case at which the effective prestress is zero. After repeated loading this case may become identical with type (e). It is seen that the ductility is greatly increased by reduction of the effective prestress. In the diagram the classification of FIP-CEB I, II and III is indicated.

COMPARATIVE BENDING MOMENT - DEFLECTION CURVES OF UNDER-REINFORCED RECTANGULAR PRESTRESSED CONCRETE BEAMS [ALL STEEL MEMBERS TENSIONED]

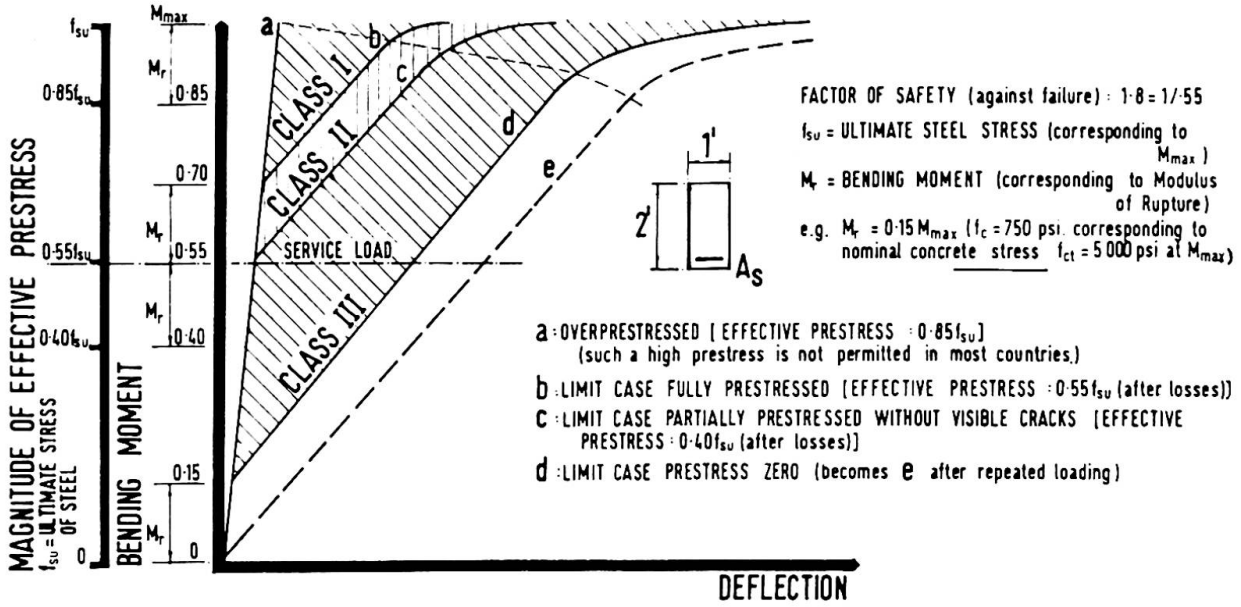

The ductility of prestressed concrete is essential where impact has to be absored. This has been demonstrated by impact tests on partially prestressed poles which I had shown at the Lisbon Congress twelve years ago. Reference is made to Figs. 5-7 in publication (1), the first shows the impact when a wagon of 45 kips weight was propagated with a speed of 10 miles per hour into a pole and cut off part of the flange. The pole was still capable of carrying the design load in spite of some wires in the flange being cut off. This demonstrates the ductility to impact.

---

(1) Impact Resistance of Prestressed Concrete Masts" by P. W. Abeles, 17th Volume of Publications of IABSE (originally presented at Lisbon Congress at theme (b)

V

CONCLUSIONS / SCHLUSSFOLGERUNGEN / CONCLUSIONS

GEORG WÄSTLUND
Chairman of Working Commission III

1. Outstanding achievements in high-rise concrete buildings are to be noted.

2. Such matters as economics, vertical transportation, fire safety, as well as convenience and comfort of building occupants deserve careful consideration.

3. Interesting new results have been obtained from field measurements of the effects produced by shrinkage, temperature, and creep on high-rise buildings.

4. Structural lightweight aggegate concrete has been used in buildings up to 60 storeys. In comparison with heavyweight aggregate concrete, only some modifications in design are necessary, and these modifications concern the differences in unit weight, modulus of elasticity, bond, and shear.

5. Significant concepts relating to the dynamic behaviour of concrete buildings were considered with special reference to earthquake, wind, blast, and also sonic boom. Strength and ductility requirements were discussed. Results of laboratory tests were presented. Field observations on buildings damaged by earthquake action were reported.

Chairman of Working Commission III
Georg Wästlund

Leere Seite
Blank page
Page vide